New Ideas for Effective Higgs Measurements

Dissertation

Johann Brehmer

New Ideas for Effective Higgs Measurements

Dissertation

submitted to the Combined Faculties for the Natural Sciences and for Mathematics of the Ruperto-Carola University of Heidelberg, Germany for the degree of Doctor of Natural Sciences

Put forward by

Johann Brehmer

born in Bremen, Germany

Oral examination: July 26, 2017

9th March 2017

Referees: Prof. Dr. Tilman Plehn

Prof. Dr. Björn Malte Schäfer

After years of expensive education
A car full of books and anticipation
I'm an expert on Shakespeare and that's a hell of a lot
But the world don't need scholars as much as I thought

— J. Cullum [1]

Abstract in deutscher Übersetzung

Abstract

Contents

Preface

This thesis is based on research conducted between 20014 and 2017 at the Institute for Theoretical Physics at Heidelberg University. Chapter 3 is based on two papers, which later became part of a CERN report:

[2] J. Brehmer, A. Freitas, D. López-Val, and T. Plehn:
Pushing Higgs Effective Theory to its Limits.
Phys. Rev. D 93, 075014 (2016). arXiv:1510.03443.

[3] A. Biekötter, J. Brehmer, and T. Plehn:
Extending the Limits of Higgs Effective Theory.
Phys. Rev. D 94, 055032 (2016). arXiv:1602.05202.

[4] D. de Florian, C. Grojean, F. Maltoni, et al.:
Handbook of LHC Higgs Cross Sections: 4. Deciphering the Nature of the Higgs Sector.
LHC Higgs Cross Section Working Group Yellow Report. arXiv:1610.07922.

Chapter 4 is based on the following publication:

[5] J. Brehmer, K. Cranmer, F. Kling, and T. Plehn:
Better Higgs Measurements Through Information Geometry.
arXiv:1612.05261.

In addition, it includes some original results and yet unpublished work in progress with F. Kling and T. Plehn.

Chapter 2 consists of introductory material that can be found in many textbooks and review articles, as well as on a lecture on effective field theories given by the author to fellow PhD students in Heidelberg:

[6] J. Brehmer:
Higgs Effective Field Theory.
Student lecture, research training group "Particle Physics Beyond the Standard Model".

Finally, some of the work done during my PhD is not included in this thesis:

[7] J. Brehmer, J. Hewett, J. Kopp, T. Rizzo, and J. Tattersall:
Symmetry Restored in Dibosons at the LHC?
JHEP 1510, 182 (2015). arXiv:1507.00013.

[8, 9] G. Brooijmans, C. Delaunay, A. Delgado, et al.:
Les Houches 2015: Physics at TeV Colliders – New Physics Working Group Report.
arXiv:1605.02684.
Part of these proceedings were published separately as
J. Brehmer, G. Brooijmans, G. Cacciapaglia, et al.:
The Diboson Excess: Experimental Situation and Classification of Explanations; A Les Houches Pre-Proceeding.
arXiv:1512.04357.

Chapter 1

Introduction

"Begin at the beginning," the King said, very gravely,
"and go on till you come to the end: then stop."
— L. Carroll [10]

The Higgs boson [11–13] is a key element of the Standard Model of particle physics (SM). Its discovery in 2012 [14, 15] completed the particle zoo of the SM. It is a triumph of a decade-old model, but it also offers us a way forward: the Higgs provides us with an unprecedented chance to understand some of the biggest unsolved mysteries of physics.

As the only known fundamental scalar, it suffers from the famous electroweak hierarchy problem: why is its mass scale (and therefore the electroweak scale) so much smaller than the Planck scale, while there is no sign of a symmetry protecting it against quantum corrections? Is the electroweak vacuum, defined by the Higgs potential, stable? Why are the Yukawa couplings, and consequently the fermion masses, spread out over so many orders of magnitude? Is the Higgs related to Dark Matter, for instance as mediator to a dark sector? Or might it even be the source of inflation, explaining the surprising level of isotropy in the Cosmic Microwave Background?

Many models of physics beyond the Standard Model have been proposed to answer at least some of these questions. Very often they predict Higgs coupling patterns different from the SM. A precise measurement of the Higgs properties thus provides a crucial probe of such models, and might be one of the most important missions for present and future runs of the Large Hadron Collider (LHC).

This poses two immediate questions:

1. Which framework should be used to parametrise the Higgs properties?
2. How can these parameters be measured efficiently at the LHC experiments?

These two questions drive the research presented in this thesis, and we will tackle them one by one.

Ideally, all Higgs measurements should use the same universal language to parametrise their results, allowing for an efficient comparison and combination. Such a framework should be general enough to describe the effects of any interesting new physics scenario without strong model assumptions. On the other hand, too large a number of parameters makes combinations of different experiments and global fits impractical.

A simple example for such a universal parametrisation is the κ framework, which was widely used during run 1 of the LHC. It is based on the SM Lagrangian, but promotes all Higgs couplings to free parameters. There are several issues with this approach: it is not gauge-invariant, and it can only describe structures that are already present in the SM. So while a measurement based on the κ framework can be useful for total rates, it will not be able to utilise information in kinematic distributions.

Instead, we work in an approach based on effective field theory (EFT) [16–18]. Based only on the assumption that new physics has a typical energy scale significantly larger than the experimental energies, all new physics effects are captured by a tower of higher-dimensional operators. The leading effects for Higgs physics should come from only a handful of operators with mass dimension 6 [19–21]. These operators are manifestly gauge-invariant and can be used beyond tree level. They describe both coupling rescalings as well as novel kinematic structures not present in the SM, allowing us to access information in distributions in addition to total rates [22, 23]. Effective operators also let us combine Higgs data with results from other experiments, including electroweak precision data or gauge boson production at the LHC [24]. However, the limited precision of the LHC Higgs measurements means that only models that are either strongly coupled or relatively light can be probed. In the latter case, the characteristic energy scale of new physics is not sufficiently separated from the momentum transfers in the experiments, casting doubt on the validity of the EFT approach.

We analyse the usefulness of higher-dimensional operators at the LHC by comparing the predictions of UV-complete scenarios of new physics to their dimension-six approximations [2]. Our analysis covers additional scalar singlets, two-Higgs-doublet models, scalar top partners, and heavy vector bosons, focusing on parameter ranges that the LHC will be sensitive to. We take into account rates and distributions in the most important Higgs production modes and various representative decay channels as well as Higgs pair production. For this array of models, benchmark points, and observables, we ask if and where the effective description of new physics breaks down, and how it can be improved.

As it turns out, the agreement between the approaches crucially depends on the matching procedure that links the coefficients of the dimension-six model to the full theory. We introduce v-improved matching, a procedure that improves the performance of the dimension-six model by resumming certain terms that arise during electroweak symmetry breaking. While formally of

higher order in the EFT expansion, these effects can be large under LHC conditions. With such a matching, the effective model provides a good description even in many scenarios where the EFT validity is not obvious. We then discuss a number of practical questions on the role of squared dimension-six terms in the differential cross sections, effects on fits, and the correlation between different observables and the momentum transfer [3].

Having established that Higgs EFT works well as a largely model-independent language for Higgs physics at the LHC, the next question is how its parameters can be measured optimally. Higgs measurements are affected by many different operators, and each of them affects different couplings, often introducing non-trivial kinematic structures. This leads to a complicated relation between the high-dimensional model parameter space and often also high-dimensional phase spaces.

Traditional analyses based on selection cuts and histograms of kinematic observables are often not sensitive to such subtle signatures. At the other end of the spectrum, experiments resort more and more to high-level statistical tools, including machine learning techniques or the matrix element method [25–29]. Many of these tools are designed for the comparison between two discrete hypotheses, and applying them to high-dimensional parameter spaces such as Higgs EFT is computationally expensive. Extending machine learning techniques to such high-dimensional spaces is a current area of research [30]. These multivariate techniques are powerful, but can be non-transparent. It is therefore increasingly important to be able to characterise the information contained in LHC signatures.

We use information geometry to understand and optimise Higgs measurements [5]. The central building block is the Fisher information, which according to the Cramér-Rao bound encodes the maximal knowledge on theory parameters we can derive from an experiment. Unlike many other statistical tools, the Fisher information is intrinsically designed for continuous, high-dimensional parameter spaces, and this approach does not require any discretisation of the theory space and leads to results that do not depend on arbitrary parameter or basis choices. In addition, the Fisher information defines a metric on the model parameter space. This not only provides an intuitive geometric picture of the sensitivity of measurements, but also allows us to track the impact of higher orders in the EFT expansion.

We calculate the Fisher information for Higgs production in weak boson fusion with decays into tau pairs and four leptons, and for Higgs production in association with a single top quark. To this end, we develop an algorithm to calculate the Fisher information in particle-physics observables based on Monte-Carlo methods. Our results give the maximum precision with which dimension-six operators can be measured in these processes, or the maximal new physics reach of these signatures. We then analyse how the differential information is distributed over phase space, which defines optimal event selections. In a next step, we calculate the information in individual kinematic distributions, and compare it to the maximal information in the full event kinematics. This provides a ranking of the most powerful production and decay observables. It allows us to

compare how much we can learn from a simple fit to histograms compared to fully multivariate methods.

This is the first application of information geometry to high-energy physics. While there is no shortage of statistical tools in the field, these new methods can help to plan and optimise measurement strategies for high-dimensional continuous models in an intuitive but powerful way. While we demonstrate this approach in different Higgs channels for dimension-six operators, our tools can easily be translated to other processes and models.

This thesis begins by recapitulating some basic ideas of Higgs physics and effective field theory in Chapter 2. In Chapter 3, we discuss the validity of effective field theory for LHC measurements and the matching between full models and effective operators. Chapter 4 presents our work on information geometry and optimal Higgs measurements. Both of these chapters will contain separate and more detailed introductions and conclusions. We summarise the results in Chapter 5.

Chapter 2

Foundations

"It is known," Irri agreed.

— G. R. R. Martin [31]

In this chapter we review some of the essential concepts that underlie the research presented in the rest of this thesis. First, we briefly summarise the role of the Higgs boson in the Standard Model (SM) and its phenomenology at the LHC. Section 2.2 then presents a pedagogical introduction to the effective field theory (EFT) concept. In Section 2.3 we combine these ideas and introduce Standard Model effective field theory as a universal language for Higgs physics.

Our introduction to Higgs physics will be superficial, and the EFT part eschews mathematical rigour for a broad picture of the central ideas. For a more thorough introduction to Higgs physics, see for instance Reference [32]. For an extensive introduction to EFTs, see References [33, 34].

The EFT section is based on a lecture given by the author and largely identical to the lecture notes [6]. Some of the examples are taken from References [33, 34].

2.1 Higgs phenomenology recap

2.1.1 The Standard Model Higgs

In the Standard Model, the Higgs field appears as an $SU(2)$ doublet ϕ as

$$\begin{aligned}\mathcal{L}_{\text{SM}} \supset\ & (D^\mu \phi)^\dagger (D_\mu \phi) - \mu^2 \phi^\dagger \phi - \lambda (\phi^\dagger \phi)^2 \\ & - \sum_{\text{generations}} \left(y_u \begin{pmatrix} \bar{u} \\ \bar{d} \end{pmatrix}_L \tilde{\phi}\, u_R + y_d \begin{pmatrix} \bar{u} \\ \bar{d} \end{pmatrix}_L \phi\, d_R + y_\ell \begin{pmatrix} \bar{\nu} \\ \bar{\ell}^- \end{pmatrix}_L \phi\, \ell_R \right) \end{aligned} \tag{2.1}$$

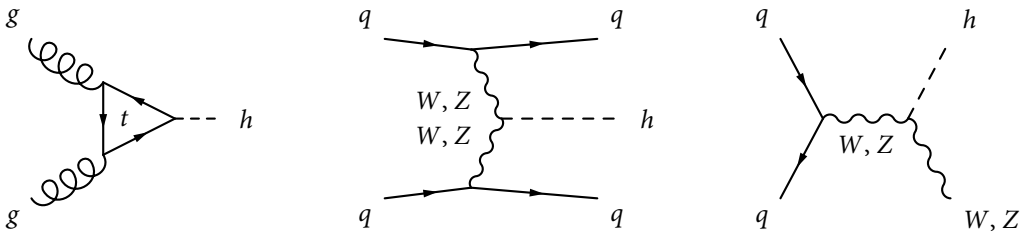

Figure 2.1: Feynman diagrams for the most important Higgs production modes considered in this thesis. Left: gluon fusion. Middle: weak boson fusion. Right: Higgs-strahlung.

with

$$D_\mu \phi = \left(\partial_\mu - \mathrm{i} g \frac{\sigma^a}{2} W_\mu^a - \mathrm{i} \frac{g'}{2} B_\mu \right) \phi \tag{2.2}$$

and $\tilde{\phi} = \mathrm{i}\tau_2 \phi^*$. For $\mu^2 < 0$, the Higgs doublet develops a non-zero vacuum expectation value (VEV)

$$v^2 \equiv 2 \left| \langle \phi \rangle \right|^2 = -\frac{\mu^2}{\lambda} \,. \tag{2.3}$$

Using some of the gauge freedom, we can rotate the Higgs field such that

$$\phi = \frac{1}{\sqrt{2}} \begin{pmatrix} -w_2 - \mathrm{i} w_1 \\ v + h + \mathrm{i} w_3 \end{pmatrix} , \tag{2.4}$$

where w_i are the would-be Goldstone bosons that give mass to the W and Z bosons, and h is the physical Higgs boson.

Plugging Equation (2.4) into Equation (2.1), we find the Higgs mass

$$m_h^2 = -2\mu^2 = 2\lambda v^2 \,. \tag{2.5}$$

The fermions and the massive vector bosons $W^\pm$ and Z get mass terms proportional to v, as well as couplings to the Higgs boson h. Since both terms stem from the same coupling to $\phi \sim v + h$, the Higgs couplings to other particles are always proportional to $g_{hxx} \sim m_x / v$. Finally, there are h^3 and h^4 self-couplings. The SM Higgs sector is very predictive: With the measurement of the Higgs mass $m_h = 125$ GeV [14, 15, 35], there are no more free parameters in the SM and all couplings are fixed.

2.1.2 Production and decay channels at the LHC

At the LHC, most Higgs bosons are produced in **gluon-gluon fusion** as shown in the left panel of Figure 2.1. Due to its large Yukawa coupling, the top plays the dominant role in the loop, with

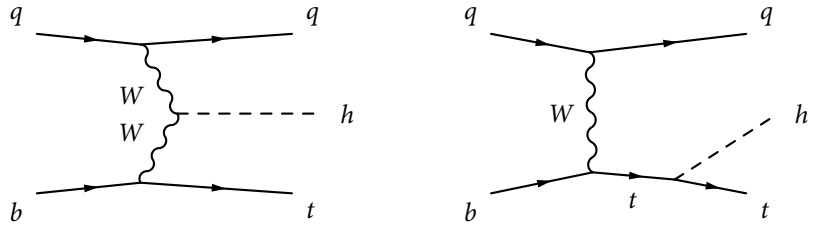

Figure 2.2: Feynman diagrams for Higgs production with a single top quark.

small contributions from the bottom. The total cross section at $\sqrt{s} = 13$ TeV is approximately 49 pb [4], a large part of which comes NLO and NNLO corrections. This sizeable rate comes at the price of a lack of discerning kinematic features that could help to separate the Higgs from backgrounds.

This is certainly different for Higgs production in **weak boson fusion** (WBF)[1], as shown in the middle panel of Figure 2.1. The production rate for this quark-initiated process is only 3.8 pb [4], but the Higgs is accompanied by two high-energetic jets that point nearly back-to-back in the two forward regions of the detector. This translates to a large invariant mass m_{jj} between them as well as a large separation in (pseudo-)rapidity $\Delta\eta_{jj}$. A second important property is provided by the colour structure of the process: at leading order, there is no colour exchange between the two quark lines, which means there is very little QCD radiation in this process. Both of these features set the WBF process apart from QCD backgrounds, which typically have many central jets. Backgrounds can therefore be reduced significantly by requiring two so-called "tagging jets" with large $\Delta\eta_{jj}$ and large m_{jj}, and vetoing any additional central jets [36].

But the tagging jets are not only useful to discriminate Higgs production from non-Higgs backgrounds. Since they recoil against the intermediate vector bosons that couple to the Higgs, they provide access to the momentum flow through the Higgs production vertex. Their properties, in particular their transverse momenta and the angular correlations between them, thus provide probes of the Higgs-gauge coupling. We will revisit this point from different perspectives, and tagging jet observables will play an important role throughout this thesis.

The right panel of Figure 2.1 shows Higgs production in association with a vector boson, or **Higgs-strahlung**. The rate is 1.4 pb for a Wh final state plus 0.9 pb for Zh. Similarly to the tagging jets in WBF, the final-state gauge boson both helps to discriminate the Higgs from backgrounds and provides a handle to access the momentum flow through the virtual intermediate vector boson.

We will also briefly analyse **Higgs production with a single top quark**. This process exists as an s-channel and a t-channel version with very different kinematic features, and can be calculated either in the four-flavour scheme (with a gluon in the initial state) or in the five-flavour scheme

[1] The common name Vector Boson Fusion (VBF) forgets that the gluon also has spin 1.

(with a b quark in the initial state). We will focus on the dominant t-channel process and calculate it in the five-flavour scheme, as shown in Figure 2.2. Diagrams where the Higgs is radiated off a top quark interfere destructively with amplitudes in which the Higgs couples to a W. The SM rate is small at 74 fb [4], but this interference pattern makes it very sensitive to changes in the top Yukawa coupling. This process is in fact the only direct probe of the sign or phase of the top Yukawa coupling ($t\bar{t}h$ production is only sensitive to the absolute value of the top Yukawa, while the total rate in gluon fusion can be influenced by many effects such as new particles in the loop).

Finally, we will take a look at **Higgs pair production** which provides a measurement of the Higgs self-coupling [37, 38], see Figure 2.3. It is another example of destructive interference between different amplitudes: diagrams in which the two Higgses couple to a top box loop interfere with those in which a single Higgs is produced in gluon fusion and then splits into two Higgses through the self-coupling. Close to threshold, these two contributions approximately cancel in the SM [37, 39], and the total rate is very small at 33 fb. Modified Higgs sectors can spoil this cancellation and increase the rate drastically.

The Higgs decay patterns are rather simple. Since it couples to all particles proportional to their mass, it prefers to decay into the heaviest particles allowed by phase space. The dominant decay mode with a branching ratio of 58% [4] are therefore $b\bar{b}$ pairs. This signature is clearly useless for Higgs bosons produced in gluon fusion because of the overwhelming QCD $gg \to b\bar{b}$ background. WBF and Vh production provide handles to tame these backgrounds, but the channel is still difficult. Easier to detect are $\tau^+\tau^-$ pairs with a branching ratio of 6.3%. Their semi-leptonic and purely leptonic decays involve neutrinos. But if the taus are boosted enough and not exactly back-to-back, the neutrino momentum can be reconstructed for instance using a collinear approximation [32].

The decays through W^+W^- or ZZ pairs into four-lepton final states are particularly important due to their clean signatures and because they provide access to Higgs-gauge couplings. Since the Higgs mass is below the W^+W^- and ZZ thresholds, one of the vectors has to be off-shell.[2]

[2] This also means that branching ratios for $h \to ZZ$ and $h \to WW$ are not really well-defined. What is often quoted is in fact a term like $\mathrm{BR}(h \to 4\ell)/(\mathrm{BR}(Z \to \ell^+\ell^-))^2$.

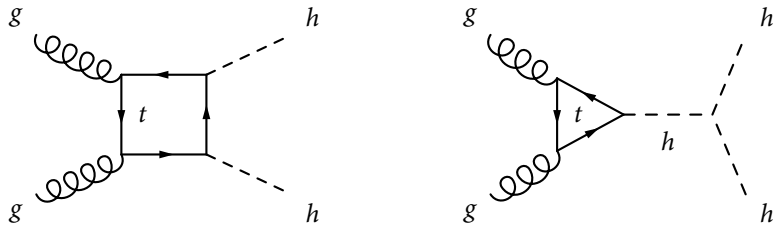

Figure 2.3: Feynman diagrams for Higgs pair production.

$h \to W^+W^- \to (\ell^+\nu)(\ell^-\bar{\nu})$ with $\ell = e, \mu$ has a respectable branching fraction of 1.1% [4], but comes with two neutrinos in the final state. Still, it is one of the most important channels to measure WBF Higgs production. The decay $h \to ZZ \to 4\ell$ with $\ell = e, \mu$ provides an extremely clean signal. Despite its small branching ratio of $1.3 \cdot 10^{-4}$, it was one of the main Higgs discovery channels [14, 35]. From a post-discovery perspective, its four leptons provide a rich spectrum of angular correlations and other observables that allow us to measure the Higgs behaviour in detail. We will discuss this feature in more detail later.

Finally, the small tree-level couplings of the Higgs to light particles mean that the loop-induced decay into photon pairs can compete with them. The dominant contribution comes from a W loop, which interferes destructively with the top loop, resulting in a branching ratio of 0.23% [4]. The ATLAS and CMS detectors are designed to reconstruct photons well, in fact with exactly this Higgs decay channel in mind. Together with $h \to 4\ell$ it constitutes the most important channel for the discovery.

2.1.3 How I Learned to Stop Worrying and Love the Higgs

There are several facets of the Higgs boson that make it special. From an experimental point of view, the properties of this shiny new thing in particle physics are still relatively unknown. Its couplings to vector bosons and heavy fermions are constrained at the $\mathcal{O}(10\%)$ level, while for the couplings to light fermions, invisible decays, and the total decay width of the Higgs there are only weak upper bounds [23, 35]. Many of these limits also rely on specific model assumptions. The top Yukawa coupling, for instance, is most strongly constrained from the total Higgs production rate, but only under the assumption that there no new physics plays a role in the gluon-fusion loop. The total Higgs width can be constrained indirectly from the contribution of $gg \to h \to ZZ \to 4\ell$ in the off-shell Higgs region, but again relying on strong model assumptions. All in all, the Higgs is still the least well measured elementary particle (in some sense with the exception of neutrinos), leaving plenty room for physics beyond the Standard Model.

From a theory perspective, there are several reasons to suspect manifestations of new physics in the Higgs sector. Starting with a rather general argument, the Higgs doublet is the key component of electroweak symmetry breaking (EWSB), which is often seen as the very core of the SM construction. A test of the Higgs properties therefore provides a test of the fundamental structure of Nature.

The Higgs boson is the only fundamental scalar discovered so far. This is interesting in its own right, but also leads to the famous electroweak **hierarchy problem**: in the absence of any protective symmetry, the mass of a scalar field should receive quantum corrections of the order of the largest scale in the theory. If the SM is valid all the way to the Planck scale, severe fine-tuning between the bare parameter and these quantum corrections is necessary to keep the electroweak mass scale at the observed value. Note that this argument interchangeably applies to the mass

parameter of the Higgs doublet μ^2, the physical Higgs mass m_h, or the electroweak VEV v. Since the strength of the weak force is suppressed by powers of $m_W \sim v$, and the gravitational force by the Planck scale, the hierarchy problem is often phrased in terms of the surprising weakness of gravity compared to the weak force. This naturalness problem is of a purely aesthetic nature, but similar aesthetic problems have in the past led to new insights. Many models have been proposed to solve the hierarchy by introducing a new symmetry that protects the Higgs mass against quantum corrections.[3] Famous examples are supersymmetry, composite Higgs models in which the Higgs is the pseudo-Goldstone boson of some broken symmetry, conformal symmetries [51], or extra dimensions. To reduce tuning to an acceptable level, this new physics should reside at energy scales not too far from the electroweak scale. These models usually modify the Higgs sector in a way that translates into Higgs couplings different from their SM values.

Citation needed for criticism of anthropic principle.

Another hierarchy unexplained in the SM is the large difference between the **fermion masses**. There are more than five orders of magnitude between the top and the electron mass, and neutrinos are even lighter. Since the fermion masses are generated by the Yukawa couplings of the Higgs doublet, models that explain the fermion masses will usually also shift the Higgs-fermion coupling patterns.

The question of **vacuum stability** is still being discussed. The renormalisation group (RG) allows us to link this question to the running the quartic coupling λ to higher energies. Current results [52] indicate that indeed the quartic coupling becomes negative at large energies, leading to a second vacuum with lower energy at much larger values of ϕ. Fortunately for us, the tunnelling probability is very small, and in the SM "our" vacuum with $v \approx 246$ GeV seems to be metastable with a lifetime longer than the age of the universe. While this indicates there is no pressing need for physics below the Planck scale to save the electroweak vacuum from a horrible fate, this result crucially depends on the measured top and Higgs masses, higher-order corrections to the beta functions, and higher-dimensional operators stemming from UV physics [53].

In addition to these theoretical and to some degree aesthetic arguments, there is solid experimental evidence for physics beyond the SM that might be linked to the Higgs sector. First, the nature of **dark matter** (DM) [54] is still unclear. It is experimentally established that this form of matter is electrically neutral, stable over cosmological timescales, clumps (i. e. is now

[3] An entirely different and somewhat metaphysical argument is based on the (weak) anthropic principle that observations of the universe are conditional upon its laws of physics allowing conscious life [40, 41]. First, this explanation requires some mechanism that generates many different vacua with different values of the physics parameters, including the Higgs mass. Most of these vacua will have "natural" parameters in which the weak and gravitational scales are comparable. String theory is hypothesised to provide such a sampling mechanism (the "multiverse"). Second, there has to be a reason why larger (and thus more abundant) values of the weak scale would not allow any type of intelligent life to form and make observations. This question is difficult to answer, and the jury is still out [42–48]. Given the speculative nature of the two questions, anthropic reasoning is being criticised as unverifiable or as based on arguments from lack of imagination. Some other models such as the relaxion [49] or Nnaturalness [50] modify the cosmological evolution such that a small Higgs mass is generated dynamically during inflation or reheating.

non-relativistic), and makes up roughly a fourth of the energy density of the universe. In many models DM is in thermal equilibrium with ordinary matter in the early universe. Interestingly, the observed dark matter density is in good agreement with electroweak-scale masses and weak couplings. This "WIMP miracle" is one main reason behind the popularity of weakly interacting massive particles (WIMPs) as DM candidates. In this scenario, good candidates for the mediator between dark matter and the SM are the Higgs boson or other scalars in an extended Higgs sector. Such "Higgs portal" scenarios often predict signatures in Higgs physics such as modified couplings or invisible Higgs decays.

Another mystery is the **matter-antimatter asymmetry** of the universe. Assuming that the cosmos was initially perfectly symmetric, the observed excess of matter can be generated dynamically if the three Sakharov conditions are satisfied: there have to be processes with baryon-number violation as well as C and CP violation, which take place out of thermal equilibrium. In the SM, these effects are too small to account for the observed asymmetry. Models that accommodate larger effects often affect the Higgs sector. In particular, extended Higgs sectors allow for electroweak symmetry breaking to be a strong first-order phase transition, providing the required out-of-equilibrium dynamics. Again, such scenarios predict signatures in Higgs measurements.

Finally, the Higgs could play another role in the cosmological evolution of the universe. The origin of the large-scale structure of the cosmos, the surprising isotropy of the cosmic microwave background (CMB), and the flatness of the Universe are all explained by an epoch of exponential expansion of space in the early universe called **inflation**. This process is often thought to be cause by a scalar field, the inflaton, slowly rolling down a potential of a certain shape. In principle the Higgs can be the inflaton, though this scenario of Higgs inflation requires unnaturally large couplings between the Higgs and the Ricci scalar, and requires a UV completion.

The null results of the LHC searches for new particles have led to some disappointment among particle physicists. But with the discovery of the Higgs boson, the LHC might not only have completed the SM particle zoo, but rather opened the door to the unknown. The Higgs boson is not just another SM particle. Some of the big open questions of fundamental physics are deeply rooted in the Higgs sector, and many other ideas can at least be linked to the Higgs sector under some assumptions. On the other hand, the current experimental precision leaves quite some room for signatures of new physics in Higgs observables. A precise determination of the Higgs properties might be one of the most exciting measurements at the LHC, and will hopefully improve our understanding of Nature significantly. Hopefully, the Higgs boson is not just the last puzzle piece of the Standard Model, but the first sign of what lies beyond.

2.2 The effective field theory idea

Check that all arguments of http://indico.cern.ch/event/477407/contributions/2200060/attachments/1369793/2076900/AM_HiggsCouplings2016.pdf are in this section. In particular slide 5.

This plethora of possible BSM models means that a model-independent universal theory framework is invaluable for TeV signatures of new physics. We will consider such a model based on the effective field theory (EFT) paradigm. Before discussing the specific realisation for Higgs physics in the next section, here we introduce the general EFT idea.

Effective field theories are a powerful tool that play a role in many, if not all, areas of physics. Whenever phenomena are spread out over different energy or length scales, an effective description can be valuable, either to simplify calculations, or to actually allow model-independent statements that would be impossible without such a framework.

2.2.1 Different physics at different scales

Our world behaves very differently depending on which energy and length scales we look at. At extremely high energies (or short distances), Nature might be described by a quantum theory of gravity. At energies of a few hundred GeV, the Standard Model is (disappointingly) in agreement with all measurements. Going to lower energies (or larger distances), we do not have to worry about Higgs or W bosons anymore: electromagnetic interactions are described by QED, weak interactions by Fermi theory, strong physics by QCD. Below a GeV, quarks and gluons are replaced by pions and nucleons as the relevant degrees of freedom. Then by nuclei, atoms, molecules. At this point most physicists give up and let chemists (and ultimately biologists and sociologists) analyse the systems.

The important point here is that the observables at one scale are not directly sensitive to the physics at significantly different scales. This is nothing new: for molecules to stick together, the details of the Higgs sector are not relevant, just as we can calculate how an apple falls from a tree without knowing about quantum gravity. To do physics at one scale, we do not have to (and often cannot) take into account the physics from all other scales. Instead, we isolate only those features that play a role at the scale of interest.

An effective field theory is a physics model that includes all effects relevant at a given scale, but not those that only play a role at significantly different scales. In particular, EFTs ignore spatial substructures much smaller than the lengths of interest, or effects at much higher energies than the energy scale of interest.

We will often use examples with one full or underlying theory and one effective theory. For simplicity, we pretend that the full theory describes physics correctly at all scales. The EFT is a simpler model than the full theory and neglects some phenomena (such as heavy particles) at energy scale Λ. However, it correctly describes the physics as long as the observables probe energy scales

$$E \ll \Lambda\,, \tag{2.6}$$

within some finite precision. This **scale hierarchy** between the energy of interest and the scale of high-energy physics not included in the EFT is the basic requirement for the EFT idea. A validity range (2.6) is a fundamental property of each EFT.

Fermi theory

The textbook example for an EFT is Fermi theory, which describes the charged current interactions between quarks (or hadrons), leptons and neutrinos at low energies. The underlying model here is the SM, in which this weak interaction is mediated by the exchange of virtual W bosons with mass m_W and coupling constant g:

$\mathcal{M}_{\text{full}} \sim$ 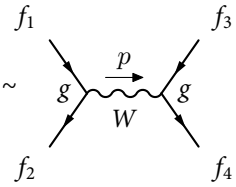

$\sim -\dfrac{g^2}{p^2 - m_W^2}$ (2.7)

In Fermi theory, there are no W bosons, just a direct interaction between four fermions with coupling constant $G_F \propto g^2/m_W^2$:

$\mathcal{M}_{\text{EFT}} \sim$ 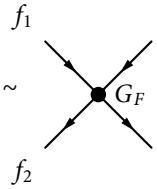

$\sim G_F \propto \dfrac{g^2}{m_W^2}$ (2.8)

So the EFT turns the W propagator into a contact interaction between the fermions, shrinking the distance bridged by the virtual W to zero. Clearly, the two amplitudes agree as long as the momentum transfer through the vertex is small, $E^2 = p^2 \ll \Lambda^2 = m_W^2$:

$$-\frac{g^2}{p^2 - m_W^2} = \frac{g^2}{m_W^2}\left(1 + \frac{p^2}{m_W^2} + \mathcal{O}\left(p^4/m_W^4\right)\right) \approx \frac{g^2}{m_W^2}\,. \tag{2.9}$$

One process described by this interaction is muon decay. Its typical energy scale $E \approx m_\mu$ is well separated from $\Lambda = m_W$, and Fermi theory will describe the process quite accurately. The relative **EFT error**, i. e. the mistake we make when calculating an observable with the EFT rather than with the full model, should be of order $\Delta_{\text{EFT}} = \Gamma_{\text{EFT}}/\Gamma_{\text{full}} \sim E^2/\Lambda^2 \sim m_\mu^2/m_W^2 \approx 10^{-6}$.

In proton collisions at the LHC the same interaction takes place, but at potentially much larger momentum transfer $E < 13$ TeV. The EFT error increases with E. For $E \gtrsim m_W$, the full model allows on-shell W production, a feature entirely missing in the EFT. Here the two descriptions obviously diverge and Fermi theory is no longer a valid approximation of the weak interaction.

Down and up the theory ladder

In reality there are of course more than two theories, and the notion of underlying and effective model becomes relative. The SM itself is not valid up to arbitrary large energies: it does not explain dark matter, the matter-antimatter asymmetry, or gravity. It is probably also internally inconsistent since at some very large energy the quartic coupling λ and the coupling constant g' hit Landau poles. So the SM is an effective theory with validity range $E \ll \Lambda \leq M_{Pl}$ and has to be replaced by some other description at larger energies. On the other hand, going to energies lower than a few GeV, the relevant physics changes again and we should switch to a new effective theory. In this way, all theories can be thought of as a series of EFTs, where the model valid at one scale is the underlying model for the effective theory at the next lower scale.

If you think you know a theory that describes our world at sufficiently large energies, then in principle there is no need to use effective theories: you can calculate every single observable in your full model (at least if the full model is perturbative at these energies or other approximations such as lattice calculations are available). This will however make hard calculations necessary even for the simplest low-energy processes. One can save a lot of computational effort and focus on the relevant physics by dividing the phase space into regions with different appropriate effective descriptions.

Starting from a high energy scale where the parameters of the fundamental theory are defined, these parameters are run to lower energies until the physics changes substantially. At this **matching scale** an effective theory is constructed from the full model, and its coefficients are determined from, or matched to, the underlying model. Then the coefficients of this EFT are run down to the next matching scale, where a new EFT is defined and its parameters are calculated, and so on. This is the **top-down** view of EFTs. For instance, we can start from the SM and construct Fermi theory as a simpler model valid at low energies. While we can certainly use the SM to calculate the muon lifetime, it is not necessary, and a calculation in Fermi theory is quite accurate and simpler.

But often we do not know the underlying theory. As mentioned above, there has to be physics beyond the SM, and there is still hope it will appear around a few TeV. If we want to parametrise the effects of such new physics on electroweak-scale observables, we do not know how the full model looks like. But even without knowing the underlying model, we can still construct an effective field theory based on a few very general assumptions. We will go through these ingredients in the next section. For this **bottom-up** approach, an effective theory is not only useful, but actually the only way we can discuss new physics without choosing a particular model of BSM physics.

High-energy physics can be seen as the field of working ourselves up a chain of EFTs to ever higher energies. But how does this chain end? Does it end at all? Even if we one day find a consistent theory that can explain all observations to date, how would we check if it indeed describes Nature up to arbitrarily high energies? Understanding all theories as effective, these questions do not matter! The EFT framework provides us with the tools to do physics without having to worry about the far ultraviolet.

2.2.2 EFT construction and the bottom-up approach

EFTs are especially useful in the framework of quantum field theory (QFT). Before showing how to construct the effective operators of such a theory in a bottom-up approach, let us recapitulate how QFTs are organised.

Reminder: operators and power counting

The basic object describing perturbative QFTs in $d = 4$ flat space-time dimensions is the action

$$S = \int \mathrm{d}^4x \, \mathcal{L}(x) \,. \tag{2.10}$$

The Lagrangian $\mathcal{L}(x)$ is a sum of couplings times operators, where the operators are combinations of fields and derivatives evaluated at one point x. These are either kinematic terms, mass terms or represent interactions between three or more fields. For instance, the Lagrangian

$$\mathcal{L} = \mathrm{i}\bar{\psi}_i \gamma^\mu \partial_\mu \psi_i - \frac{1}{4} V_{\mu\nu} V^{\mu\nu} - m_i \bar{\psi}_i \psi_i + m_V^2 V_\mu V^\mu - g \bar{\psi}_i \gamma_\mu \psi_i V^\mu \tag{2.11}$$

with implicit sum over i describes fermions ψ_i, a massive vector boson V_μ, and an interaction between them with coupling g.[4]

A key property of each coupling or operator is its **canonical dimension** or mass dimension. In simple terms this can be formulated as the following question: if you assign a value to a quantity, which power of a mass unit such as GeV would this value carry? Since we work in units with $\hbar = c = 1$, length and distance dimensions are just the inverse of mass dimensions. We will denote the mass dimension of any object with squared brackets, where $[\mathcal{O}] = D$ means that $\mathcal{O}$ is of dimension mass^D, or mass dimension D.

In QFT, the action can appear in exponentials such as $e^{\mathrm{i}S}$, so it must be dimensionless: $[S] = 0$. The space-time integral in Equation (2.10) then implies $[\mathcal{L}] = d = 4$, so every term in the Lagrangian has to be of mass dimension 4. Applying this to the kinetic terms, we can calculate the mass dimension of all fields. This then allows us to calculate the mass dimension or canonical dimension of operators and couplings in the theory.

In the example in Equation (2.11), the kinetic term for the fermions contains one space-time derivative, $[\partial] = 1$. To get $[\bar{\psi}\partial\psi] = 4$, the fermion fields must have dimension $[\psi_i] = 3/2$. Similarly, the field strength $V_{\mu\nu}$ contains a derivative, so we end up with $[V_\mu] = 1$. With these numbers we can check the other operators. In addition to the expected $[m] = [m_V] = 1$, we find $[\bar{\psi}\psi V^\mu] = 4$ or $[g] = 0$.

The canonical dimension of an operator has two important consequences. First, the renormalisation group flow of a theory, i. e. the running of the couplings between different energy scales,

[4] Massive vector bosons have issues with renormalisability and unitarity, which can be solved by generating the mass in a Higgs mechanism at a higher scale, but this irrelevant for the discussion here.

largely depends on the mass dimensions of the operators. Operators with mass dimension $D < d$ ("relevant" operators) receive large quantum corrections when going from large energies to low energies. This is a key argument for many fine-tuning problems such as the hierarchy problem or the cosmological constant problem. On the other hand, operators with $D > d$ ("irrelevant" ones) are typically suppressed when going to lower energies. Operators with $D = d$ are called "marginal".

The second consequence of the mass dimension affects the renormalisability of a theory. Theories with operators with $D > d$ are **non-renormalisable**:[5] particles in loops with energies $E \to \infty$ will lead to infinities in observables, and they are too many to be hidden in a renormalisation of the parameters.

Effective operators

From now on we will only consider EFTs realised as a local QFT in 4 space-time dimensions, an approach that has proven very successful in high-energy physics so far. EFTs are then defined as a sum of operators $\mathcal{O}_i$, each with a specific canonical dimension D_i. We can split the coupling in front of each operator into a dimensionless constant, the **Wilson coefficient** f_i, and some powers of a mass scale, for which we use the scale of heavy physics Λ:

$$\mathcal{L}_{\text{EFT}} = (\text{kinetic and mass terms}) + \sum_i \frac{f_i}{\Lambda^{D_i - d}} \mathcal{O}_i \,. \tag{2.12}$$

Why do we force Λ to appear in front of the operators like this? If we do not know anything about the underlying model at scale Λ, our best guess (which can be motivated with arguments based on the renormalisation group flow) is that it consists of dimensionless couplings $g \sim \mathcal{O}(1)$ and mass scales $M \sim \mathcal{O}(\Lambda)$. Indirect effects mediated by this high-energy physics should therefore be proportional to a combination of these factors, as given in Equation (2.12) with couplings $f_i \sim \mathcal{O}(1)$. This is certainly true in Fermi theory, where the effective coupling G_F is suppressed by $\Lambda^2 = m_W^2$.

Ingredients

How the operators $\mathcal{O}_i$ look like might be clear in a top-down situation where we know the underlying theory. In a bottom-up approach, however, we need a recipe to construct a list of operators in a model-independent way. It turns out that this is surprisingly straightforward, and the list of operators we need to include in the EFT is defined by three ingredients: the particle content, the symmetries, and a counting scheme that decides which operators are relevant at the scale of interest. We will go through them one by one.

[5] The opposite is not true: some theories contain only operators with $D \leq d$, but are still not renormalisable.

1. **Particle content**: one has to define the fields that are the dynamical degrees of freedoms in the EFT, i. e. that can form either external legs or internal propagators in Feynman diagrams. At least all particles with masses $m \ll \Lambda$ should be included. The operators are then combinations of these fields and derivatives.
2. **Symmetries**: some symmetry properties of the world have been measured with high precision, and we can expect that a violation of these symmetries has to be extremely small or happens at very high energies. These can be gauge symmetries (such as the $SU(3) \times SU(2) \times U(1)$ of the SM), space-time symmetries (such as Lorentz symmetry), or other global symmetries (such as flavour symmetries). Requiring that the effective operators do not violate these symmetries is well motivated and can reduce the complexity of the theory significantly.
3. **Counting scheme**: with a set of particles and some symmetry requirements we can construct an infinite tower of different operators. We therefore need some rule to decide which of the operators we can neglect. Here the dimensionality of the operators becomes important. As argued above, we expect an operator with canonical dimension $D > d$ to be suppressed by a factor of roughly $1/\Lambda^{D-d}$. Operators of higher mass dimension are therefore more strongly suppressed. Setting a maximal operator dimension is thus a way of limiting the EFT to a finite number of operators that should include the leading effects at energies $E \ll \Lambda$.

One property that is often required of theories is missing in this list: an EFT (with its intrinsic UV cutoff Λ) does not have to be renormalisable in the traditional sense. In fact, most EFTs include operators with mass dimension $D > d$ and are thus non-renormalisable. However, EFTs are still renormalisable order by order in the counting scheme, and loop effects can be calculated without any fundamental issues.

Basis choices

Usually not all operators that can be constructed in this way are independent. This can be seen from a field redefinition of the form

$$\phi(x) \to \phi'(x) = \phi(x) + \varepsilon f(x) \tag{2.13}$$

where ε is some small parameter and $f(x)$ can contain any combination of fields evaluated at x. The action in terms of the new field is then (after integration by parts)

$$\int \mathrm{d}^4x\, \mathcal{L}[\phi] \to \int \mathrm{d}^4x\, \mathcal{L}[\phi'] = \int \mathrm{d}^4x \left(\mathcal{L}[\phi] + \varepsilon \left[\frac{\delta \mathcal{L}}{\delta \phi} - \partial_\mu \frac{\delta \mathcal{L}}{\delta \partial_\mu \phi} \right] f + \mathcal{O}\left(\varepsilon^2\right) \right). \tag{2.14}$$

Such a transformation does not change the physics, i. e. the S-matrix elements [55–58], so we can equivalently use the new action instead of the original one. In this way, each equation of motion

provides us with a degree of freedom to swap operators for a combination of other operators. Similarly, Fierz identities and integration by parts can be used to manipulate the form of operators. Together these tools reduces the number of operators and coefficients necessary in an EFT basis, and lead to some freedom to choose which operators to work with.

Why is the sky blue?

Following Reference [34], we will demonstrate this bottom-up approach with a simple question: why is the sky blue? In other words, why is blue light coming from the sun scattered more strongly by particles in the atmosphere than red light? A full derivation of this takes some time and requires knowledge of the underlying electrodynamic interactions. Instead, we will write down an effective field theory for this process of Rayleigh scattering. The only thing we have to know are the basic scales of the process: photons with energy E_γ scatter off basically static nuclei characterised by an excitation energy ΔE, mass M and radius a_0. Looking at these numbers, we see that these scales are clearly separated:

$$E_\gamma \ll \Delta E, a_0^{-1} \ll M\,. \tag{2.15}$$

This is good news, since such a scale hierarchy is the basic requirement for an EFT. We are interested in elastic scattering, so we set the cutoff of the EFT as[6]

$$\Lambda \sim \Delta E, a_0^{-1}\,. \tag{2.16}$$

With this we can put together the building blocks for our EFT as discussed above:

1. As fields we will need photons and atoms, where we can approximate the latter as infinitely heavy.
2. The relevant symmetries are the $U(1)_{em}$ and Lorentz invariance. At these energies we will also not be able to create or destroy atoms, which you can see as another symmetry requirement on the effective Lagrangian.
3. We will include the lowest-dimensional operators that describe photon-atom scattering.

The kinetic part of such an EFT reads

$$\mathcal{L}_{\text{kin}} = \phi_v^\dagger \mathrm{i} v^\alpha \partial_\alpha \phi_v - \frac{1}{4} F_{\mu\nu} F^{\mu\nu}\,, \tag{2.17}$$

where ϕ_v is the field operator representing an infinitely heavy atom at constant velocity v, and $F_{\mu\nu}$ is the photon field strength tensor. Boosting into the atom's rest frame, $v = (1,0,0,0)$ and the first term becomes the Lagrangian of the Schrödinger equation.

[6] In reality there are two orders of magnitude between ΔE and a_0^{-1}, but this does not affect the line of argument at all and we choose to ignore this fact.

The usual power counting based on $[\mathcal{L}] = 4$ gives the mass dimensions

$$[\partial] = 1\,, \quad [v] = 0\,, \quad [\phi] = \frac{3}{2} \quad \text{and} \quad [F_{\mu\nu}] = 2\,. \tag{2.18}$$

The interaction operators must be Lorentz-invariant combinations of $\phi^\dagger\phi$, $F_{\mu\nu}$, v_μ, and ∂_μ. Note that operators directly involving A_μ instead of $F_{\mu\nu}$ are forbidden by gauge invariance, and single instances of ϕ correspond to the creation or annihilation of atoms which is not possible at these energies. The first such operators appear at mass dimension 7,

$$\mathcal{L}_{\text{int}} = \frac{f_1}{\Lambda^3}\phi_v^\dagger\phi_v F_{\mu\nu}F^{\mu\nu} + \frac{f_2}{\Lambda^3}\phi_v^\dagger\phi_v v^\alpha F_{\alpha\mu}v_\beta F^{\beta\mu} + \mathcal{O}\big(1/\Lambda^4\big)\,, \tag{2.19}$$

and we expect them to contain the dominant effects of Rayleigh scattering at energies $E_\gamma \ll \Lambda$.

The scattering amplitude of light off the atmospheric atoms should therefore scale as $\mathcal{M} \sim 1/\Lambda^3$, which means that the cross section scales with $\sigma \sim 1/\Lambda^6$. Since the cross section has the dimension of an area, $[\sigma] = -2$, and the only other mass scale in this low-energy process is the photon energy E_γ, we know that the effective cross section must be proportional to

$$\sigma \propto \frac{E_\gamma^4}{\Lambda^6}\big(1 + \mathcal{O}\big(E_\gamma/\Lambda\big)\big)\,. \tag{2.20}$$

In other words, blue light is much more strongly scattered than red light. Our effective theory, built just from a few simple assumptions, explains the colour of the sky!

Finally, we should check the validity range of our EFT. We expect it to work as long as

$$E_\gamma \ll \Lambda \sim \Delta E \sim \mathcal{O}(\text{eV}) \tag{2.21}$$

which is equivalent to wavelengths above $\mathcal{O}(100\,\text{nm})$. Our approximation is probably safe for visible light! In the near ultraviolet we expect deviations from the E_γ^4 proportionality and our EFT to break down.

2.2.3 Top-down approach and matching

In the top-down approach to effective field theories, we start from a known model of UV physics and calculate the corresponding effective operators and Wilson coefficients in the EFT. The defining criterion of this **matching procedure** is that at low energies the effective and underlying descriptions agree, at least up to a given order in the loop expansion (e. g. in α_s) and up to a given order in the EFT expansion in $1/\Lambda$.

This can be achieved either by functional methods or with Feynman diagrams. Here we will sketch the conceptual foundation involving functional methods, before arriving at a simple diagrammatic method. Note that the matching cannot be reversed: one cannot uniquely reconstruct a full theory only based on the EFT. Details of the matching procedure will play a crucial role in Chapter 3.

The effective action

The central object that allows us to systematically analyse the low-energy effects of heavy physics is the effective action S_{eff}. Following Reference [59, 60], we now outline its calculation at the one-loop level. Note that this is just a conceptual sketch and not mathematically rigorous, and that we omit higher-order terms irrelevant for this thesis as well as certain cases of mixed loops with light and heavy particles [61]. For a more thorough derivation see the quantum field theory textbook of your choice.

For simplicity, let us assume that our theory $S[\phi, \Phi]$ consists of light particles ϕ and a heavy scalar Φ that should not be part of the effective theory as dynamical degree of freedom. The effective action is calculated by **integrating out** the heavy particles from the partition function,

$$e^{iS_{\text{eff}}[\phi]} = \int \mathcal{D}\Phi \, e^{iS[\phi,\Phi]} \,. \tag{2.22}$$

While the path integral over the heavy fields is computed, the light fields are kept fixed as "background fields".

The effective action can be calculated with a saddle-point approximation. For this we expand Φ around its classical value Φ_c:

$$\Phi(x) = \Phi_c(x) + \eta(x) \,. \tag{2.23}$$

Φ_c is defined by the classical equation of motion

$$\left.\frac{\delta S[\phi,\Phi]}{\delta\Phi}\right|_{\Phi=\Phi_c} = 0 \,, \tag{2.24}$$

so expanding the action around this extremum leads to

$$S[\phi, \Phi_c + \eta] = S[\phi, \Phi_c] + \frac{1}{2} \left.\frac{\delta^2 S[\phi,\Phi]}{\delta\Phi^2}\right|_{\Phi=\Phi_c} \eta^2 + \mathcal{O}\left(\eta^3\right) \,. \tag{2.25}$$

Plugging this into Equation (2.22), we find

$$e^{iS_{\text{eff}}[\phi]} \approx e^{iS[\phi,\Phi_c]} \int \mathcal{D}\eta \, \exp\left(\frac{1}{2} \left.\frac{\delta^2 S[\phi,\Phi]}{\delta\Phi^2}\right|_{\Phi=\Phi_c} \eta^2\right) \,. \tag{2.26}$$

The last term is a Gaussian integral with a known solution,

$$e^{iS_{\text{eff}}[\phi]} \approx e^{iS[\phi,\Phi_c]} \left[\det\left(-\left.\frac{\delta^2 S}{\delta\Phi^2}\right|_{\Phi=\Phi_c}\right)\right]^{-1/2} \tag{2.27}$$

and finally

$$S_{\text{eff}}[\phi] \approx S[\phi, \Phi_c] + \frac{\mathrm{i}}{2} \operatorname{tr} \log \left(- \left. \frac{\delta^2 S}{\delta \Phi^2} \right|_{\Phi=\Phi_c} \right) , \tag{2.28}$$

where the functional trace is defined as an integral over momentum space k together with a sum over internal states i such as spin or flavour,

$$\operatorname{tr} x \equiv \sum_i \int \frac{\mathrm{d}^4 k}{(2\pi)^4} \, \langle k, i | x | k, i \rangle \, . \tag{2.29}$$

This result can be directly evaluated with functional methods. The first term in Equation (2.28) can be easily calculated by solving the classical equations of motions in Equation (2.24). Computing the functional trace is more involved, but can be simplified with a procedure called **covariant derivative expansion** [59, 62, 63]. Universal results that can be adapted to many scenarios are available in the literature [60, 61, 64].

The effective action is in general non-local, visible as (covariant) derivatives D appearing in the denominator (formally defined as Green's functions). We expand these terms schematically as

$$\phi^\dagger \frac{1}{D^2 - M^2} \phi = -\phi^\dagger \frac{1}{M^2} \left[1 + \frac{D^2}{M^2} \right] \phi + \mathcal{O}\left(1/M^6\right) , \tag{2.30}$$

so that only a rest term of higher order in $1/\Lambda = 1/M$ remains non-local [61]. In a last step, we truncate the resulting tower of operators at some order in our counting scheme, in our case in the expansion in $1/\Lambda$. The resulting effective theory consists of a finite set of local operators up to some order in a counting scheme, compatible with our definition of effective theories in the previous section. Unlike in the bottom-up approach, not all operators have to appear, and we can calculate the Wilson coefficients based on the underlying theory.

Scalar example

As a simple example consider a theory of two real scalar fields. The light field ϕ has mass m, the heavy field Φ with mass M will be integrated out. The underlying theory is given by

$$\begin{aligned} S[\phi, \Phi] = \int \mathrm{d}^4 x \Bigg[& \frac{1}{2} \partial_\mu \phi \partial^\mu \phi - \frac{m^2}{2} \phi^2 + \frac{1}{2} \partial_\mu \Phi \partial^\mu \Phi - \frac{M^2}{2} \Phi^2 \\ & - \frac{\lambda_0}{4!} \phi^4 - \frac{\lambda_2}{4} \phi^2 \Phi^2 - \frac{\lambda_4}{4!} \Phi^4 \Bigg] . \end{aligned} \tag{2.31}$$

Odd interactions and a mixing term $\phi\Phi$ are forbidden with suitable $\mathbb{Z}_2$ symmetries.

The classical equation of motion for Φ is

$$\left(\partial^2 + M^2 + \frac{\lambda_2}{2}\phi^2 + \frac{\lambda_4}{3!}\Phi_c^2\right)\Phi_c = 0 \tag{2.32}$$

with the trivial solution $\Phi_c = 0$.

The first term in the effective action then just gives back ϕ^4 theory for the light field, without any new effective interactions:

$$S[\phi, \Phi_c] = \int \mathrm{d}^4x \left[\frac{1}{2}\partial_\mu\phi\partial^\mu\phi - \frac{m^2}{2}\phi^2 - \frac{\lambda_0}{4!}\phi^4\right]. \tag{2.33}$$

The second term is

$$\begin{aligned}\frac{\mathrm{i}}{2}\operatorname{tr}\log\left(-\left.\frac{\delta^2 S}{\delta\Phi^2}\right|_{\Phi=\Phi_c}\right) &= \frac{\mathrm{i}}{2}\operatorname{tr}\log\left(\partial^2 + M^2 + \frac{\lambda_2}{2}\phi^2\right)\\ &= \frac{\mathrm{i}}{2}\operatorname{tr}\log\left(\partial^2 + M^2\right) + \frac{\mathrm{i}}{2}\operatorname{tr}\log\left(1 + \frac{\lambda_2}{2}\frac{1}{\partial^2 + M^2 + \mathrm{i}\varepsilon}\phi^2\right),\end{aligned} \tag{2.34}$$

where derivatives in the denominator are defined as Green's functions. Since $\operatorname{tr}\log\left(\partial^2 + M^2\right)$ is just a constant that can be calculated for instance in dimensional regularisation, the first part does not give us any higher-dimensional operators of the light fields ϕ. Expanding the logarithm in the second term, we find

$$S_{\text{eff}} \supset \frac{\mathrm{i}\lambda_2}{4}\operatorname{tr}\frac{1}{\partial^2 + M^2 - \mathrm{i}\varepsilon}\phi^2 - \frac{\mathrm{i}\lambda_2^2}{8}\operatorname{tr}\left(\frac{1}{\partial^2 + M^2 - \mathrm{i}\varepsilon}\phi^2\right)^2 + \frac{\mathrm{i}\lambda_2^3}{12}\operatorname{tr}\left(\frac{1}{\partial^2 + M^2 - \mathrm{i}\varepsilon}\phi^2\right)^3 + \mathcal{O}\left(\lambda_2^4\right). \tag{2.35}$$

The first of these terms will renormalise the ϕ mass term, and the second will contribute to the ϕ^4 interaction. This is important for RG running, but will not create the kind of new effective interactions we are interested in here. We instead focus on the last term and evaluate the functional trace:

$$\begin{aligned}S_{\text{eff}} &\supset -\frac{\mathrm{i}\lambda_2^3}{12}\int\frac{\mathrm{d}^4k}{(2\pi)^4}\ \langle k|\left(\frac{1}{\partial^2 + M^2 - \mathrm{i}\varepsilon}\phi^2\right)^3|k\rangle\\ &\supset -\frac{\mathrm{i}\lambda_2^3}{12}\int\mathrm{d}^4x\int\mathrm{d}^4y\int\mathrm{d}^4z\int\frac{\mathrm{d}^4k}{(2\pi)^4}\int\frac{\mathrm{d}^4p}{(2\pi)^4}\int\frac{\mathrm{d}^4q}{(2\pi)^4}\ \langle k|\frac{1}{\partial^2 + M^2 - \mathrm{i}\varepsilon}|x\rangle\langle x|\phi^2|p\rangle\\ &\quad\times\langle p|\frac{1}{\partial^2 + M^2 - \mathrm{i}\varepsilon}|y\rangle\langle y|\phi^2|q\rangle\langle q|\frac{1}{\partial^2 + M^2 - \mathrm{i}\varepsilon}|z\rangle\langle z|\phi^2|k\rangle.\end{aligned} \tag{2.36}$$

Here we have used the definition of the functional trace in Equation (2.29) and inserted unity, $1 = \int\mathrm{d}^4x\ |x\rangle\langle x| = \int\frac{\mathrm{d}^4p}{(2\pi)^4}\ |p\rangle\langle p|$. $|k\rangle$, $|p\rangle$, and $|q\rangle$ are eigenstates of the derivative operator

∂, i. e. $\langle k|\, \mathrm{i}\partial_\mu = \langle k|\, k_\mu$, while $|x\rangle$, $|y\rangle$, and $|z\rangle$ denote the eigenstates of local operators, $\langle x|\, \phi^2 = \langle x|\, \phi^2(x)$. Their inner product is $\langle x|k\rangle = e^{-\mathrm{i}kx}$. Using these properties and shifting the integration variables, we get

$$\begin{aligned} S_{\text{eff}} \supset & -\frac{\mathrm{i}\lambda_2^3}{12} \int \mathrm{d}^4x \int \mathrm{d}^4y \int \mathrm{d}^4z \int \frac{\mathrm{d}^4k}{(2\pi)^4} \int \frac{\mathrm{d}^4p}{(2\pi)^4} \int \frac{\mathrm{d}^4q}{(2\pi)^4}\, \frac{1}{-k^2+M^2-\mathrm{i}\varepsilon} e^{\mathrm{i}kx} \phi(x)^2 e^{-\mathrm{i}px} \\ & \times \frac{1}{-p^2+M^2-\mathrm{i}\varepsilon} e^{\mathrm{i}py} \phi(y)^2 e^{-\mathrm{i}(p+Q)y}\, \frac{1}{-q^2+M^2-\mathrm{i}\varepsilon} e^{\mathrm{i}qz} \phi(z)^2 e^{-\mathrm{i}kz} \\ \supset & \frac{\mathrm{i}\lambda_2^3}{12} \int \mathrm{d}^4x \int \mathrm{d}^4y \int \mathrm{d}^4z \int \frac{\mathrm{d}^4k}{(2\pi)^4} \int \frac{\mathrm{d}^4p}{(2\pi)^4} \int \frac{\mathrm{d}^4q}{(2\pi)^4}\, \phi(x)^2 \phi(y)^2 \phi(z)^2 \\ & \times \frac{e^{\mathrm{i}p(z-x)}\, e^{\mathrm{i}q(z-y)}}{(k^2-M^2+\mathrm{i}\varepsilon)\left((k+p)^2-M^2+\mathrm{i}\varepsilon\right)\left((k+p+q)^2-M^2+\mathrm{i}\varepsilon\right)}\,. \end{aligned} \tag{2.37}$$

We can now perform the integral over the loop momentum k with Feynman parameters:

$$\begin{aligned} T_3(p,q) &\equiv \int \frac{\mathrm{d}^4k}{(2\pi)^4}\, \frac{1}{(k^2-M^2+\mathrm{i}\varepsilon)\left((k+p)^2-M^2+\mathrm{i}\varepsilon\right)\left((k+p+q)^2-M^2+\mathrm{i}\varepsilon\right)} \\ &= 2\int_0^1 \mathrm{d}x \int_0^{1-x} \mathrm{d}y \int \frac{\mathrm{d}^4k}{(2\pi)^4} \Big[x(k^2-M^2+\mathrm{i}\varepsilon) + y((k+p)^2-M^2+\mathrm{i}\varepsilon) \\ &\qquad + (1-x-y)((k+p+q)^2-M^2+\mathrm{i}\varepsilon)\Big]^{-3} \\ &= 2\int_0^1 \mathrm{d}x \int_0^{1-x} \mathrm{d}y \int \frac{\mathrm{d}^4k}{(2\pi)^4}\, \frac{1}{\left[(k+a)^2-B+\mathrm{i}\varepsilon\right]^3} \end{aligned} \tag{2.38}$$

with $a = (1-x)p + (1-x-y)q$ and $B = M^2 - (1-x-y)(p+q)^2 - yp^2 + a^2$. Shifting the loop momentum as $k \to k+a$, we finally arrive at

$$T_3(p,q) = 2\int_0^1 \mathrm{d}x \int_0^{1-x} \mathrm{d}y \int \frac{\mathrm{d}^4k}{(2\pi)^4}\, \frac{1}{\left[k^2-B+\mathrm{i}\varepsilon\right]^3}\,. \tag{2.39}$$

To evaluate this, we first Wick-rotate $k^0 = \mathrm{i}k_E^0$. Formally, this means shifting the integration path in the complex plane of k^0 from along the real axis to along the imaginary axis. The Cauchy theorem assures that this does not change the value of the integral as long as we chose the contour such that the poles are not caught between the two contours. Defining $k_E^2 = (k_E^0)^2 + \boldsymbol{k}^2 = -k^2$, we find

$$I_{0,3} \equiv \int \frac{\mathrm{d}^4k}{(2\pi)^4}\, \frac{1}{\left[k^2-B+\mathrm{i}\varepsilon\right]^3} = \mathrm{i}\int \frac{\mathrm{d}^4k_E}{(2\pi)^4}\, \frac{1}{\left[-k_E^2-B\right]^3}\,, \tag{2.40}$$

where the $+\mathrm{i}\varepsilon$ is no longer necessary. With $\bar{k} = |k_E|$ we can finally calculate the integral:

$$I_{0,3} = \frac{2\pi^2}{(2\pi)^4} \int \mathrm{d}\bar{k}\bar{k}^3\, \frac{1}{\left[\bar{k}^2+B\right]^3} = \frac{-\mathrm{i}}{32\pi^2 B}\,. \tag{2.41}$$

Collecting all the pieces, we have

$$S_{\text{eff}} \supset \frac{\lambda_2^3}{192\pi^2} \int \mathrm{d}^4x \int \mathrm{d}^4y \int \mathrm{d}^4z\, \phi(x)^2\phi(y)^2\phi(z)^2 \int \frac{\mathrm{d}^4p}{(2\pi)^4} \int \frac{\mathrm{d}^4q}{(2\pi)^4}\, e^{\mathrm{i}p(z-x)}\, e^{\mathrm{i}q(y-z)} \times \int_0^1 \mathrm{d}x \int_0^{1-x} \mathrm{d}y \left[M^2 - (1-x-y)(p+q)^2 - yp^2 + ((1-x)p + (1-x-y)q)^2\right]^{-1} . \tag{2.42}$$

At first glance, this is disappointing: this effective action looks non-local and involves highly non-trivial integrals. It turns out that these can in fact be calculated and give a finite result [65, 66]. The full expression is extremely ugly. Fortunately, we do not need it. Instead, we expand the integrand in powers of $1/M^2$. We will only calculate the leading term at $\mathcal{O}\left(1/M^2\right)$. We will show that it produces a finite result as well, so the rest term at $\mathcal{O}\left(1/M^4\right)$ also has to be finite. Even more, we can argue that the rest term at $\mathcal{O}\left(1/M^4\right)$ has to vanish: the coefficient at a given order $1/M^k$ in this expansion is an integral without any mass scales, and has to lead to a result of mass dimension $k-2$. Only $k=2$ can give a non-zero and finite result, all higher orders therefore have to vanish. In this way, we find the much simpler result

Just like the dear proof reader…

Something is fishy. Check this argument, and check discrepancy with Denner's habil!

$$\begin{aligned} S_{\text{eff}} &\supset \frac{\lambda_2^3}{384\pi^2 M^2} \int \mathrm{d}^4x \int \mathrm{d}^4y \int \mathrm{d}^4z\, \phi(x)^2\phi(y)^2\phi(z)^2 \int \frac{\mathrm{d}^4p}{(2\pi)^4} \int \frac{\mathrm{d}^4q}{(2\pi)^4}\, e^{\mathrm{i}p(z-x)} e^{\mathrm{i}q(y-z)} \\ &\qquad + \mathcal{O}\left(1/M^4\right) \\ &\supset \frac{\lambda_2^3}{384\pi^2 M^2} \int \mathrm{d}^4x \int \mathrm{d}^4y \int \mathrm{d}^4z\, \phi(x)^2\phi(y)^2\phi(z)^2\, \delta(z-x)\delta(y-z) \\ &\supset \frac{\lambda_2^3}{384\pi^2 M^2} \int \mathrm{d}^4x\, \phi(x)^6 . \end{aligned} \tag{2.43}$$

After the expansion in $1/M$, we have finally arrived at a local theory!

What about the higher terns in Equation (2.35)? Their calculation is analogous to the one presented here and will lead to operators like ϕ^8 and higher. They will be suppressed at least with $1/M^4$ and are thus irrelevant for our dimension-six effective theory.

Collecting the pieces in Equation (2.33) and Equation (2.43), up to one loop and $\mathcal{O}\left(1/M^2\right)$ the full effective action is given by

$$S_{\text{eff}}[\phi] = \int \mathrm{d}^4x \left[\frac{1}{2}\partial_\mu\phi\partial^\mu\phi - \frac{m^2}{2}\phi^2 - \frac{\lambda_0}{4!}\phi^4 + \frac{\lambda_2^3}{384\pi^2M^2}\phi^6\right] . \tag{2.44}$$

As expected, the dimension-six operator is suppressed by two powers of the heavy scale $\Lambda \equiv M$, and the Wilson coefficient consists of the couplings λ_2^3 times a loop factor.

Diagrammatic matching

As an alternative to this functional approach, the effective action in Equation (2.28) can be calculated in an intuitive diagrammatic way. Since the light fields are kept fixed in Equation (2.22),

the effective action is given by all connected Feynman diagrams with only ϕ as external legs and only Φ fields as internal propagators. A more rigorous derivation than the one in the precious section in fact reveals that also certain connected loop diagrams with only ϕ as external legs and both Φ and ϕ fields as internal propagators contribute if they cannot be disconnected by cutting a single internal ϕ line [61]. The first term in Equation (2.28) corresponds to all such tree-level diagrams, the second term describes one-loop pieces. Higher-loop corrections will play no role in this thesis and were left out.

In practice, the effective operators and their Wilson coefficients can be calculated without the need for any functional methods as follows:

1. Start with the particle content of the full model. Choose Λ and divide the particles of the full model into light and heavy fields. Light fields, which should include at least those with masses below Λ, will make up the particle content of the effective theory. Heavy fields will be integrated out, that is, removed as dynamical degrees of freedom in the EFT.
2. Based on the particles and interactions of the full model, draw all connected Feynman diagrams in which
   - all external legs are light fields, and
   - that cannot be disconnected by cutting a single internal light field line. For tree-level diagrams this is equivalent to requiring that only heavy fields appear as internal lines.

   Using the Feynman rules of the full model, calculate the expressions for these diagrams. Do not treat the external legs as incoming or outgoing particles, but keep the field operator expressions.
3. Express quantities of the full model in terms of Λ. Truncate this infinite series of diagrams at some order in $1/\Lambda$, depending on the dimension of the operators that you want to keep. Together with kinetic and mass terms for the light fields, these form the Lagrangian of the EFT.

Fermi theory again

Let us apply this top-down procedure to our standard example of Fermi theory. For simplicity, we do not take the full SM, but just the interactions between massive W bosons and fermions as the underlying theory. The Lagrangian of these interactions is similar to that given in Equation (2.11).

1. Our full model consists of the quarks and leptons and the W boson. We want to analyse weak interactions below the W mass, so we set $\Lambda = m_W$. So all quarks and leptons except for the top are the light particles of the EFT, while the W boson and the top quark are heavy and have to be integrated out.
2. The only diagram with the requested features that has only one heavy propagator has the

form

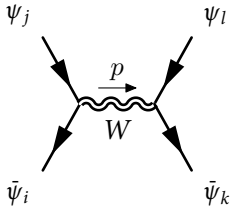

(2.45)

Double lines denote a heavy field. There are additional diagrams with W self-interactions or W loops, but they involve at least two W propagators, which means that all contributions from them will be of order $\mathcal{O}\left(1/\Lambda^4\right)$, which we will neglect.

This diagram evaluates to

$$\begin{aligned}&\left(\bar{\psi}_i \frac{\mathrm{i}g}{\sqrt{2}} \frac{1-\gamma_5}{2} \gamma^\mu \psi_j\right) \frac{-g_{\mu\nu}}{p^2 - m_W^2} \left(\bar{\psi}_k \frac{\mathrm{i}g}{\sqrt{2}} \frac{1-\gamma_5}{2} \gamma^\nu \psi_l\right) \\ &= \frac{g^2 \left(\bar{\psi}_i (1-\gamma_5) \gamma^\mu \psi_j\right) \left(\bar{\psi}_k (1-\gamma_5) \gamma_\mu \psi_l\right)}{8(p^2 - m_W^2)}\end{aligned} \tag{2.46}$$

3. The only dimensionful parameter is $m_W = \Lambda$, and for the EFT to be valid we assume $p^2 \ll \Lambda^2$. We can then expand this expression as

$$\frac{g^2}{8m_W^2} \left(\bar{\psi}_i (1-\gamma_5) \gamma^\mu \psi_j\right) \left(\bar{\psi}_k (1-\gamma_5) \gamma_\mu \psi_l\right) + \mathcal{O}\left(1/\Lambda^4\right) . \tag{2.47}$$

With this, we again rediscover the dimension-six EFT matched to the weak interactions of the SM:

$$\mathcal{L} = \mathrm{i}\bar{\psi}_i \gamma^\mu \partial_\mu \psi_i - m_i \bar{\psi}_i \psi_i + \frac{c}{\Lambda^2} \left(\bar{\psi}_i (1-\gamma_5) \gamma_\mu \psi_j\right) \left(\bar{\psi}_k (1-\gamma_5) \gamma^\mu \psi_l\right) . \tag{2.48}$$

with heavy scale $\Lambda = m_W$ and Wilson coefficient $c = g^2/8$. Replacing c/Λ^2 by $G_F/\sqrt{2} = g^2/(8m_W^2)$ restores the historic form of Fermi theory.

Operator mixing

So far we have neglected that like all parameters in a QFT, the Wilson coefficients of an EFT depend on the energy scale. Running the model from one energy to a different one leads to **operator mixing**: loop effects from one operator will affect the coefficients of other operators. If the Wilson coefficients are given at the matching scale Λ (we use this symbol since the matching scale is usually chosen only slightly below the EFT cutoff), at the scale of interest E they will take on values of the form

$$f_i(E) \sim f_i(\Lambda) \pm \sum_j \frac{g^2}{16\pi^2} \log \frac{\Lambda^2}{E^2} f_j(\Lambda) , \tag{2.49}$$

where g are the typical couplings in the loops.

If the matching scale is not too far away from the energy scale of interest and if all Wilson coefficients are already sizeable at the matching scale, this is often negligible. There is an important consequence, though: even if an operator is zero at the matching scale, operator mixing will give it a small but non-zero value at lower energies. So regardless of what the underlying model is, it can be expected that eventually all effective operators allowed by the symmetries will receive contributions from it.

2.3 Dimension-six Higgs physics

We now apply these general ideas to electroweak and in particular Higgs physics at the TeV scale and construct the Standard Model effective field theory (interchangeably called linear Higgs effective field theory) up to dimension six [19–21, 67]. This is the framework we will use throughout this thesis. We will first argue why such an effective theory is very useful, and then construct its effective operators following the recipe laid out in Section 2.2.2. Section 2.3.3 will take a closer look at the phenomenology of these operators. Finally, in Section 2.3.4 we briefly discuss a few alternative frameworks.

2.3.1 Motivation

As argued in Section 2.1.3, there are many reasons to suspect new physics in the Higgs sector. Some of these arguments, such as the hierarchy problem or the WIMP miracle of dark matter, point towards BSM physics close to the electroweak scale or, depending on the level of acceptable fine-tuning, up to a few TeV. Unfortunately these (purely aesthetic) arguments do not tell us how exactly such physics should look like.

This leaves us with a question highly relevant for upcoming ATLAS and CMS analyses: what is the best language to discuss indirect signs of new physics at the electroweak scale, in particular in the Higgs sector? Which parameterisation of Higgs properties provides a good interface between different experiments, and between experiment and theory?

Directly interpreting measurements in complete models of new physics is impractical: for $n_y \gg 1$ signatures and $m_a \gg 1$ models this requires $m_a n_y$ limits to be derived.[7] Also, the parameter space of such models (think of the relatively simple MSSM) can be huge, and many of their features do not matter at the electroweak scale at all. It makes more sense to define an intermediate framework that can be linked both to measurements and to full theories, so only n_y sets of limits plus m_a translation rules from complete theories to the intermediate language have to be calculated. Such a framework should include all necessary physics, but no phenomena irrelevant at this scale… exactly the defining feature of an effective field theory.

[7] The weird notation is necessary because the author cannot resist a stupid pun.

2.3.2 Operators

Building blocks

Since we do not know what physics lays beyond the SM, we have to construct our EFT from a bottom-up perspective. As discussed above, this means we have to write down all operators based on a set of particles that are compatible with certain symmetries and are important according to some counting scheme. Let us go through these one by one:

1. As degrees of freedoms we use the SM fields. In particular, we assume the Higgs boson h and the Goldstone bosons w_i are combined in a $SU(2)_L$ doublet ϕ as in the SM, see Equation (2.4). This is consistent with correct data and the correct choice if new physics decouples, that is, if in the limit $\Lambda \to \infty$ the SM is recovered [68]. We will discuss an alternative construction based on the physical scalar h instead of ϕ as the fundamental building block in Section 2.3.4.
2. All operators have to be invariant under Lorentz transformations and under the SM gauge group $SU(3)_C \times SU(2)_L \times U(1)_Y$, and conserve lepton and baryon number.
3. We order the operators by their mass dimension and thus their suppression in powers of $1/\Lambda$. We will keep those up to mass dimension 6, i. e. $\mathcal{O}\left(1/\Lambda^2\right)$.

Simple dimensional analysis of the kinetic terms of the SM fields tells us the mass dimensions of all building blocks:

$$[f] = \frac{3}{2}\,, \quad [V_\mu] = 1\,, \quad [V_{\mu\nu}] = 2\,, \quad [\phi] = 1\,, \quad [\partial_\mu] = 1 \quad \text{and} \quad [D_\mu] = 1\,. \tag{2.50}$$

The only dimension-five operator that can be built from the SM fields is the Weinberg operator $(\bar{L}_L \tilde{\phi} *)(\tilde{\phi}^\dagger L_L)$. It generates a Majorana mass term for the neutrinos and violates lepton number, and is entirely irrelevant for Higgs physics. The leading effects in our EFT are expected to come from dimension-six operators:

$$\mathcal{L}_{\text{EFT}} = \mathcal{L}_{\text{SM}} + \sum_i \frac{f_i}{\Lambda^2} \mathcal{O}_i + \mathcal{O}\left(1/\Lambda^4\right) \tag{2.51}$$

with unknown cutoff scale Λ and Wilson coefficients f_i. For convenience, we will from now on drop the higher-order terms.

As discussed in Section 2.2.2, field redefinitions (or, relatedly, equations of motions), Fierz identities and integration by parts provide equivalence relations between certain operators and give us some freedom to define a basis of operators. Taking these into account, there are 59 independent types of dimension-six operators, not counting flavour structures and Hermitian conjugation [69]. Counting all possible flavour structures, there are 2499 distinct operators. Fortunately, in practice only a small subset of these are relevant: first, the strong constraints on

$\mathcal{O}_{\phi 1} = (D_\mu \phi)^\dagger \, (\phi \, \phi^\dagger) \, (D^\mu \phi)$	$\mathcal{O}_{GG} = (\phi^\dagger \phi) \, G^a_{\mu\nu} \, G^{\mu\nu \, a}$
$\mathcal{O}_{\phi 2} = \frac{1}{2} \partial^\mu (\phi^\dagger \phi) \, \partial_\mu (\phi^\dagger \phi)$	$\mathcal{O}_{BB} = -\frac{g'^2}{4} (\phi^\dagger \phi) \, B_{\mu\nu} \, B^{\mu\nu}$
$\mathcal{O}_{\phi 3} = \frac{1}{3} (\phi^\dagger \phi)^3$	$\mathcal{O}_{WW} = -\frac{g^2}{4} (\phi^\dagger \phi) \, W^k_{\mu\nu} \, W^{\mu\nu \, k}$
$\mathcal{O}_{\phi 4} = (\phi^\dagger \phi) \, (D_\mu \phi)^\dagger (D^\mu \phi)$	$\mathcal{O}_{BW} = -\frac{g \, g'}{4} (\phi^\dagger \sigma^k \phi) \, B_{\mu\nu} \, W^{\mu\nu \, k}$
	$\mathcal{O}_B = \frac{ig}{2} (D^\mu \phi^\dagger)(D^\nu \phi) \, B_{\mu\nu}$
	$\mathcal{O}_W = \frac{ig}{2} (D^\mu \phi^\dagger) \sigma^k (D^\nu \phi) \, W^k_{\mu\nu}$

Table 2.1: Bosonic *CP*-conserving dimension-six operators relevant for Higgs physics.

flavour-changing neutral currents motivates the assumption of flavour-diagonal or even flavour-universal Wilson coefficients. Second, only a small number of these operators directly affects Higgs physics. At higher orders in the EFT expansion, the number of operators increases rapidly, explaining why we stick to the leading effects at dimension 6: not counting flavour structures, there are $\mathcal{O}(1000)$ operators at dimension 8 and $\mathcal{O}(10\,000)$ dimension-10 operators [70].

Three different conventions have become popular: in addition to the complete "Warsaw" basis [69], there is the SILH convention [71, 72] and the HISZ basis [73]. All three maximize the use of bosonic operators to describe Higgs and electroweak observables. For a comparison of and conversion between these bases see References [2, 74]. Throughout this thesis we use the basis developed in References [22, 75], which is strongly based on the HISZ basis and now widely used in global fits [23, 24].

More references?

We classify the operators based on their field content and on their behaviour under *CP* transformations. This combined charge conjugation and parity inversion is an approximate symmetry of the SM that is only violated by the complex phase of the CKM matrix. In addition, there are rather tight bounds on *CP* violation in many processes. This motivates many analyses to restrict their set of operators to the *CP*-conserving ones. On the other hand, new sources of *CP* violation are needed to explain the matter-antimatter asymmetry in the universe, and their effects at low energies could be visible as *CP*-violating effective operators. Both types of operators will be analysed in this thesis.

Operator basis

We begin with the *CP*-conserving dimension-six operators relevant for Higgs physics, following References [22, 75]. In Table 2.1 we list the bosonic ones, Table 2.2 gives the Higgs-fermion

$\mathcal{O}_\ell = (\phi^\dagger\phi)\, L_L \phi\, \ell_R$	$\mathcal{O}_{\phi L}^{(1)} = \mathrm{i}(\phi^\dagger \overleftrightarrow{D}_\mu \phi)(\bar{L}_L \gamma^\mu L_L)$	$\mathcal{O}_{\phi L}^{(3)} = \mathrm{i}(\phi^\dagger \overleftrightarrow{D}^a_\mu \phi)(\bar{L}_L \gamma^\mu \sigma_a L_L)$
$\mathcal{O}_u = (\phi^\dagger\phi)\, Q_L \tilde{\phi}\, u_R$	$\mathcal{O}_{\phi Q}^{(1)} = \mathrm{i}(\phi^\dagger \overleftrightarrow{D}_\mu \phi)(\overline{Q}_L \gamma^\mu Q_L)$	$\mathcal{O}_{\phi Q}^{(3)} = \mathrm{i}(\phi^\dagger \overleftrightarrow{D}^a_\mu \phi)(\overline{Q}_L \gamma^\mu \sigma_a Q_L)$
$\mathcal{O}_d = (\phi^\dagger\phi)\, Q_L \phi\, d_R$	$\mathcal{O}_{\phi \ell}^{(1)} = \mathrm{i}(\phi^\dagger \overleftrightarrow{D}_\mu \phi)(\bar{\ell}_R \gamma^\mu \ell_R)$	
	$\mathcal{O}_{\phi u}^{(1)} = \mathrm{i}(\phi^\dagger \overleftrightarrow{D}_\mu \phi)(\bar{u}_R \gamma^\mu u_R)$	
	$\mathcal{O}_{\phi d}^{(1)} = \mathrm{i}(\phi^\dagger \overleftrightarrow{D}_\mu \phi)(\bar{d}_R \gamma^\mu d_R)$	
	$\mathcal{O}_{\phi ud}^{(1)} = \mathrm{i}(\phi^\dagger \overleftrightarrow{D}_\mu \phi)(\bar{u}_R \gamma^\mu d_R)$	

Table 2.2: *CP*-conserving dimension-six operators relevant for the Higgs-fermion couplings. For readability, flavour indices and Hermitian conjugation are omitted.

$\mathcal{O}_{uW} = (\overline{Q}_L \sigma^{\mu\nu} u_R)\sigma^a \tilde{\phi} W^a_{\mu\nu}$	$\mathcal{O}_{uB} = (\overline{Q}_L \sigma^{\mu\nu} u_R)\tilde{\phi} B_{\mu\nu}$	$\mathcal{O}_{uG} = (\overline{Q}_L \sigma^{\mu\nu} T^a u_R)\tilde{\phi} G^a_{\mu\nu}$
$\mathcal{O}_{dW} = (\overline{Q}_L \sigma^{\mu\nu} d_R)\sigma^a \phi W^a_{\mu\nu}$	$\mathcal{O}_{dB} = (\overline{Q}_L \sigma^{\mu\nu} d_R)\phi B_{\mu\nu}$	$\mathcal{O}_{dG} = (\overline{Q}_L \sigma^{\mu\nu} T^a d_R)\phi G^a_{\mu\nu}$
$\mathcal{O}_{\ell W} = (\bar{L}_L \sigma^{\mu\nu} \ell_R)\sigma^a \phi W^a_{\mu\nu}$	$\mathcal{O}_{\ell B} = (\bar{L}_L \sigma^{\mu\nu} \ell_R)\phi B_{\mu\nu}$	

Table 2.3: Dipole operators affecting the Higgs-gauge-fermion couplings. For readability, flavour indices and Hermitian conjugation are omitted.

$\mathcal{O}_{G\widetilde{G}} = (\phi^\dagger\phi)\, G^a_{\mu\nu}\, \widetilde{G}^{\mu\nu\, a}$	$\mathcal{O}_{\widetilde{B}} = \frac{ig}{2}(D^\mu\phi^\dagger)(D^\nu\phi)\, \widetilde{B}_{\mu\nu}$
$\mathcal{O}_{B\widetilde{B}} = -\frac{g'^2}{4}(\phi^\dagger\phi)\, B_{\mu\nu}\, \widetilde{B}^{\mu\nu}$	$\mathcal{O}_{B\widetilde{W}} = -\frac{g\, g'}{4}(\phi^\dagger\sigma^k\phi)\, B_{\mu\nu}\, \widetilde{W}^{\mu\nu\, k}$
$\mathcal{O}_{W\widetilde{W}} = -\frac{g^2}{4}(\phi^\dagger\phi)\, W^k_{\mu\nu}\, \widetilde{W}^{\mu\nu\, k}$	

Table 2.4: Bosonic CP-violating dimension-six operators relevant for Higgs physics. The dual field strengths are defined in Equation (2.53).

operators, and the "dipole operators" made of Higgs fields, gauge bosons, and fermions are listed in Table 2.3. We use the convention for the sign in the covariant derivative given in Equation (2.2), T^a are the $SU(3)$ generators, and

$$\phi^\dagger \overleftrightarrow{D}_\mu \phi \equiv \phi^\dagger D_\mu \phi - (D_\mu\phi)^\dagger \phi \quad \text{and} \quad \phi^\dagger \overleftrightarrow{D}^a_\mu \phi \equiv \phi^\dagger \sigma^a D_\mu \phi - (D_\mu\phi)^\dagger \sigma^a \phi\,. \tag{2.52}$$

In addition to these CP-conserving structures, there are a number of CP-violating operators. We only list the bosonic ones relevant for Higgs physics [76, 77] in Table 2.4. They involve the dual field strength tensors

$$\widetilde{V}_{\mu\nu} = \frac{1}{2}\varepsilon_{\mu\nu\rho\sigma} V^{\mu\nu}\,, \quad V = B, W, G\,. \tag{2.53}$$

Finally, there are a few pure CP-even and CP-odd pure gauge operators made from field strength tensors and (covariant) derivatives, and a large number of four-fermion operators similar to the one in Equation (2.48), which will not be important in this thesis.

As argued above, not all of these operators are independent. The equations of motions for the Higgs field and the electroweak gauge bosons read [69]

$$D^2\phi = -\mu^2\phi - 2\lambda(\phi^\dagger\phi)\phi - \sum_f y_f \bar{f}_R f_L + \mathcal{O}\big(1/\Lambda^2\big)\,, \tag{2.54}$$

$$\partial^\rho B_{\rho\mu} = -\frac{g'}{2}\left(i\phi^\dagger \overleftrightarrow{D}_\mu \phi + \sum_f Y_f \bar{f}\gamma_\mu f\right) + \mathcal{O}\big(1/\Lambda^2\big)\,, \tag{2.55}$$

$$(D^\rho W_{\rho\mu})^a = \frac{g}{2}\left(i\phi^\dagger \overleftrightarrow{D}^a_\mu \phi + \bar{q}_L\gamma_\mu\sigma^a q_L + \bar{\ell}_L\gamma_\mu\sigma^a \ell_L\right) + \mathcal{O}\big(1/\Lambda^2\big)\,, \tag{2.56}$$

where Y_f are the weak hypercharges of the fermions. Following Equation (2.14), this provides us with three equivalence relations between dimension-six operators [22, 75]:

$$\mathcal{O}_{\phi,2} + \mathcal{O}_{\phi,4} - \mu^2(\phi^\dagger\phi)^2 - 6\lambda\mathcal{O}_6 = \sum_f y_f \mathcal{O}_f + \mathcal{O}\big(1/\Lambda^4\big) \tag{2.57}$$

$$2\mathcal{O}_B + \mathcal{O}_{BW} + \mathcal{O}_{BB} + g'^2\left(\mathcal{O}_{\phi,1} - \frac{1}{2}\mathcal{O}_{\phi,2}\right) = -\frac{g'^2}{2}\sum_f Y_f \mathcal{O}_{\phi f}^{(1)} + \mathcal{O}\left(1/\Lambda^4\right) \tag{2.58}$$

$$2\mathcal{O}_W + \mathcal{O}_{BW} + \mathcal{O}_{WW} + g^2\left(\mathcal{O}_{\phi,4} - \frac{1}{2}\mathcal{O}_{\phi,2}\right) = -\frac{g^2}{4}\left(\mathcal{O}_{\phi L}^{(3)} + \mathcal{O}_{\phi Q}^{(3)}\right) + \mathcal{O}\left(1/\Lambda^4\right). \tag{2.59}$$

This lets us eliminate three of the operators listed in Tables 2.1 to 2.4.

There are different strategies for picking the operators to keep. In a top-down approach, one could choose operators based on the underlying physics. In a bottom-up approach, calculations can be simplified if the operators are chosen based on their contributions to physical observables, for instance to avoid blind directions. Applied to Higgs physics, this logic suggests to discard $\mathcal{O}_{\phi L}^{(1)}$, $\mathcal{O}_{(3)}$, and $\mathcal{O}_{\phi,4}$ [22].

Constraints

Some of the remaining operators are tightly constrained experimental data. Electroweak precision measurements limit the Wilson coefficients of $\mathcal{O}_{\phi,1}$, $\mathcal{O}_{BW}$, $\mathcal{O}_{\phi f}^{(1)}$, $\mathcal{O}_{\phi f}^{(3)}$, $\mathcal{O}_{B\widetilde{W}}$, and $\mathcal{O}_{\widetilde{B}}$ to a level where their effects in Higgs physics are small. Measurements of electric dipole moments put tight constrains on the dipole operators. We will ignore all these operators.[8]

Limits on flavour-changing neutral currents constrain off-diagonal fermion-Higgs couplings. Also, flavour-diagonal $\mathcal{O}_f$ involving fermions of the first and second generation will be irrelevant for many signatures considered in this thesis. We therefore only keep the Higgs-fermion operators $\mathcal{O}_f$ of the third generation.

This leaves us with a list of thirteen operators relevant for LHC Higgs physics: ten CP-even operators,

$$\mathcal{O}_{\phi,2}\,, \quad \mathcal{O}_{\phi,3}\,, \quad \mathcal{O}_{GG}\,, \quad \mathcal{O}_{BB}\,, \quad \mathcal{O}_{WW}\,, \quad \mathcal{O}_{B}\,, \quad \mathcal{O}_{W}\,, \quad \mathcal{O}_{\tau}\,, \quad \mathcal{O}_{t}\,, \quad \text{and} \quad \mathcal{O}_{b}\,; \tag{2.60}$$

and three CP-odd ones,

$$\mathcal{O}_{G\widetilde{G}}\,, \quad \mathcal{O}_{B\widetilde{B}}\,, \quad \text{and} \quad \mathcal{O}_{W\widetilde{W}}\,. \tag{2.61}$$

Renormalisation group evolution

The Wilson coefficients of these operators depend on the energy scale. In the last years, the contributions of all dimension-six operators on the running of the SM parameters, as well as the whole 59×59 anomalous dimension matrix of dimension-six operators, have been calculated

[8] This simple argument is suitable for our rather conceptual work. In a thorough global fit, however, it should be checked carefully whether these constraints are actually strong enough to make all these operator irrelevant for Higgs physics in all cases. Such a check should include RGE effects when comparing constraints from different scales. The increasing precision in Higgs observables means that many of these operators will become relevant again in the future.

at one-loop level [78–80]. This provides all necessary tools to run the EFT parameters from the matching scale Λ to the experimental scale E. Following Equation (2.49), this shifts the Wilson coefficients by a term proportional to a loop factor and $\log \Lambda^2/E^2$.

As we will discuss in some length in Chapter 3, the LHC Higgs measurements are only sensitive to new physics scales between the electroweak scale and the TeV scale. The corresponding logarithm typically cannot compensate for the loop factor, and the RGE effects on Wilson coefficients that are already non-zero at the matching scale are small. We will therefore neglect operator running for our analyses.

2.3.3 Phenomenology

After picking a set of operators, the next question is how they affect Higgs observables. We will first discuss two examples, $\mathcal{O}_{\phi,2}$ and $\mathcal{O}_W$, in detail, before listing the effects of all operators in Equations (2.60) and (2.60).

$\mathcal{O}_{\phi 2}$: rescaled Higgs couplings

Our first example is the operator $\mathcal{O}_{\phi,2}$. Ignoring the Goldstones, it consists only of derivatives and Higgs fields $\phi^\dagger\phi = (v^2 + 2v\tilde{h} + \tilde{h}^2)/2$, where we use a tilde on h for reasons that will become clear soon. Its contribution to the Lagrangian reads

$$\begin{aligned}\mathcal{L}_{\text{EFT}} &\supset \frac{f_{\phi,2}}{2\Lambda^2}\,\partial^\mu(\phi^\dagger\phi)\,\partial_\mu(\phi^\dagger\phi)\\ &= \frac{f_{\phi,2}v^2}{2\Lambda^2}\,\partial_\mu\tilde{h}\partial^\mu\tilde{h} + \frac{f_{\phi,2}\,v}{\Lambda^2}\,\tilde{h}\partial_\mu\tilde{h}\partial^\mu\tilde{h} + \frac{f_{\phi,2}\,v}{2\Lambda^2}\,\tilde{h}^2\partial_\mu\tilde{h}\partial^\mu\tilde{h}\,.\end{aligned} \tag{2.62}$$

The first term rescales the kinetic term of the Higgs boson:

$$\mathcal{L}_{\text{EFT}} \supset \left(1 + \frac{f_{\phi 2}v^2}{\Lambda^2}\right)\frac{1}{2}\,\partial_\mu\tilde{h}\partial^\mu\tilde{h}\,. \tag{2.63}$$

To restore the canonical form of the kinetic term, we have to rescale the Higgs boson $\tilde{h}$ to

$$h = \sqrt{1 + \frac{f_{\phi 2}v^2}{\Lambda^2}}\,\tilde{h}\,. \tag{2.64}$$

On the one hand, this universally shifts all Higgs couplings to other particles as

$$g_{hxx} = \frac{1}{\sqrt{1 + \frac{f_{\phi 2}v^2}{\Lambda^2}}}\,g^{\text{SM}}_{hxx}\,. \tag{2.65}$$

The effect on the Higgs self-coupling is more involved. First, the rescaling in Equation (2.64) also affects the Higgs mass term given in Equation (2.5). For fixed v and m_h, this amounts to shifting the Higgs self-coupling λ to

$$\lambda = \frac{m_h^2}{2v^2}\left(1 + \frac{f_{\phi 2} v^2}{\Lambda^2}\right). \tag{2.66}$$

In addition, the second term in Equation (2.62) introduces a new Lorentz structure into the Higgs self-interaction that depends on the Higgs momenta. A non-zero Wilson coefficients $f_{\phi 2}$ will therefore have a strong impact on Higgs pair production, not only on the total rate, but also on kinematic distributions.

$\mathcal{O}_W$: new Higgs-gauge structures

Our second example is $\mathcal{O}_W$, which contracts covariant derivatives acting on Higgs doublets, defined in Equation (2.2), with a field strength tensor $W^k_{\mu\nu} = \partial_\mu W^k_\nu - \partial_\nu W^k_\mu + g\varepsilon^{kmn} W^m_\mu W^n_\nu$. Expanding $\mathcal{O}_W$ and only keeping the pieces that will affect the hWW coupling, we find

$$\begin{aligned}
\mathcal{L}_{\text{EFT}} &\supset \frac{f_W}{\Lambda^2}\frac{\mathrm{i}g}{2}\,(D^\mu\phi)^\dagger \sigma^k (D^\nu\phi)\, W^k_{\mu\nu} \\
&= \frac{\mathrm{i}g f_W}{2\Lambda^2}\left(\partial^\mu\phi^\dagger + \frac{\mathrm{i}g}{2} W^{m\,\mu}\phi^\dagger\sigma^m + \frac{\mathrm{i}g'}{2}B^\mu\phi^\dagger\right)\sigma^k\left(\partial^\nu\phi - \frac{\mathrm{i}g}{2}\sigma^n W^{n\,\nu}\phi - \frac{\mathrm{i}g'}{2}B^\nu\phi\right) W^k_{\mu\nu} \\
&\supset \frac{\mathrm{i}g f_W}{2\Lambda^2}\left\{\frac{\partial^\mu h}{\sqrt{2}}\left[\sigma^k\sigma^n\right]_{22}\frac{-\mathrm{i}g}{2}\,W^{n\,\nu}\,\frac{v}{\sqrt{2}} + \frac{\mathrm{i}g}{2}\,W^{m\,\nu}\,\frac{v}{\sqrt{2}}\left[\sigma^m\sigma^k\right]_{22}\frac{\partial^\mu h}{\sqrt{2}}\right\} W^k_{\mu\nu} \\
&= \frac{f_W}{\Lambda^2}\frac{g^2 v}{8}\left[\sigma^k,\sigma^n\right]_{22}(\partial^\mu h)\,W^{n\,\nu}\,W^k_{\mu\nu} \\
&= \frac{f_W}{\Lambda^2}\frac{\mathrm{i}g^2 v}{4}\,\varepsilon^{nk3}\,(\partial^\mu h)\,W^{n\,\nu}\,W^k_{\mu\nu}\,.
\end{aligned} \tag{2.67}$$

With $m_W = gv/2$ and $W^\pm_\mu = (W^1_\mu \mp \mathrm{i}W^2_\mu)/\sqrt{2}$ this finally fields

$$\mathcal{L}_{\text{EFT}} \supset \frac{f_W}{\Lambda^2}\frac{\mathrm{i}g m_W}{2}\,(\partial^\mu h)\left(W^{+\,\nu}\,W^-_{\mu\nu} + W^{-\,\nu}\,W^+_{\mu\nu}\right). \tag{2.68}$$

This is another contribution to the hWW vertex. But unlike the SM-like coupling

$$\mathcal{L}_{\text{SM}} \supset g m_W\, h W^{+\,\mu}\,W^-_\mu\,, \tag{2.69}$$

the $\mathcal{O}_W$ term includes derivatives. This means that the interaction gains a momentum dependence:

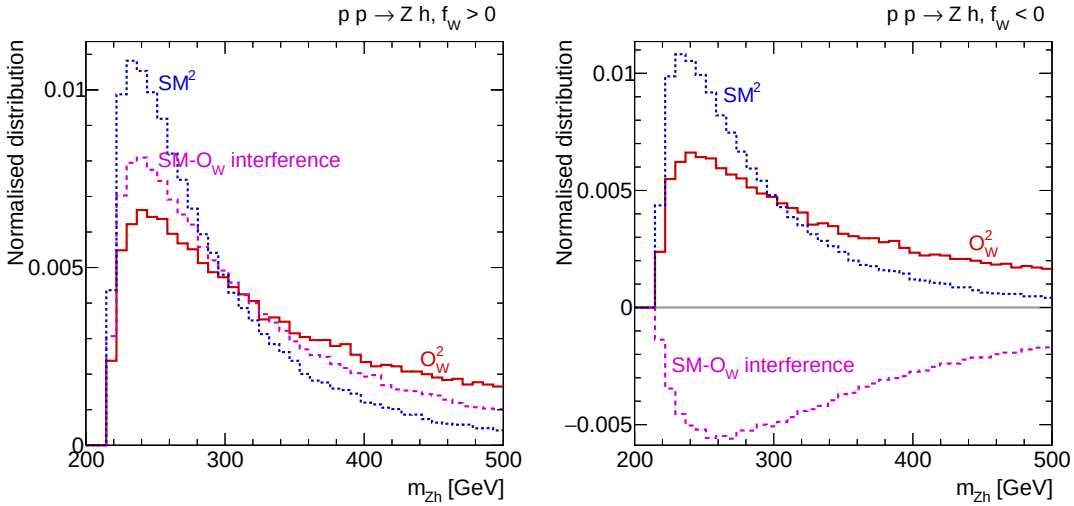

Figure 2.4: Distribution of the Zh invariant mass in the Higgs-strahlung process $pp \to Zh$ at LHC conditions. We compare the contributions from the SM, the operator $\mathcal{O}_W$ squared, and their interference, which can be constructive (left) or destructive (right).

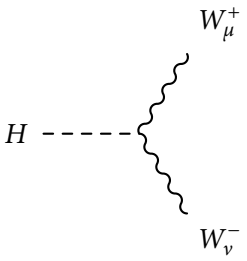

$$= \mathrm{i} g m_W \left[g_{\mu\nu} + \frac{f_W}{2\Lambda^2} p_H^2 \, g_{\mu\nu} + \frac{f_W}{2\Lambda^2} \left(p_\mu^H p_\nu^+ + p_\mu^- p_\nu^H \right) \right] , \tag{2.70}$$

where $p_\mu^\pm$ and p_μ^H are the incoming momenta of the $W^\pm$ and the H, respectively.

This operator illustrates two key features of the EFT approach. First, $\mathcal{O}_W$ does not only affect the hWW vertex, but also hZZ interactions and triple-gauge couplings such as WWZ. This means that the dimension-six operator language allows us to combine different measurements in a global fit.

Second, $\mathcal{O}_W$ changes the shape of distributions, for instance in Higgs-strahlung at the LHC,

$$pp \to Zh \, . \tag{2.71}$$

In this process, the intermediate Z can carry arbitrary large energy and momentum, which we can measure for instance as the invariant mass of the final Zh system. From Equation (2.70) we expect that the effects from $\mathcal{O}_W$ will grow with m_{Zh}. In Figure 2.4 we demonstrate this by comparing

the distribution of m_{Zh} based on only the SM couplings, on the dimension-six operator $\mathcal{O}_W$ only, and on the interference between the two components. Indeed we see that $\mathcal{O}_W$ contributes mostly in the high-energy tail of the distribution.

All those couplings

After these two worked-out examples, we now give the complete list of single-Higgs couplings induced by the dimension-six operators of Equations (2.60) and (2.61), some of which were calculated in References [22, 75] and cross-checked by us.

Check signs due to different conventions for the covariant derivative!

These interactions read

$$\begin{aligned}\mathcal{L}_{\text{EFT}} \supset\ & g^{(1)}_{hgg}\, h G^a_{\mu\nu} G^{a\,\mu\nu} + g^{(2)}_{hgg}\, \varepsilon_{\mu\nu\rho\sigma} h G^{a\,\mu\nu} G^{a\,\rho\sigma} + g_{h\gamma\gamma}\, h A_{\mu\nu} A^{\mu\nu} \\ & + g^{(1)}_{hZ\gamma}\, A_{\mu\nu} Z^\mu \partial^\nu h + g^{(2)}_{hZ\gamma}\, h A_{\mu\nu} Z^{\mu\nu} \\ & + g^{(1)}_{hZZ}\, Z_{\mu\nu} Z^\mu \partial^\nu h + g^{(2)}_{hZZ}\, h Z_{\mu\nu} Z^{\mu\nu} + g^{(3)}_{hZZ}\, h Z_\mu Z^\mu + g^{(4)}_{hZZ}\, h \varepsilon_{\mu\nu\rho\sigma} Z^{\mu\nu} Z^{\rho\sigma} \\ & + g^{(1)}_{hWW} \left(W^+_{\mu\nu} W^{-\,\mu} \partial^\nu h + \text{h. c.} \right) + g^{(2)}_{hWW}\, h W^+_{\mu\nu} W^{-\,\mu\nu} + g^{(3)}_{hWW}\, h W^+_\mu W^{-\,\mu} \\ & \qquad\qquad + g^{(4)}_{hWW}\, h \varepsilon_{\mu\nu\rho\sigma} W^{+\,\mu\nu} W^{-\,\rho\sigma} \\ & + \sum_{f=\tau,t,b} \left(g_{hff} h \bar{f}_L f_R + \text{h. c.} \right) \end{aligned} \tag{2.72}$$

with couplings

$$\begin{aligned}
g^{(1)}_{hgg} &= \frac{f_{GG} v}{\Lambda^2}\,, & g^{(1)}_{hZ\gamma} &= \frac{g^2 v s (f_W - f_B)}{4c\Lambda^2}\,, \\
g^{(2)}_{hgg} &= \frac{f_{G\widetilde{G}} v}{2\Lambda^2}\,, & g^{(2)}_{hZ\gamma} &= \frac{g^2 v s (2s^2 f_{BB} - 2c^2 f_{WW})}{4c\Lambda^2}\,, \\
g_{h\gamma\gamma} &= -\frac{g^2 v s^2 (f_{WW} + f_{BB})}{4\Lambda^2}\,, & g_{hff} &= -\frac{m_f}{v}\left(1 + \frac{v^2 f_{\phi,2}}{\Lambda^2}\right)^{-1/2} + \frac{v^2 f_f}{\sqrt{2}\Lambda^2}\,, \\
g^{(1)}_{hZZ} &= \frac{g^2 v (c^2 f_W + s^2 f_B)}{4c^2\Lambda^2}\,, & g^{(1)}_{hWW} &= \frac{g^2 v f_W}{4\Lambda^2}\,, \\
g^{(2)}_{hZZ} &= -\frac{g^2 v (s^4 f_{BB} + c^4 f_{WW})}{4c^2\Lambda^2}\,, & g^{(2)}_{hWW} &= -\frac{g^2 v f_{WW}}{2\Lambda^2}\,, \\
g^{(3)}_{hZZ} &= \frac{g^2 v}{4c^2}\left(1 + \frac{v^2 f_{\phi,2}}{\Lambda^2}\right)^{-1/2}\,, & g^{(3)}_{hWW} &= \frac{g^2 v}{2}\left(1 + \frac{v^2 f_{\phi,2}}{\Lambda^2}\right)^{-1/2}\,, \\
g^{(4)}_{hZZ} &= -\frac{g^2 v (s^4 f_{B\widetilde{B}} + c^4 f_{W\widetilde{W}})}{8c^2\Lambda^2}\,, & g^{(4)}_{hWW} &= -\frac{g^2 v f_{W\widetilde{W}}}{4\Lambda^2}\,.
\end{aligned} \tag{2.73}$$

Check CP-odd ones.

Here $s \equiv g'/\sqrt{g^2 + g'^2}$ and $c = \sqrt{1 - s^2}$ are the sine and cosine of the weak mixing angle, and $V_{\mu\nu} = \partial_\mu V_\nu - \partial_\nu V_\mu$ for $V = A, W^\pm, Z$.

Note that the clear majority of the couplings in Equation (2.72) does not exist in the SM and contains derivatives. Dimension-six operators predict a variety of novel kinematic features in Higgs interactions, making their measurement at the LHC both exciting and challenging.

2.3.4 Alternative frameworks

The linear Higgs EFT discussed above is not the only useful parametrisation of Higgs properties. We will briefly go through some of the alternative frameworks and explain their main properties, before finishing this chapter with a comparison of the different approaches.

Non-linear Higgs effective field theory

In the SM EFT (or linear Higgs EFT) constructed in Section 2.3.2 the Higgs boson h and the Goldstone bosons w_a form an $SU(2)$ doublet ϕ as given in Equation (2.4). But in some models of new physics the Higgs is not part of an elementary $SU(2)$ doublet. Typical examples are composite Higgs models in which the Higgs boson is a pseudo-Goldstone from some strongly interacting dynamics [81–85]. Non-linear Higgs EFT, sometimes simply called "Higgs EFT", is an effective theory designed for these scenarios [76, 86–95]. This model is also often referred to as "chiral Lagrangian", and indeed its structure is similar to that of chiral perturbation theory, for an introduction see for instance References [96, 97]. Again, we begin by going through the ingredients to the effective theory before constructing the Lagrangian.

The **particle content** of the non-linear Higgs EFT constitutes the main difference to the linear Lagrangian: the physical scalar h is separated from the Goldstones w_a, both are included as independent degrees of freedom rather than as part of the doublet ϕ. The Higgs boson h is now a singlet under the SM gauge symmetry. The Goldstone bosons w_a, no longer a part of a Higgs doublet, are organised in the exponential form

$$U = e^{i\sigma_a w_a} . \tag{2.74}$$

The Goldstones transform non-linearly under the (approximate) global custodial symmetry $SU(2)_L \times SU(2)_R$, giving the EFT its name.

The **symmetries** are the same as in the linear case. We require invariance under Lorentz transformations as well as under the SM gauge group $SU(3)_C \times SU(2)_L \times U(1)_Y$ and baryon and lepton number conservation. For simplicity, we will also restrict our brief discussion to CP-even operators that conserve lepton flavour.

Choosing the **counting scheme** is a little more involved. To account for strongly interacting scenarios, we now have to distinguish three different scales [92]:

- The electroweak scale $v = 246$ GeV, which defines the W and Z mass, but is not necessarily the Higgs VEV.

- The scale f associated to the Goldstone bosons w_a and the Higgs boson h due to some breaking of the underlying dynamics, in analogy to the pion decay constant f_π.[9]
- The cut-off Λ of the theory. For weakly coupled physics this can be arbitrary. But one can calculate that the low-energy effective theories from spontaneously broken strongly coupled dynamics break down around $\Lambda \approx 4\pi f$ [96]. A cut-off of this size guarantees for the EFT to be renormalisable order by order.

The existence of three scales means there are two dimensionless parameters, so in general the EFT terms are organised in a double expansion [92]. The first is

$$\xi \equiv \frac{v^2}{f^2}\,. \tag{2.75}$$

The value of ξ defines the non-linearity of the model: the limit $\xi \to 0$ restores the linear Lagrangian. An expansion in ξ exactly corresponds to the power-counting scheme of linear EFT, i. e. ordering operators by their canonical dimension.

The second dimensionless parameter is

$$\frac{f^2}{\Lambda^2} \approx \frac{1}{16\pi^2} \tag{2.76}$$

for strongly coupled scenarios. Expanding in f^2/Λ^2 corresponds to a loop expansion similar to that in chiral perturbation theory. Equivalently, one can define a **chiral dimension** $\chi = [\mathcal{O}]_c$ for each operator $\mathcal{O}$ with the assignments [92]

$$\begin{aligned} &[f]_c = 1\,, && [V_\mu]_c = 0\,, && [V_{\mu\nu}]_c = 1\,, && [U]_c = 0\,, && [h]_c = 0\,, \\ &[\partial_\mu]_c = 1\,, && [D_\mu]_c = 1\,, && [g]_c = 1\,, && [y_f]_c = 1\,. \end{aligned} \tag{2.77}$$

The loop order L of an operator is equivalent to chiral dimension $\chi = 2L + 2$. This chiral counting can also be linked to an expansion in $\hbar$ [98].

The correct expansion scheme depends on the value of ξ. For $\xi \gg 1/16\pi^2$ or $f \ll 3$ TeV, the chiral expansion is more appropriate. For $\xi \ll 1/16\pi^2$ or $f \gg 3$ TeV, the canonical expansion is correct. In the intermediate region, a combined expansion gives the best results. Since LHC Higgs physics is mostly sensitive to NP scenarios with $f \ll 3$ TeV, the chiral expansion is phenomenologically more relevant and we will stick to it. For a more thorough discussion of power counting in this framework, see Reference [68].

[9] In general, the scales associated with w_a and h, f_w and f_h, can be different, making the power-counting even more complicated.

At the leading chiral order $\chi = 2$ or $L = 0$, the Higgs sector of the Lagrangian is given by [90][10]

$$\begin{aligned}\mathcal{L}_{\text{non-linear EFT}} \supset & \frac{1}{2}\partial_\mu h \partial^\mu h \left(1 + c_H \xi \mathcal{F}_H(h)\right) - V(h) \\ & - \frac{v^2}{4}\,\mathrm{tr}[V_\mu V^\mu]\mathcal{F}_C(h) + c_T \xi \frac{v^2}{4}\,\mathrm{tr}[T V^\mu]\,\mathrm{tr}[T V_\mu]\mathcal{F}_T(h) \\ & - \frac{v}{\sqrt{2}}\left[\sum_f \bar{f}_L U y_f \mathcal{F}_Y^f(h) P_f f_R + \text{h. c.}\right] \end{aligned} \tag{2.78}$$

with $V_\mu \equiv (D_\mu U)U^\dagger$, $T \equiv U\sigma_3 U^\dagger$ and projectors $P_u = (\mathbb{1} + \sigma_3)/2$, $P_d = P_\ell = (\mathbb{1} - \sigma_3)/2$. The functions $\mathcal{F}_C(h)$, $V(h)$, $\mathcal{F}_T(h)$, $\mathcal{F}_T(h)$, $\mathcal{F}_Y^u(h)$, $\mathcal{F}_Y^d(h)$, and $\mathcal{F}_Y^\ell(h)$ encode the coupling of the Higgs h and are arbitrary functions. They can be expanded as a power series in h/f, or to simplify the expressions in h/v, for instance

$$\mathcal{F}_C(h) = 1 + 2a_C\frac{h}{v} + b_C\left(\frac{h}{v}\right)^2 + \dots . \tag{2.79}$$

At next-to-leading order in the chiral expansion many more terms relevant for Higgs physics appear. We do not list them here and refer the interested reader for instance to Reference [93].

Finally, the relationship between the linear and non-linear effective theories deserves some discussion. The two approaches in principle provide different parameterisations of the same physics, as can be seen by expanding the non-linear Lagrangian in ξ rather then χ. The difference is the ordering of the operators in the EFT expansion and, equivalently, the expected size of different effects. Operators that appear at one order in the $1/\Lambda$ expansion of the linear EFT may appear at a very different order in the chiral expansion of the non-linear EFT.

Since the symmetry requirements on the non-linear setup are smaller, we expect it to be more general than the linear Lagrangian at a comparable order in the expansions. This is exactly what is found when comparing the linear dimension-six operators to the NLO chiral Lagrangian: the dimension-six operators predict certain correlations, while the non-linear description has more operators that can break these correlations [93]. A straightforward example is the relation between hxx and $hhxx$ couplings. For dimension-six operators, it is fixed doe to the appearance of $\phi^\dagger\phi \sim (v^2 + 2vh + h^2)/2$, while these couplings are always independent in the chiral approach, as can be seen in Equation (2.78).

The current experimental limits leave room for both strongly or weakly coupled new physics, for ξ smaller or larger than $1/(16\pi^2)$, for scenarios in which the linear or non-linear effective

[10] Two comments on this Lagrangian are in order. First, in principle there could be further functions of h coupling to the kinetic terms of the gauge bosons. Such interactions arise in typical strongly coupled theories at one-loop level with a coefficient $\sim 1/(16\pi^2)$ and are therefore usually classified as NLO operators [90, 91]. Second, the function $\mathcal{F}_C(h)$ (and a corresponding one to the fermion kinetic terms) can be removed with field redefinitions, shifting its physics into the other couplings [91, 95].

theories work better. Only a precise measurement of the Higgs properties and a global analysis of correlations will tell us which approach is correct. As a general rule, more SM-like results favour the linear approach that we follow throughout this thesis. On the other hand, certain deviations that do not follow the correlations predicted by dimension-six operators point towards non-linear physics.

κ framework

Effective field theories are of course not the only way to describe the Higgs sector. During run 1 of the LHC, the most widely used parametrisation was the κ framework [99] or the closely related Δ framework [100]. Its construction is remarkably simple: starting from the SM Higgs sector, all Higgs couplings are dressed with form factors,

$$g_{hxx} = \kappa_x g_{hxx}^{\text{SM}} = (1 + \Delta_x) g_{hxx}^{\text{SM}} . \tag{2.80}$$

Some care has to be taken to treat the Higgs-gluon and Higgs-photon couplings consistently, where indirect effects of shifted Higgs-top or Higgs-W couplings compete with direct effects from new physics [100].

From a theoretical point of view, the κ framework is not gauge-invariant and does not present a consistent quantum field theory. In practice, this means that electroweak loop effects may introduce divergences that cannot be renormalised. This problem can be solved by embedding the κ framework in a UV completion [101].

Citation?

From a more phenomenological point of view, this approach is well suited to parametrise measurements of total rates. Simple shifts of SM-like Higgs coupling structures are expected in some scenarios of new physics, for instance in many scalar extensions of the Higgs sector [101]. But many other models predict new kinematic features, visible as changed kinematic shapes, and the κ framework is unable to describe these. For better or worse, it is also agnostic about correlations between different Higgs couplings, and about correlations between Higgs observables and triple gauge vertices or electroweak precision measurements.

The strength of the κ framework is clearly not its theoretical foundation. Its allure comes from its simplicity and the fact that it is designed around the simple question of measuring the couplings of the (SM-like) Higgs boson. This parametrisation made sense as a common denominator for the first Higgs measurements with limited statistics of run 1 of the LHC. But the increased amount of data and crucial kinematic information collected during run 2 require a different, more sophisticated language.

Pseudo-Observables

Higgs pseudo-observables (POs) [102–104] are designed as a generalisation of the κ framework to include BSM kinematic features. In a very broad sense, this term encompasses any number that is

field theoretically defined and can be experimentally accessed [68]. Signal strengths, cross sections, partial widths, total widths, and individual form factors or couplings all fall under this umbrella term. Here we follow the more narrow definition of effective-coupling PO [4]. Pseudo-observables are then constructed process by process by writing down all contributing amplitudes under some broad assumptions on new physics. These expressions are then decomposed in a pole expansion, and the resulting residues are identified as pseudo-observables. This procedure also requires an expansion in the inverse of the new physics scale Λ. This means that just as the EFT approach, pseudo-observables rely on new physics being heavy, $E \ll \Lambda$. So far, this framework has been developed for Higgs production in WBF or Higgs-strahlung, as well as for all phenomenologically relevant Higgs decays.

Phenomenologically, pseudo-observables can describe shifts in SM couplings as well as kinematic shapes. Like the EFT approach, their construction requires certain minimal assumptions on the symmetries of new physics as well as an expansion in $1/\Lambda$. In fact, at tree level pseudo-observables can be mapped linearly to an EFT constructed with the same ingredients (which is the non-linear Higgs EFT discussed below).

The main difference between pseudo-observables and the EFT approach is a conceptual one. Pseudo-observables are designed from the perspective of a given process: they describe the coefficients of the different contributing amplitudes. They are not parameters of a Lagrangian and do not define a consistent quantum field theory. In particular, the values of POs measured in one process have no meaning for other processes. Effective operators on the other hand are a proper, gauge-invariant quantum field theory that universally describes any physics below the cutoff scale, and the same Wilson coefficients predict the behaviour of very different processes.

Proponents of the PO approach favour a multi-layer interpretation of LHC data, where the data is first presented in terms pseudo-observables, which can then be interpreted in terms of EFTs or specific models of UV physics. They argue that this approach provides a clear separation between measurement and interpretation [4]. On the other hand, proponents of the "direct EFT approach" argue that there is no need for such an intermediate layer, and suggest to directly fit effective operators. The debate about which approach is better is still ongoing [4]. Ultimately, both effective operators and POs are well-defined frameworks that can describe all relevant kinematic effects, and thus present a suitable interface between experiment and theory.

Simplified models

All these approach have in common that they assume the absence of new light particles. Simplified models are designed to close this gap and to describe kinematic effects from new light resonances. In addition to resonance peaks these include threshold effects in loops and Higgs decays into (invisible) new light degrees of freedom. Simplified models also allow to combine information from direct searches with indirect measurements. Except for the key element of adding new light propagating degrees of freedom to the SM, the term is not particularly well-defined, and there is a

lot of freedom to construct such models.

The simplest version of a simplified model consists of the SM supplemented with another particle, with ad-hoc coupling structures based on phenomenological requirements. Such a setup might even be not gauge-invariant and thus inconsistent beyond tree level. We will discuss one example introduced in Reference [3] in Chapter 3. At the other end of the spectrum, simplified models can be consistently defined quantum field theories, potentially involving higher-dimensional operators. The only difference to the linear and non-linear EFT approaches discussed above is the extended particle content. The additional flexibility of course comes at the price of an increased number of parameters.

Examples of such models for Higgs physics include an extended Higgs sector with an additional singlet and a doublet, which offers great flexibility to tune the Higgs couplings [101]. The authors of Reference [105] develop a model with an additional singlet and vector-like quarks. Finally, References [106, 107] discuss additional scalar singlets supplemented with higher-dimensional operators.

Comparison

All these approaches define parametrisations of the Higgs properties that can be used as interfaces between different measurements and between experiment and theory. In Table 2.5 we summarise and compare their different properties.

The different frameworks can be classified into consistent quantum field theories, which includes the EFTs, and process-based parameterisations of amplitudes through form factors. The κ framework and pseudo-observables belong to the latter category. Simplified models can fall into either category. The QFT formalism allows to link different processes and to incorporate any loop effects.

More important for practical purposes is the range of phenomena that can be described. The κ framework is limited to rescalings of the SM Higgs couplings and is not able to incorporate kinematic information. Pseudo-observables and the two EFT approaches are much more flexible and can describe a large number of kinematic features. However, they rely on new physics being substantially heavier than the experimentally probed energies around the weak scale. Features from light new particles, for instance resonances or loop thresholds, are only covered by appropriate simplified models. The dimension-six operators of linear Higgs EFT and to a lesser extent the leading operators of the chiral EFT also predict certain correlation between different couplings and measurements, while by definition the pseudo-observables are only valid for a given process.

To summarise, in the absence of new light particles, Higgs properties can be adequately parameterised by pseudo-observables, non-linear Higgs EFT, and linear Higgs EFT. The linear EFT approach is theoretically well-motivated, predictive, and flexible enough, and we will focus on this framework during this thesis.

	κ framework	POs	Non-linear EFT	Linear EFT	Simplified models
Motivation	experiment: simplest Higgs parametrisation	experiment: amplitude decomposition for given process	theory: complete low-energy effects of NP with singlet h	theory: complete low-energy effects of NP with doublet ϕ	exp. / theory: new light particles
Input	SM Higgs couplings	process amplitudes, pole expansion, NP expansion ($1/\Lambda$)	SM particles (h), symmetries, counting scheme (loops)	SM particles (ϕ), symmetries, counting scheme ($1/\Lambda$)	new particles (masses, charges, interactions)
Parameters	coefficients of SM amplitude	coefficients of amplitudes	Lagrangian parameters of consistent QFT	Lagrangian parameters of consistent QFT	depends
Validity conditions	SM-like	NP heavy, symmetries	NP heavy, symmetries	NP heavy, symmetries	single light new particles, other NP decouples
Shifted SM couplings	yes	yes	yes	yes	depends
Kinematic effects	no	yes	yes	yes	depends
New resonances, loop thresholds, invisible decays	no	no	no	no	yes
Correlations	no	no	some	many	depends

Table 2.5: Comparison of different parametrisations of Higgs properties. The upper part of the table focuses on the theoretical foundation, the lower the phenomenology. Since "simplified models" describe a rather general idea, many details depend on the specific realisation.

Chapter 3

Higgs effective theory at its limits

All models are wrong, but some are useful.
— G. Box [108]

Higgs effective theories can universally describe all signatures expected from new physics as long as its mass scale Λ is sufficiently separated from the experimentally accessible scale. However, the limited precision of the LHC means that Higgs measurements are often only sensitive to models with scales not much higher than the electroweak scale. In this chapter we discuss if and when the EFT approach is nevertheless useful, and how its validity can be improved.

In Section 3.1 we discuss the LHC sensitivity and its implications for effective theories, and formulate our strategy to test the dimension-six approach. In Section 3.2 we discuss some crucial details of the matching between full models and EFTs, and introduce the novel "v-improved" matching procedure. Section 3.3 contains the bulk of our results, the comparison of full models to their EFT approximations for a variety of models and observables. We go into more detail and analyse some practical questions in a specific example case in Section 3.4, and finally present our conclusions in Section 3.5.

Most of the work presented in this chapter was previously published in Reference [2], while the content of Section 3.4 was published in Reference [3]. A part of the content of this chapter was also included in Reference [4]. Nearly all of the results and most of their presentation in this chapter — including all plots, most of the tables, and a significant part of the text — are identical to that in these three publications.

3.1 Introduction

3.1.1 Energy scales in Higgs measurements

There is no doubt that effective field theories work extraordinarily well as long as there is a scale hierarchy between the experimentally probed energy and the new physics scale, $E \ll \Lambda$. On the other hand, it is clear that the EFT expansion breaks down at $E \geq \Lambda$, where an infinite number of operators contributes at the same size and the model is neither predictive nor renormalisable. The validity of the effective theory in the intermediate region,

$$E \lesssim \Lambda\,, \tag{3.1}$$

is less obvious and will depend on the specific underlying model as well as on the observable studied. So in which of these categories do LHC Higgs measurements belong?

Higgs production at hadron colliders does not probe a single experimental energy scale over the full relevant phase space. The momentum transfer is bounded from below by the Higgs mass. Selection criteria necessary to separate a signal from the QCD backgrounds often require a higher momentum transfer $E > m_h$. More importantly, most of the information on operators with derivatives comes from high-energy tails, as demonstrated in Section 2.3.3. During run 1, significant event numbers are recorded within the range

$$m_h \leq E \lesssim \mathcal{O}(400\text{ GeV})\,, \tag{3.2}$$

depending on the process, observable, collected amount of data, and analysis methods.

On the other hand, we can roughly estimate the new physics scale Λ that LHC Higgs measurements are able to probe. Assuming a 10% precision on total Higgs rate measurements and no loop suppression of new physics effects, such a signature lies within the experimental reach of the LHC if

$$\left|\frac{\sigma\times\text{BR}}{(\sigma\times\text{BR})_{\text{SM}}}-1\right| = \frac{g^2 m_h^2}{\Lambda^2} \gtrsim 10\% \qquad \Leftrightarrow \qquad \Lambda < \frac{g\,m_h}{\sqrt{10\%}} \approx g\,400\text{ GeV}\,. \tag{3.3}$$

where g are the typical couplings of the underlying theory.

This simple estimation shows that the scale separation E/Λ is limited by the experimental precision and crucially depends on the size of the couplings of underlying physics. For very weakly coupled theories, $g^2 < 1/2$, only new physics models with new particles at or below the electroweak scale can leave measurable signatures in Higgs observables, and the EFT approach clearly does not make sense. For truly strongly coupled theories, $1 < g \lesssim 4\pi$, new physics scenarios up to $\Lambda \lesssim 5$ TeV are relevant, and the EFT expansion converges flawlessly. In fact, the EFT approach to Higgs observables has largely been motivated by the desire to describe models with strongly

interacting electroweak symmetry breaking [71]. For moderately weakly to moderately strongly coupled theories, $1/2 \lesssim g^2 \lesssim 2$, the LHC Higgs programme is sensitive to scales

$$280 \text{ GeV} \lesssim \Lambda \lesssim 560 \text{ GeV} \tag{3.4}$$

This corresponds exactly to the intermediate region defined in Equation (3.1).

In this simple argument we ignored that new physics might also change distributions and especially affect the high-energy tails or off-shell regions. A thorough global fit of Higgs results including kinematic information confirms the rough estimate given in Equation (3.4) [23].

We conclude that for moderately weakly coupled scenarios of new physics, the limited precision of LHC Higgs measurements cannot guarantee a clear scale hierarchy, and the effective field theory approach cannot be trusted blindly. But this does not mean that an analysis of LHC data in terms of a truncated dimension-six Lagrangian cannot be useful. Instead, the applicability of the dimension-six model now depends on the nature of the underlying physics as well as on the process and observable, and has to be carefully checked for each situation.

From a practical perspective, in Reference [23] is has been shown that a fit of dimension-six operators to the Higgs data at Run I is a sensible and practicable extension of the usual Higgs couplings fit. As discussed at length in the previous chapter, dimension-six operators including derivatives complement the Higgs coupling modifications and allow us to extract information from kinematic distributions. Even if the LHC constraints do not induce a hierarchy of scales, and the EFT approach is not formally well defined, there appears to be no problem in using the truncated dimension-six Lagrangian as a phenomenological model to describe the LHC Higgs data. This description induces theory uncertainties if we want to interpret the LHC results in terms of an effective field theory [109].

3.1.2 Questions for the EFT approach

In this chapter we analyse the usefulness of the dimension-six description of the Higgs sector with a comprehensive comparison of full models and their dimension-six description. As argued above, the EFT validity has to be tested on a process-to-process as well as model-to-model basis. We therefore select four represantative models of new physics, map them onto dimension-six operators, and compare the predictions of the full and the effective model in various Higgs observables.

We select moderately weakly interacting extensions of the Higgs sector of the Standard Model by

1. a scalar singlet,
2. a scalar doublet,
3. a coloured top-partner scalar, and
4. a massive vector triplet.

For each of these models we pick a number of parameter benchmark points, designed to highlight phenomenogical features of the model, and to be within the experimental reach of the LHC Higgs programme.

The corresponding EFT descriptions are constructed by integrating out the heavy fields and expanding the effective action to $\mathcal{O}\left(1/\Lambda^2\right)$. In other words, we match the theories to the dimension-six operators of the linear Higgs EFT introduced in Section 2.3.2. The details of this matching procedure are a key element of our analysis and will be discussed in detail in the next section.

For all these scenarios, we calculate the Higgs couplings, and in a next step rates and distributions for selected Higgs production modes and decay channels. The key questions we aim to address are:

- Which masses and coupling predict Higgs signatures relevant for the LHC? Is the corresponding new physics scale sufficiently separated from v?
- Which observables are correctly described by dimension-six model? Where does the EFT description break down, and why?
- Does this breakdown pose a problem for LHC analyses?

In this way, we analyse what problems the lack of a clear hierarchy of scales leads to in practice, and discuss how these might affect global LHC-Higgs fits including kinematic distributions. Turning the argument around, we ask whether and when the analysis of a UV-complete model offers an advantage compared to the effective theory.

After this broad survey of the applicability of dimension-six operators, we focus on the vector triplet scenario and WBF Higgs production and briefly discuss some practical aspects. The first question is whether it is justified or preferable to include the square of dimension-six operators in calculations while neglecting dimension-eight operators interfering with the SM. Both contribute at the same order $\mathcal{O}\left(1/\Lambda^4\right)$ to the squared amplitude.

We also discuss is whether a naive simplified model with a new light scalar can improve the description where the EFT breaks down, analyse the correlation of different kinematic observables with the unobservable momentum transfer in WBF Higgs production, and check whether the differences between full and effective descriptions survive a realistic parton shower and jet reconstruction.

In addition and mostly simultanously to our work, published in References [2, 3], the applicability of EFTs to Higgs physics at the LHC was studied in a range of different situations [4, 110–122]. The differences to our work lies in the considered new physics scenarios and observables. A lot of attention focussed on Higgs production in weak boson fusion and its sensitivity to UV physics [123–126]. Similar points were discussed for Higgs-strahlung [110], in the production of (potentially off-shell) Higgs bosons in gluon fusion [115, 119, 127–129], and in electroweak precision observables as well as Higgs decays to photons [122]. With the notable exception of Reference [122],

these other studies generally do not discuss ambiguities in the matching procedure, a central aspect of the research presented here.

The problem of a lack of scale hierarchy is not unique to the EFT approach. As discussed at the end of Section 2.3.4, pseudo-observables rely on the same expansion in $1/\Lambda$, and the breakdown of this expansion has been studied in Reference [104].

As an aside, similar concerns have fuelled an intense investigation in the context of dark matter searches [130–135]. While in that field EFT-based predictions are usually robust for early-universe and late-time annihilation rates as well as for dark matter-nucleon scattering, the required hierarchy of scales often breaks down for dark matter signals at colliders.

3.2 Matching in the Time of LHC Run 2

3.2.1 Ambiguities

Before discussing the individual models and presenting our results, we have to define how we construct the effective models. Matching the dimension-six Lagrangian to a full model is a three-step procedure. Its starting point is the definition of a heavy mass scale Λ. Second, we integrate out the degrees of freedom above Λ as described in Section 2.2.3, which leads to an infinite tower of higher-dimensional operators. Finally, this effective action is truncated so that only the dimension-six terms, suppressed by $1/\Lambda^2$, remain.

The matching is not unambiguous: on the one hand, Λ is usually not uniquely defined. A typical case is a new physics scenario with only one heavy mass scale M in the Lagrangian, but also some mixing terms of the new fields with the SM Higgs doublet. In the unbroken electroweak phase the only new physics scale is then

$$\Lambda_1 = M\,. \tag{3.5}$$

But after electroweak symmetry breaking, the electroweak VEV contributes through the mixing term to the actual physical masses m of the new particles. Even if there is only one dimensionful scale of new physics in the Lagrangian, this defines additional scales of the form

$$\Lambda_2^2 = m^2 = M^2 \pm g^2 v^2\,, \tag{3.6}$$

where g is a combination of couplings or mixing angles. Of course there can be many such scales.

Further ambiguities arise in the third step since we can choose which parameters to keep constant while expanding in $1/\Lambda$. For instance we can often choose to define Wilson coefficients in terms of Lagrangian couplings or in terms of mixing angles. Again, the first choice corresponds to the natural choice in the unbroken phase of the electroweak symmetry, while the latter is often only defined in the broken phase.

In both scenarios, switching from one choice to another corresponds to including additional contributions suppressed by v^2/Λ^2 to the Wilson coefficients of the dimension-six operators. In the first example,

$$\begin{aligned}\frac{f_x}{\Lambda_2^2}\,\mathcal{O}_x &= \frac{f_x}{M^2 \pm g^2 v^2}\,\mathcal{O}_x = \frac{f_x}{M^2}\left(1 \mp \frac{g^2 v^2}{M^2} + \mathcal{O}\big(1/M^4\big)\right)\mathcal{O}_x \\ &= \left(\frac{f_x}{\Lambda_1^2} \mp \frac{f_x g^2 v^2}{\Lambda_1^4}\right)\mathcal{O}_x + \mathcal{O}\big(1/\Lambda_1^6\big)\,. \end{aligned} \tag{3.7}$$

It should be stressed that these effects always contribute to observables at $\mathcal{O}\big(1/\Lambda^4\big)$, the same order in the EFT expansion as the leading effects from dimension-eight operators, which we always neglect. From a purely theoretical point of view these terms are subleading, and indeed in the obvious validity regime of the EFT they are irrelevant. But this is not the situation we find at the LHC. In practice, these formally suppressed terms may be important even if the dimension-eight terms are small.

These ambiguities in the matching procedure raise the question if we can improve the agreement between full model and dimension-six Lagrangian by incorporating effects of the non-zero electroweak VEV in the matching. To answer this question we now define two different matching prescriptions.

3.2.2 Default vs. v-improved matching

Our **default matching** follows a purely theoretical motivation and represents the conventional approach to matching. The linear Higgs EFT is formulated in terms of the doublet ϕ and based on the assumption $\Lambda \gg v$. It should therefore be matched to the full theory in the unbroken phase of the electroweak symmetry. An obvious choice for the matching scale is then the mass scale of new particles in the limit of $v \to 0$, which as in our simple example above we denote

$$\Lambda_{\text{default}} = M\,. \tag{3.8}$$

For simplicity we assume there is only one such scale, i. e. that all new particles are mass-degenerate in the unbroken electroweak phase. Otherwise the new particles would have to be integrated out consecutively at different scales M_i. We then expand the effective action, expressed in parameters of the Lagrangian, and drop all terms of $\mathcal{O}\big(\Lambda^{-4}\big)$.

Alternatively, we define a v-**improved matching** procedure that accounts for additional terms suppressed by v^2/Λ^2 in the Wilson coefficients of the dimension-six Lagrangian. This corresponds to matching the linear EFT in the broken electroweak phase. In the first matching step, we define Λ as the physical mass m of the new particles in the broken phase including contributions from v,

$$\Lambda_{v\text{-improved}} = m\,, \tag{3.9}$$

rather than the mass scale in the unbroken phase. Again, multiple particles with substantial mass splittings will require a multi-step matching procedure, but there is no fundamental problem to describe them. The Wilson coefficients are expressed in terms of phenomenologically relevant quantities such as mixing angles and physical masses, again defined in the broken phase. This is a somewhat subjective criterion that depends on model and process: the v-improved matching procedure is not a unique definition, but rather a general guideline. We will demonstrate an example for a natural choice in the singlet scenario.

3.2.3 Making sense of v-improvement

We can interpret the two matching schemes from two different perspectives. First we analyse it from the unbroken electroweak phase. Some of the operators with dimension 8 or higher are of the form

$$\mathcal{O}_i^{(d=6+2n)} = (\phi^\dagger\phi)^n \mathcal{O}_i^{(6)}\,, \tag{3.10}$$

where $\mathcal{O}_i^{(6)}$ is a dimension-six operator. The untruncated, infinite tower of higher-dimensional operators generated from the full theory can be re-organised as

$$\begin{aligned}\mathcal{L}_{\text{EFT}} &\equiv \mathcal{L}_{\text{SM}} + \sum_{d=6}^{\infty}\sum_i \frac{f_i^{(d)}}{\Lambda^{d-4}}\mathcal{O}_i^{(d)} \\ &= \mathcal{L}_{\text{SM}} + \sum_i \sum_{n=0}^{\infty} \frac{f_i^{(6+2n)}}{\Lambda^{2+2n}} \left(\phi^\dagger\phi\right)^n \mathcal{O}_i^{(6)} + \sum_{d=8}^{\infty}\sum_k \frac{f_k^{(d)}}{\Lambda^{d-4}}\mathcal{O}_k^{(d)}\,,\end{aligned} \tag{3.11}$$

where $\mathcal{O}_k^{(d)}$ are the dimension-eight and higher operators of a different form than Equation (3.10). A v-improved matching corresponds to replacing $\phi^\dagger\phi \to v^2/2$ in (part of) the first sum:[1]

$$\mathcal{L}_{v\text{-improved dim-6}} = \mathcal{L}_{\text{SM}} + \sum_i \frac{\overbrace{\sum_{n=0}^{\infty} f_i^{(6+2n)} \left(\frac{v^2}{2\Lambda^2}\right)^n}^{f_i^{(6),v\text{-improved}}}}{\Lambda^2}\mathcal{O}_i^{(6)}\,. \tag{3.12}$$

So from the perspective of the unbroken phase of the electroweak symmetry, v-improvement corresponds to a **partial resummation of dimension-eight and higher operators** into the Wilson coefficients of the dimension-six operators.

[1] The argument is slightly more complicated if additional powers of ϕ appear in $\mathcal{O}_i^{(6)}$. One can then also take into account terms where instances of ϕ in $\mathcal{O}_i^{(6)}$ are replaced by the VEV and fields in the prefactor are left alone. This effectively adds a combinatorical factor to Equation (3.12).

From an experimental point of view, or in the broken electroweak phase, physical masses and mixing angles are simply the natural choices to describe a model. We then expect that the v-improved matching procedure can improve the validity of the dimension-six model. For a more precise statement we have to distinguish between an expansion in v/Λ and $\mathbf{p}/\Lambda$. We expect the v-improved matching prescription can lead to a better agreement with the full models in situations where the expansion in v/Λ is relevant, while it cannot help with the expansion in $\mathbf{p}/\Lambda$, corresponding to genuine new dimension-eight operators not of the form in Equation (3.10). We will come back to this difference later and demonstrate it in the vector triplet scenario.

Again, the truncation of the EFT Lagrangian is formally justified as long as $v \ll \Lambda$ and we only probe energies $E \ll \Lambda$. In this limit the dimension-eight operators as well as the Λ-suppressed terms in the Wilson coefficients are negligible; our two matching procedures then give identical results. In the absence of a large enough scale separation, our bottom-up approach allows us to treat them independently. This way we can use the v-improved matching to enhance the validity of the dimension-six Lagrangian.

3.3 Full models vs. effective theory

The main aim of this chapter is to compare a comprehensive set of LHC predictions from specific new physics models to their corresponding effective field theory predictions. In this way we test the applicability of the dimension-six model for four different, more or less UV-complete, scenarios of underlying physics:

1. a scalar singlet extension with mixing effects and a second scalar resonance;
2. a two-Higgs doublet model, adding a variable Yukawa structure, a CP-odd, and a charged Higgs;
3. scalar top partners, contributing to Higgs couplings at one loop; and
4. a vector triplet with gauge boson mixing.

This ensemble of models covers a wide range of CP-even new physics signatures in the Higgs sector.

After describing our technical setup, we analyse these four scenarios one by one. For each model we first define the theory and introduce the main phenomenological features at the LHC. We discuss the decoupling in the Higgs sector, and derive the dimension-six setup. Finally, we define a number of benchmark points and give a detailed account of the full and dimension-six phenomenology at the LHC.

Effects in the SM-like Higgs couplings will be parametrised with the relative shifts from the SM values

$$\Delta_x \equiv \frac{g_{hxx}}{g_{hxx}^{\text{SM}}} - 1 \,, \tag{3.13}$$

as defined in Equation (2.80). Unlike in the published version [2], we express the effective Lagrangian in the HISZ basis with the ten dimension-six operators of Equation (2.60).

3.3.1 Setup

Our comparison covers the most relevant observables for LHC Higgs physics. Acceptance and background rejections cuts are kept to a minimum to be able to test the effective field theory approach over as much of the phase space as possible.

In the case of Higgs production through gluon fusion, we analyse the production process with a Higgs decay to four leptons or to photons,

$$\begin{aligned} gg &\to h \to 4\ell\,, \\ gg &\to h \to \gamma\gamma\,. \end{aligned} \tag{3.14}$$

For the photons we do not apply any cuts, while for $\ell = e, \mu$ we require

$$m_{4\ell} > 100\ \text{GeV} \quad \text{and} \quad m_{\ell^+\ell^-}^{\text{same flavour}} > 10\ \text{GeV} \tag{3.15}$$

to avoid too large contributions from the Z peak and bremsstrahlung.

For Higgs production in weak boson fusion (WBF), we evaluate the production process

$$ud \to h\,ud \to W^+W^-\,ud \to (\ell^+\nu)\,(\ell^-\bar{\nu})\,ud\,, \tag{3.16}$$

which is the dominant partonic contribution at the LHC. We require the standard WBF cuts

$$\begin{aligned} &p_{T,j} > 20\ \text{GeV}\,, && \Delta\eta_{jj} > 3.6\,, && m_{jj} > 500\ \text{GeV}\,, \\ &p_{T,\ell} > 10\ \text{GeV}\,, && \not{E}_T > 10\ \text{GeV}\,. \end{aligned} \tag{3.17}$$

Unlike for gluon fusion, the kinematics of the final state can now introduce new scales and a dependence on the UV structure of the model. The process is particularly interesting in the context of perturbative unitarity [136–142]. While the latter is satisfied in a UV-complete model by construction, deviations from the SM Higgs-gauge couplings in the EFT may lead to an increasing rate at very large energies [126, 143], well outside the EFT validity range $E/\Lambda \ll 1$. To look for such signatures, we focus on the high-energy tail of the transverse mass distribution,

$$m_T^2 = \left(E_{T,\ell\ell} + E_{T,\nu\nu}\right)^2 - \left(\mathbf{p}_{T,\ell\ell} + \mathbf{p}_T^{\text{miss}}\right)^2 \tag{3.18}$$

with

$$E_{T,\ell\ell} = \sqrt{\mathbf{p}_{T,\ell\ell}^2 + m_{\ell\ell}^2}\,, \quad E_{T,\nu\nu} = \sqrt{\not{E}_T + m_{\ell\ell}^2}\,. \tag{3.19}$$

As the last single Higgs production process we evaluate Higgs-strahlung

$$qq \to Vh \tag{3.20}$$

with $V = W^\pm, Z$. We do not simulate the Higgs and gauge boson decays, assuming that we can always reconstruct for example the full $Zh \to \ell^+\ell^- b\bar{b}$ final state. No cuts are applied.

Finally, Higgs pair production,

$$gg \to hh\,, \tag{3.21}$$

is well known to be problematic when it comes to the effective theory description [38, 144, 145]. Again, neither Higgs decays nor kinematic cuts are expected to affect our analysis, so we leave them out.

We test all these channels for the singlet and doublet Higgs sector extensions. For the top partner and vector triplet models we focus on the WBF and Higgs-strahlung modes.

In the dimension-six simulations we always include the square of the dimension-six operator contributions. While these terms are technically of the same mass dimension as dimension-eight operators, which we neglect, we keep them to avoid negative values of the squared matrix element in extreme phase-space regions. Notice that these situations do not necessarily imply a breakdown of the EFT expansion. On the contrary, they may appear in scenarios where new physics contributions dominate over the SM part, while the EFT expansion is fully valid (with $E/\Lambda \ll 1$). In such cases, the bulk effects stem from the squared dimension-six terms instead of the interference with the SM, while the effects from dimension-eight operators are smaller and can be safely neglected. We will discuss this aspect in more detail in the next section.

Most amplitudes are calculated at leading order in α_s and α_{ew}, which is sufficient given the size of new physics effects that the LHC is sensitive to. We always take into account interference terms between Higgs and gauge amplitudes.

For tree-level processes we generate event samples with `MadGraph 5` [146], using publicly available our own model files implemented in `FeynRules` [147], which provides the corresponding UFO files [148]. For the dimension-six predictions we resort to a modified version of the `HEL` model file [149].

The Higgs-gluon and Higgs-photon couplings are evaluated with the full one-loop form factors [150], including top, bottom and W loops as well as new particles present in the respective models. For Higgs pair production, we use a modified version of Reference [151], see also Reference [152].

Other loop effects are analysed using reweighting: we generate event samples using appropriate general couplings. Next, we compute the one-loop matrix element for each phase space point and reweight the events with the ratio of the renormalised one-loop matrix element squared to the tree-level model. For the one-loop matrix elements we utilise `FeynArts` and `FormCalc` [153] with our own model files that include the necessary counterterms. The loop form factors are handled with dimensional regularisation in the 't Hooft-Veltman scheme, and written in terms of standard loop integrals. These are further reduced via Passarino-Veltman decomposition and evaluated with the help of `LoopTools` [154].

Generally we create event samples of at least 100 000 events per benchmark point and process for pp collisions at $\sqrt{s}$ = 13 TeV. We use the `CTEQ6L` pdf [155] and the default dynamical choices of the factorisation and renormalisation scale implemented in `MadGraph`. For this broad survey of EFT validity we limit ourselves to parton level and do not apply a detector simulation, a more realistic simulation will be discussed in the next section. The mass of the SM-like Higgs is fixed to m_h = 125 GeV [156]. For the top mass we take m_t = 173.2 GeV [157, 158]. The Higgs width in each model is based on calculations with `Hdecay` [159], which we rescale with the appropriate coupling modifiers and complement with additional decay channels where applicable.

3.3.2 Singlet extension

Model setup

The simplest extension of the minimal Higgs sector of the Standard Model is by a real scalar singlet S [160–166]. For the sake of simplicity we consider a minimal version of the singlet model, in which a discrete $\mathbb{Z}_2$ parity forbids additional (e. g. cubic) terms in the potential. The theory is then given by

$$\mathcal{L}_{\text{singlet}} \supset (D_\mu \phi)^\dagger (D^\mu \phi) + \frac{1}{2}\, \partial_\mu S\, \partial^\mu S - V(\phi, S)\,, \tag{3.22}$$

where the scalar potential has the form

$$V(\phi, S) = \mu_1^2\, \phi^\dagger \phi + \lambda_1 \left(\phi^\dagger \phi\right)^2 + \mu_2^2\, S^2 + \lambda_2\, S^4 + \lambda_3 \left(\phi^\dagger \phi\right) S^2\,. \tag{3.23}$$

The new scalar S can mix with the SM doublet ϕ provided the singlet develops a VEV,

$$\langle S \rangle = \frac{v_s}{\sqrt{2}}\,. \tag{3.24}$$

The mixing angle is given by

$$\tan(2\alpha) = \frac{\lambda_3 v v_s}{\lambda_2 v_s^2 - \lambda_1 v^2}\,. \tag{3.25}$$

Details on the parametrisation and Higgs mass spectrum are given in Appendix 2.1.

Signatures and decoupling patterns

The additional scalar singlet affects Higgs physics in three ways. First, it mixes with the Higgs via the mixing angle α, which leads to a universal rescaling of all Higgs couplings to fermions and vectors. Second, it modifies the Higgs self-coupling. Finally, it introduces a new, heavy resonance H coupled to the Standard Model through mixing.

The key parameter is the portal interaction between the doublet and the singlet fields $\lambda_3(\phi^\dagger\phi)\,S^2$, which is responsible for the mixed mass eigenstates. The mixing reduces the coupling of the SM-like Higgs h to all Standard Model particles universally,

$$\Delta_x = \cos\alpha - 1 \tag{3.26}$$

for $x = W, Z, t, b, \tau, g, \gamma, \ldots$. It also affects the self-coupling of the light Higgs, which takes on the form

$$g_{hhh} = 6\cos^3\alpha\,\lambda_1 v - 3\cos^2\alpha\sin\alpha\,\lambda_3 v_s + 3\cos\alpha\sin^2\alpha\,\lambda_3 v - 6\sin^3\alpha\,\lambda_2 v_s\,. \tag{3.27}$$

The parameter $\sin\alpha$ quantifies the departure from the SM limit $\alpha \to 0$. This limit can be attained in two ways: first, a small mixing angle can be caused by a weak portal interaction,

$$|\tan(2\alpha)| = \left|\frac{\lambda_3\, v\, v_s}{\lambda_2 v_s^2 - \lambda_1 v^2}\right| \ll 1 \quad \text{if} \quad \lambda_3 \ll 1\,. \tag{3.28}$$

The Higgs couplings to SM particles approach their SM values, but there is no large mass scale associated with this limit. In the extreme case of $\lambda_2, \lambda_3 \ll \lambda_1$ we find small $\alpha \approx -\lambda_3/\lambda_1 \times v_s/(2v)$ even for $v_s \lesssim v$. This situation is to some extent the singlet model counterpart of the "alignment without decoupling" scenario in the Two-Higgs-doublet model (2HDM) [167, 168] or the MSSM [169, 170]. It relies on a weak portal coupling and a small scale separation, which cannot be properly described by an effective field theory.

As a second possibility, the additional singlet can introduce a large mass scale $v_s \gg v$, giving us

$$\tan\alpha \approx \frac{\lambda_3}{2\lambda_2}\,\frac{v}{v_s} \ll 1 \quad \text{if} \quad v \ll v_s\,, \tag{3.29}$$

where $\lambda_3/(2\lambda_2)$ is an effective coupling of up to order one. In this limit the heavy Higgs mass, which we identify as the heavy mass scale, is given by

$$m_H \approx \sqrt{2\lambda_2}\, v_s\,. \tag{3.30}$$

In terms of m_H, the Higgs couplings scale like

$$\Delta_x = -\frac{\alpha^2}{2} + \mathcal{O}\big(\alpha^3\big) \approx -\frac{\lambda_3^2}{4\lambda_2}\left(\frac{v}{m_H}\right)^2\,. \tag{3.31}$$

This is a dimension-six effect. If we require $|\Delta_x| \gtrsim 10\%$ to keep our discussion relevant for the LHC, this implies

$$m_H \approx \sqrt{2\lambda_2}\, v_s < \frac{\sqrt{5}\lambda_3}{\sqrt{2\lambda_2}}\, v = 390\ \text{GeV} \times \frac{\lambda_3}{\sqrt{\lambda_2}}\,. \tag{3.32}$$

If we also assume that the ratio of quartic couplings is of the order of a perturbative coupling, $\lambda_3/\sqrt{\lambda_2} \lesssim 0.5$, the LHC reach in the Higgs coupling analysis translates into heavy Higgs masses below 200 GeV. For strongly coupled scenarios, $\lambda_3/\sqrt{\lambda_2} \lesssim 1 \ldots \sqrt{4\pi}$, the heavy mass reach increases to $m_H \lesssim 0.4 \ldots 1.5$ TeV. This suggests that a weakly coupled Higgs portal will fail to produce a sizeable separation of scales when looking at realistic Higgs coupling analyses. The question becomes if and where this lack of scale separation hampers our LHC analyses.

Dimension-six description

In the EFT approach the singlet model only generates $\mathcal{O}_{\phi,2}$ at dimension six [117]. Before electroweak symmetry breaking, the only mass scale in the Lagrangian that describes the new physics is $\mu_2^2 < 0$. Defining the Wilson coefficients suppressed by this new physics scale gives clearly wrong results, as we will discuss in the analogous case for the two-Higgs-doublet model in the next section. Instead identify the leading contribution to the heavy Higgs mass as the new physics scale in our default matching, in agreement with the logic Section 3.2. Following the discussion of decoupling patterns above this means

$$\Lambda_{\text{default}} = \sqrt{2\lambda_2}\, v_s \approx m_H \,. \tag{3.33}$$

The corresponding Wilson coefficient, expressed in terms of Lagrangian parameters, is

$$\tilde{f}_{\phi,2}^{\text{default}} = \frac{\lambda_3^2}{2\lambda_2} \,. \tag{3.34}$$

For the v-improved matching, we instead use the actual physical mass

$$\Lambda_{v\text{-improved}} = m_H \,. \tag{3.35}$$

In the broken phase the Higgs couplings are fully expressed through the mixing angle α as given in Equation (3.26). We define

$$f_{\phi,2}^{v\text{-improved}} = 2(1-\cos\alpha)\frac{m_H^2}{v^2} \,. \tag{3.36}$$

which ensures that the Higgs couplings exactly agree between the full model and the v-improved dimension-six description.

Benchmark points

We start our numerical analysis by defining five singlet benchmark points in Table 3.1, with heavy Higgses ranging from 200 to 1000 GeV. The first three scenarios are in agreement with current experimental and theoretical constraints. This includes direct mass bounds from heavy

	Singlet				Default EFT			v-improved EFT		
	m_H	$\sin\alpha$	v_s/v	Δ_x	Λ	$f_{\phi,2}$	Δ_x	Λ	$f_{\phi,2}$	Δ_x
S1	500	0.2	10	−0.020	491	0.14	−0.018	500	0.15	−0.020
S2	350	0.3	10	−0.046	336	0.14	−0.037	350	0.16	−0.046
S3	200	0.4	10	−0.083	190	0.04	−0.031	200	0.06	−0.083
S4	1000	0.4	10	−0.083	918	2.60	−0.092	1000	3.13	−0.083
S5	500	0.6	10	−0.200	407	1.26	−0.231	500	1.24	−0.200

Table 3.1: Benchmarks for the singlet extension. We show the model parameters and the universal coupling modification for the complete model, as well as the cutoff scales Λ, Wilson coefficients $\bar{f}_{\phi,2}$, and the universal coupling modification in the EFT approach for the default and v-improved matching schemes. All mass scales are given in GeV.

Higgs searches at colliders, Higgs coupling measurements, electroweak precision observables, perturbative unitarity and vacuum stability [163–165]. Note that for S4 and S5 the combination of large heavy Higgs masses together with large mixing angles is incompatible with perturbative unitarity and electroweak precision constraints. We nevertheless keep such benchmarks for illustration purposes.

Higgs couplings and total production rates

Table 3.1 also shows the universal shift Δ_x of the light Higgs couplings, both for the full singlet model and its dimension-six EFT descriptions. For the default matching, we find reasonable agreement with the full model for the scenarios with a heavy additional Higgs, while large discrepancies appear when the new physics is lighter. In particular, note the difference between S3 and S4. Both describe the same coupling shift $\Delta_x = -0.08$. But while S3 realises this with a weakly coupled light Higgs, which the default EFT cannot describe, S4 has a heavier, more strongly coupled Higgs, and the EFT description works. In all cases, the v-improved EFT by construction predicts the Higgs couplings correctly.

In Table 3.2 we show how well the effective models describe the total Higgs production cross sections in gluon fusion, WBF and Higgs-strahlung. These numbers confirm what we expect from the coupling modifications: while the default dimension-six model predict qualitatively similar shifts in the total rates, there are rate deviations of up to 10%. In the v-improved EFT we find that the Higgs couplings and total rates agree exactly with the full model predictions. The dimension-six operators are entirely sufficient to capture the coupling shifts, but a significant part of their coefficients are formally of $\mathcal{O}\left(v^4/\Lambda^4\right)$.

	$\sigma_{\text{default EFT}}/\sigma_{\text{singlet}}$			$\sigma_{v\text{-improved EFT}}/\sigma_{\text{singlet}}$		
	ggF	WBF	Vh	ggF	WBF	Vh
S1	1.006	1.006	1.004	1.001	1.001	1.000
S2	1.019	1.021	1.019	1.000	1.001	1.000
S3	1.119	1.118	1.118	1.000	0.999	1.000
S4	0.982	0.982	0.982	0.999	0.999	1.000
S5	0.925	0.925	0.925	0.999	0.999	1.000

Table 3.2: Cross section ratios of the matched dimension-six EFT approximation to the full singlet model at the LHC. We show the leading Higgs production channels for all singlet benchmark points. The statistical uncertainties on these ratios are below 0.4%.

Distributions

The most obvious source of discrepancy between the full model and the EFT is the heavy resonance H. It can for example be produced in gluon fusion and then observed as a peak in the $m_{4\ell}$ distribution. By construction, it will not be captured by the dimension-six model. We illustrate this in the upper left panel of Figure 3.1. For Higgs-strahlung production (Figure 3.1, upper right panel), where the novel H resonance does not appear in an intermediate Born-level propagator and hence has no impact, we find instead excellent agreement between both descriptions over the entire phase space.

The second Higgs has a second, more subtle effect. In the full model, both Higgs exchange diagrams are needed to unitarise WW scattering. Correspondingly, the EFT description breaks perturbative unitarity roughly at the scale [143]

$$m_{WW}^2 \sim \frac{16\pi}{\frac{f_{\phi,2}}{\Lambda^2}\left(1-\frac{f_{\phi,2}v^2/\Lambda^2}{4(1+f_{\phi,2}v^2/\Lambda^2)}\right)} \approx \left(\frac{1.7\text{ TeV}}{\sin\alpha}\right)^2 . \tag{3.37}$$

In our benchmark point S5, this is around 2.8 TeV. The incomplete cancellations between Higgs and gauge amplitudes means that the dimension-six model tends to have a larger rate at energies already below this scale. For this specific benchmark choice, this can be seen in the lower left panel of Figure 3.1, where we show the distribution of the transverse mass defined in Equation (3.18) in the process $ud \to W^+W^- ud \to (\ell^+\nu)\,(\ell^-\bar{\nu})\,ud$, to which WBF production of both h and H contributes. We observe that the dimension-six model predicts a slightly higher rate at large m_T than both the full singlet model and the SM. Given the very mild signal, which results from the fast decrease in the parton densities and the small mixing angle for realistic scenarios, such effect is likely of no relevance for LHC physics.

A more interesting channel to study in the singlet model is Higgs pair production. The Higgs

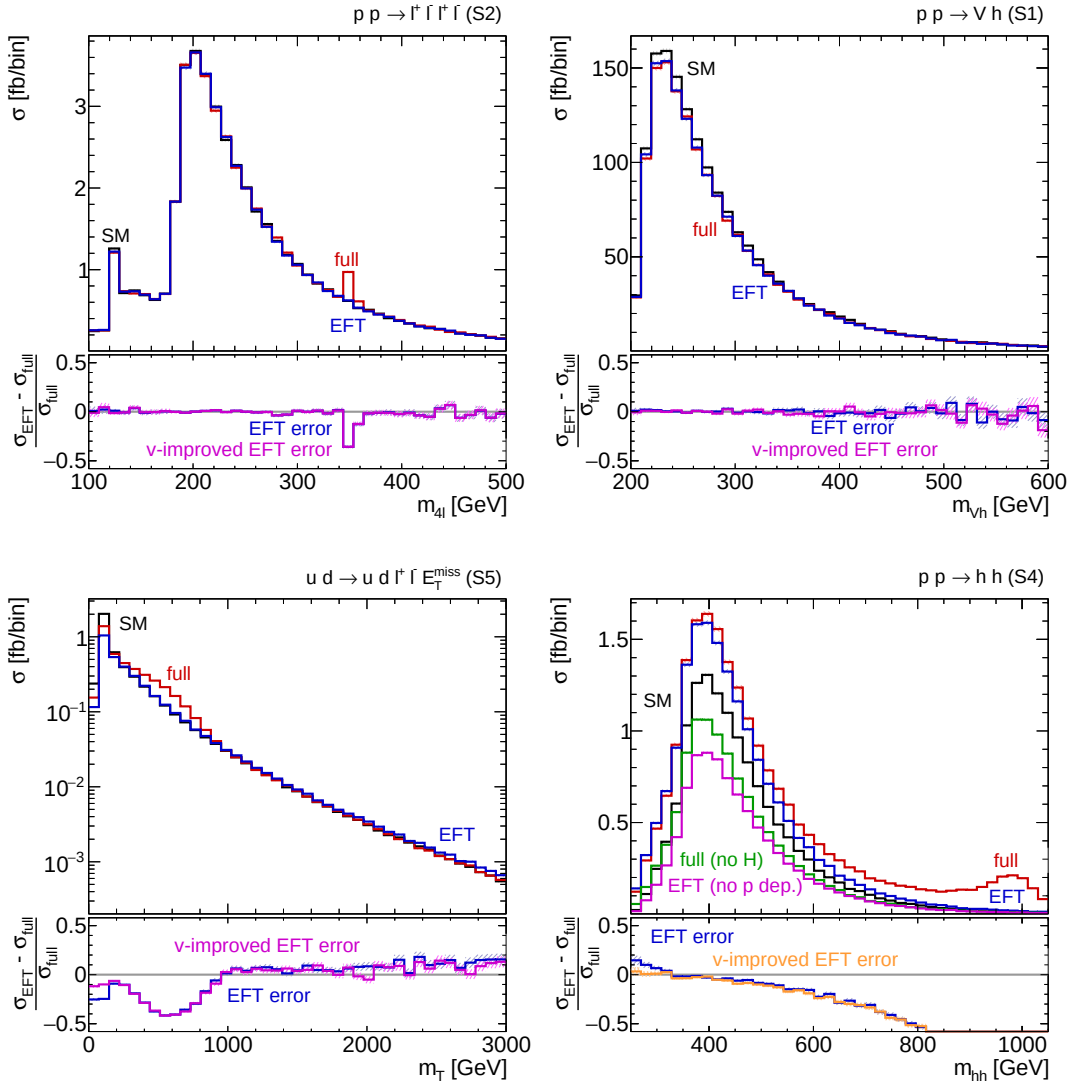

Figure 3.1: Selected kinematic distributions in the singlet model. The different curves show the SM, the full singlet model, and the dimension-six model. Top left: $m_{4\ell}$ distribution in the $gg \to h \to 4\ell$ channel for S2. Top right: m_{Vh} distribution in Vh production for S1. Bottom left: m_T distribution in the WBF $h \to \ell^+\ell^- \not{E}_T$ channel for S5. Bottom right: m_{hh} distribution in Higgs pair production for S4. For m_{hh} we show several contributions in the full theory and the dimension-six approach. In all plots, the error bars give the statistical uncertainties.

self-coupling is the only Higgs coupling which gains a momentum dependence in the matched EFT. In addition, there exists an approximate cancellation between the two leading amplitudes in the SM at threshold [37, 39]. This induces a second relevant scale and with it a sensitivity to small deviations in the Higgs couplings.

In the bottom right panel of Figure 3.1 we give the m_{hh} distribution in the full and dimension-six models. In addition, we show how the distributions would look in the full model without a H state, and in the EFT without the momentum-dependent (derivative) terms given in Equation (**??**). Already at threshold and far away from the H resonance, the interference of the SM-like terms with the H diagrams makes up a significant part of the amplitude. In the EFT, the derivative terms are similarly relevant already at low energies. Close to threshold, the (v-improved) dimension-six model approximates the full theory well. But this agreement becomes worse already at moderately larger energies, and clearly breaks down towards the H pole.

Summary

If we limit ourselves to Higgs properties relevant for single Higgs production at the LHC, the modifications from a singlet extension are very simple: all Standard Model couplings acquire a common scaling factor, and no relevant new Lorentz structures appear at tree-level. The dimension-six setup reproduces this effect correctly: the reduced couplings to all SM fields alone do not require a large hierarchy of scales. A standard matching procedure that expands the coefficients to leading order in v^2/Λ^2 may lead to sizeable deviations from the full model. However, a v-improved EFT construction that takes into account higher orders in v^2/Λ^2 gives perfect agreement with the full theory. In other words, many of the dimension-eight and higher operators generated from the singlet model are of the form $(\phi^\dagger\phi)^n\mathcal{O}_i^{(6)}$. After EWSB they can be resummed into the Wilson coefficients of the dimension-six operators as given by Eq. (3.12).

Higgs pair production is different. There is a large contribution from off-shell H, while in the EFT the h self-coupling involves a derivative. These different structures lead to discrepancies between full and effective description that increase with momentum transfer. Of course, the effective theory by definition does not include the second resonance, so it fails whenever a heavy Higgs appears on-shell in the full theory.

3.3.3 Two-Higgs-doublet model

Model setup

The two-Higgs-doublet model (2HDM) [171, 172] adds a second weak doublet with weak hypercharge $Y = +1$ to the SM Higgs sector. The combined potential reads

$$V(\phi_1, \phi_2) = m_{11}^2\, \phi_1^\dagger \phi_1 + m_{22}^2\, \phi_2^\dagger \phi_2 + \frac{\lambda_1}{2}\, (\phi_1^\dagger \phi_1)^2 + \frac{\lambda_2}{2}\, (\phi_2^\dagger \phi_2)^2 + \lambda_3\, (\phi_1^\dagger \phi_1)\, (\phi_2^\dagger \phi_2) + \lambda_4\, |\phi_1^\dagger\, \phi_2|^2 + \left[-m_{12}^2\, \phi_1^\dagger \phi_2 + \frac{\lambda_5}{2}\, (\phi_1^\dagger \phi_2)^2 + \text{h. c.} \right] . \quad (3.38)$$

The mass terms m_{ij}^2 and the dimensionless self-couplings λ_i are real parameters. The doublet VEVs $\langle \phi_j^0 \rangle = v_j/\sqrt{2}$ are parametrised by their ratio $\tan\beta = v_2/v_1$. For the Yukawa couplings, there are four possible scenarios that satisfy the SM flavour symmetry and preclude tree-level flavour-changing neutral currents (FCNCs) [173]:

- type I, where all fermions couple to just one Higgs doublet ϕ_2;
- type II, where up-type (down-type) fermions couple exclusively to ϕ_2 (ϕ_1);
- lepton-specific, with a type-I quark sector and a type-II lepton sector; and
- flipped, with a type-II quark sector and a type-I lepton sector.

For simplicity, we restrict our discussion to type I and type II. In all four cases, the absence of tree-level FCNCs is protected by a global $\mathbb{Z}_2$ discrete symmetry $\phi_i \to (-1)^i\, \phi_i$ (for $i = 1, 2$). This symmetry is softly broken by the mixed mass term m_{12}.

The physical degrees of freedoms are two neutral CP-even scalars h^0, H^0, one neutral CP-odd scalar A^0, and a set of charged scalars $H^\pm$, parametrised by the mixing angle between the CP-even scalars α. For a detailed account of the model setup, see Appendix 2.2.

Signatures and decoupling patterns

Just as the singlet extension, the 2HDM predicts two types of LHC signatures: first, scalar and VEV mixing lead to modified light Higgs couplings. Unlike for the singlet extension, these coupling modifications are not universal and reflect the more flexible flavour structure as well as the multiple scales of the model. Second, there are three new heavy resonances H^0, A^0, and $H^\pm$, which should have near-degenerate masses to avoid custodial symmetry breaking.

The light Higgs coupling to weak bosons $V = W, Z$ always scales like

$$\Delta_V = \sin(\beta - \alpha) - 1 = -\frac{\cos^2(\beta - \alpha)}{2} + \mathcal{O}\big(\cos^4(\beta - \alpha)\big) . \quad (3.39)$$

We can insert the leading contribution of a mass-degenerate heavy Higgs sector and find

$$\Delta_V \approx \frac{\sin^2(2\beta)}{8} \left(\frac{v}{m_{A^0}} \right)^4 . \quad (3.40)$$

While in the singlet model the light Higgs coupling to gauge bosons is shifted at $\mathcal{O}\left(v^2/m_H^2\right)$, see Equation (3.31), the same coupling is now affected at $\mathcal{O}\left(v^4/m_{A^0}^4\right)$, corresponding to a dimension-eight effect.

The couplings to the fermions on the other hand are modified at $\mathcal{O}\left(v^2/m_{A_0}^2\right)$. For up-type quarks, we find

$$1 + \Delta_t = \frac{\cos\alpha}{\sin\beta} \,. \tag{3.41}$$

The couplings to down-type quarks and leptons are

$$1 + \Delta_b = 1 + \Delta_\tau = \frac{\cos\alpha}{\sin\beta} \tag{3.42}$$

in a type-I model and

$$1 + \Delta_b = 1 + \Delta_\tau = -\frac{\sin\alpha}{\cos\beta} \tag{3.43}$$

in a type-II 2HDM.

Finally, a $H^\pm$ loop contributes to the Higgs-photon coupling. The expression for this coupling shift is given in Equation (33) in Appendix 2.2.

Two aspects turn the decoupling in the general 2HDM into a challenge: first, delayed decoupling effects appear after electroweak symmetry breaking [174]. For example, in type-II models we find [101]

$$\Delta_b \approx -\tan\beta\,\frac{\sin(2\beta)}{2}\left(\frac{v}{m_{A^0}}\right)^2 \,. \tag{3.44}$$

This correction to the bottom Yukawa coupling corresponds to a dimension-six effect, and already moderate values of $\tan\beta$ significantly delay the decoupling of the heavy 2HDM states in the Yukawa sector.

Second, unlike in the MSSM, the Higgs self-couplings $\lambda_1 \ldots \lambda_5$ and m_{12} are not bounded from above. In combinations like $\lambda_j v^2$, potentially enhanced with factors of $\tan' beta$, they contribute to the masses of the heavy Higgs bosons and to the interactions of the SM-like Higgs state, effectively inducing new energy scales.

Such additional mass scales driven by v leads to problems with any EFT derived from and matched to the full theory assuming only one new physics scale. While this should not be viewed as a problem of the EFT approach in general, it will require a v-improved matching procedure.

Dimension-six description

We first follow our default procedure and match the effective theory to the 2HDM in the unbroken electroweak phase. To this end, we first rotate ϕ_1 and ϕ_2 into the so-called Higgs basis, where only one Higgs doublet obtains a vacuum expectation value, $\langle\phi_l\rangle = v/\sqrt{2}$, $\langle\phi_h\rangle = 0$ [173, 175]. This doublet ϕ_l is then identified with the SM-like Higgs doublet, while the other doublet ϕ_h is integrated out. This doublet ϕ_l is then identified with the SM-like Higgs doublet, while the other doublet ϕ_h is integrated out. Its decoupling is described by the mass scale

$$\Lambda^2_{\text{default}} = m_{11}^2 \sin^2\beta + m_{22}^2 \cos^2\beta + m_{12}^2 \sin(2\beta)\,. \tag{3.45}$$

The 2HDM generates a number of dimension-six operators at tree level, for which the Wilson coefficients depend on the flavour structure. While the up-type Yukawa coupling is always modified the same way, the down-type and lepton couplings are different for type-I and type-II. With the definition

$$\bar\lambda \equiv \frac{\sin(2\beta)}{2}\left[\frac{\lambda_1}{2} - \frac{\lambda_2}{2} + \left(\frac{\lambda_1}{2} + \frac{\lambda_2}{2} - \lambda_3 - \lambda_4 - \lambda_5\right)\cos(2\beta)\right] \tag{3.46}$$

we find

$$\begin{aligned}
f_t &= -\frac{\bar\lambda y_t}{\tan\beta}\,,\\
f_b &= \begin{cases} -\dfrac{\bar\lambda y_b}{\tan\beta} & \text{type I}\,,\\ \bar\lambda y_b \tan\beta & \text{type II}\,,\end{cases}\\
f_\tau &= \begin{cases} -\dfrac{\bar\lambda y_\tau}{\tan\beta} & \text{type I}\,,\\ \bar\lambda y_\tau \tan\beta & \text{type II}\,.\end{cases}
\end{aligned} \tag{3.47}$$

Here y_t, y_b, y_τ refer to the SM values of the respective Yukawa couplings, $y_f = \sqrt{2}m_f/v$.

The contribution of the $H^\pm$ loop to the Higgs-photon coupling is mapped onto $\mathcal{O}_{BB}$ with a Wilson coefficient

$$\begin{aligned}
f_{BB} = \frac{(\tan\beta + \cot\beta)}{3072\,\pi^2}\Bigg[&\left(\lambda_1 + \lambda_2 - 2\lambda_3 + 6\lambda_4 + 6\lambda_5 - 8\frac{m_{h^0}^2}{v^2}\right)\sin(2\beta)\\
&+ 2(\lambda_1 - \lambda_2)\sin(4\beta) + (\lambda_1 + \lambda_2 - 2\lambda_3 - 2\lambda_4 - 2\lambda_5)\sin(6\beta)\Bigg]\,.
\end{aligned} \tag{3.48}$$

In the effective Lagrangian there are no non-decoupling term of $\mathcal{O}\left(\Lambda^0\right)$ because the charged Higgs loop decouples in the limit $m_{A^0} \to \infty$ with finite λ_i. If instead we keep m_{12} fixed and let

	2HDM						
	Type	$\tan\beta$	α/π	m_{12}	m_{H^0}	m_{A^0}	$m_{H^\pm}$
D1	I	1.5	−0.086	45	230	300	350
D2	II	15	−0.023	116	449	450	457
D3	II	10	0.032	157	500	500	500
D4	I	20	0	45	200	500	500

Table 3.3: Benchmarks for the 2HDM extension. We show the model parameters and the heavy Higgs masses. All masses are in GeV.

one of the couplings λ_i grow with m_{A^0}, the charged Higgs does not decouple. For a derivation of these results see Appendix 2.2.

Upon electroweak symmetry breaking, the physical heavy Higgs masses m_{H^0}, m_{A^0}, and $m_{H^\pm}$ acquire contributions $\sim \lambda_i v^2$ from the electroweak VEV in addition to the heavy scale Λ_{default} defined above. We therefore again consider an alternative v-improved matching where the matching scale is

$$\Lambda_{v\text{-improved}} = m_{A^0} \,. \tag{3.49}$$

In this setup, the Wilson coefficients in Equations (3.47) and (3.48) remain unchanged. The two matching schemes can exhibit significant differences in the 2HDM since the pseudoscalar mass $m_{A^0}^2 = m_{12}^2/(\sin\beta\cos\beta) - \lambda_5 v^2$ does not coincide with Λ_{default} over wide ranges of the parameter space.

Benchmark points

In Table 3.3 we define four benchmark points for the 2HDM. They are in agreement with all constraints at the time of publication of Reference [2], implemented with the help of `2HDMC` [176], `HiggsBounds` [177, 178], `SuperIso` [179], and `HiggsSignals` [180]. To better illustrate certain model features, in some scenarios we tolerate deviations between 1 σ and 2 σ in the Higgs couplings measurements.

The key physics properties of the different 2HDM scenarios can be summarised as:

D1 **Moderate decoupling**: with Higgs couplings shifts of up to 2σ in terms of the LHC constraints. This generates $\Delta_{\tau,b,t} \approx \mathcal{O}(15\%)$ as well as a large $h^0 H^+ H^-$ coupling. Additional Higgs masses around 250 . . . 350 GeV can leave visible imprints.

D2 **Supersymmetric**: reproducing the characteristic mass splittings and Higgs self-couplings of the MSSM with light stops [181].

	Default EFT				
	$\lvert\Lambda\rvert$ [GeV]	f_t	f_b	f_τ	f_{BB}
D1	100	0.12	0.003	0.001	0.009
D2	448	0.00	−0.006	−0.002	−0.001
D3	99	−0.07	0.206	0.077	−0.016
D4	142	0.00	0.000	0.000	−0.023

Table 3.4: Matching scales and Wilson coefficients for the effective theory matched to the 2HDM, based on the default matching in the unbroken phase.

	v-improved EFT				
	Λ [GeV]	f_t	f_b	f_τ	f_{BB}
D1	300	−0.12	−0.003	−0.001	−0.009
D2	450	0.00	−0.006	−0.002	−0.001
D3	500	−0.07	0.206	0.077	−0.016
D4	500	0.00	0.000	0.000	−0.023

Table 3.5: Matching scales and Wilson coefficients for the effective theory matched to the 2HDM, based on the v-improved matching in the unbroken phase with $\Lambda = m_{A^0}$.

D3 **Sign-flipped bottom Yukawa**: this is possible in type-II models at large $\tan\beta$, as shown in Equation (3.44) [182]. This can be viewed as a manifestation of a delayed decoupling [174].

D4 **Fermiophobic heavy Higgs**: possible only in type-I models for $\sin\alpha = 0$. The heavy Higgs H^0 is relatively light, but essentially impossible to observe at the LHC [152].

In Tables 3.4 and 3.5 we show the heavy scales Λ and the Wilson coefficients for the EFT in the two matching schemes. With the exception of benchmark D2, the suppression scales are drastically different. The matching in the unbroken phase is particular pathological in benchmark D1, where $\Lambda^2_{\text{default}}$ is negative and the signs of the Wilson coefficients are switched compared to the v-improved matching.

Higgs couplings and total production rates

Table 3.6 shows the tree-level coupling shifts of the light Higgs in the three models. The results confirm that the default matching defined in the unbroken phase does not reproduce the coupling patterns of the full model at all. We conclude that an EFT matched to the 2HDM in the unbroken electroweak phase is essentially useless, and we have to rely on v-improved matching. For simplicity,

	Δ_V		Δ_t			$\Delta_b = \Delta_\tau$		
	2HDM	EFT	2HDM	dEFT	vEFT	2HDM	dEFT	vEFT
D1	−0.05	0.00	0.16	−0.74	0.08	0.16	−0.74	0.08
D2	0.00	0.00	0.00	0.00	0.00	0.07	0.07	0.07
D3	−0.02	0.00	0.00	0.46	0.02	−2.02	−46.5	−1.84
D4	0.00	0.00	0.00	0.00	0.00	0.00	0.00	0.00

Table 3.6: Normalised tree-level couplings of the light Higgs in our 2HDM benchmarks, comparing the full 2HDM model to the EFT based on the default matching ("dEFT") and that based on v-improved matching ("vEFT").

we will from now on leave out the results based on the default matching, which only confirm these initial results.

The v-improved matching, on the other hand, essentially captures most of the coupling shifts. It still fails to describe shifts in the couplings to weak bosons, which correspond to a dimension-eight operator as discussed above.[2] Unlike in the singlet model, the v-improved EFT also struggles with scenarios of very light new physics such as D1. But all in all, it performs well in situations with a modest scale hierarchy such as benchmarks D2.

A particularly interesting scenario is described by benchmark D3. In the full model, the bottom Yukawa is exactly sign-flipped, a signature hardly visible at the LHC. Generating such a signature from higher-dimensional operators requires their contributions to be twice as large as the SM Yukawa coupling due to the enhancement of v/Λ by a large coupling. The EFT fails to capture this coupling shift fully, leading to a significantly different prediction for the Higgs decay into bottom quarks.

In Table 3.7 we repeat this analysis for the loop-induced couplings of an on-shell Higgs to gluons and photons. A large part of these coupling shifts stems from the modified Higgs-top and Higgs-W couplings, leading to good agreement in the same scenarios where the tree-level couplings were described accurately. Separating the $H^\pm$ contribution to the Higgs-photon coupling, we find that $\mathcal{O}_{BB}$ captures its effect very well.

Table 3.8 compares total production rates at the LHC. Depending on the benchmark, the dimension-six truncation leads to up to 10% departures, in agreement with the coupling deviations.

[2] Note that the operator $\mathcal{O}_{BB}$ does contribute to the $h^0 VV$ coupling, representing the effect of a charged Higgs loop. But as our results show, this effect is neglible.

	Δ_g		Δ_γ			
	2HDM	v-improved EFT	2HDM		v-improved EFT	
D1	$0.16 + 0.00\,\mathrm{i}$	$0.08 + 0.00\,\mathrm{i}$	−0.16	(−0.05)	−0.10	(−0.07)
D2	$0.00 + 0.00\,\mathrm{i}$	$0.00 + 0.00\,\mathrm{i}$	0.00	(0.00)	0.00	(0.00)
D3	$0.07 - 0.09\,\mathrm{i}$	$0.02 + 0.00\,\mathrm{i}$	−0.08	(−0.05)	−0.05	(−0.05)
D4	$0.00 + 0.00\,\mathrm{i}$	$0.00 + 0.00\,\mathrm{i}$	−0.05	(−0.05)	−0.05	(−0.05)

Table 3.7: Normalised couplings of the light Higgs to gluons and photons in our 2HDM benchmarks. The bottom loop leads to small imaginary parts of Δ_g and Δ_γ. For the Higgs-photon coupling, these imaginary parts are always smaller than 1% of the real part of the amplitude and neglected here. The numbers in parentheses ignore the modification of the Higgs-fermion couplings, allowing us to separately analyse how well the $H^\pm$ loop is captured by $\mathcal{O}_{BB}$.

	$\sigma_{v\text{-improved EFT}}/\sigma_{\text{2HDM}}$		
	ggF	WBF	Vh
D1	0.872	1.109	1.108
D2	1.001	1.000	1.000
D3	1.022	1.042	1.042
D4	1.001	1.001	1.003

Table 3.8: Cross section ratios of the v-improved dimension-six approximation to the full 2HDM at the LHC. The statistical uncertainties on these ratios are below 0.4%.

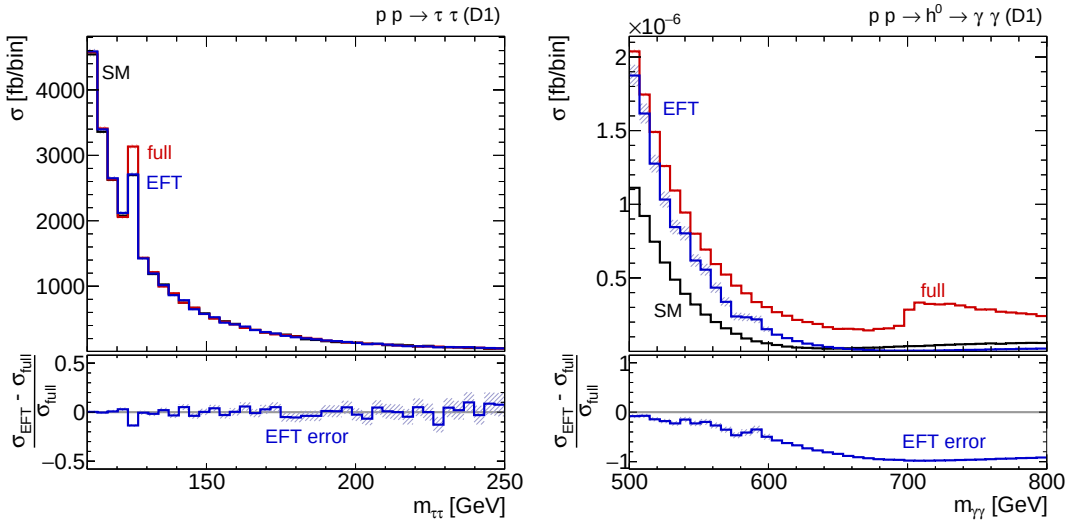

Figure 3.2: Left: $m_{\tau\tau}$ distribution in the $gg \to \tau^+\tau^-$ channel. Right: off-shell behaviour of the process $gg \to h^0 \to \gamma\gamma$ in 2HDM benchmark D1, only taking into account the Higgs diagrams. At $m_{\gamma\gamma} \gtrsim 2m_{H^\pm} = 700$ GeV, the charged Higgs threshold is visible.

Distributions

As for the singlet model, the phenomenology of the 2HDM is mostly reflected in the coupling patterns discussed above, with little new kinematic effects. In the left panel of Figure 3.2 we illustrate the coupling deviations in gluon-fusion Higgs production with a decay $h \to \tau^+\tau^-$, showing how the full 2HDM and the (v-improved) EFT give substantially different predictions for the size of the Higgs signal.

While on-shell Higgs decays to photons are generally well described by the EFT, this changes for off-shell Higgs production. At $m_{\gamma\gamma} \gtrsim 2m_{H^\pm}$, the $H^\pm$ in the loop can resolve the charged Higgs, enhancing the size of its contribution significantly. This effect is not captured by the effective operator and leads to a different behaviour of the amplitude $gg \to h^0 \to \gamma\gamma$ between the full and effective model, as shown in the right panel of Figure 3.2. However, the tiny rate and the large combinatorial background mean that this discrepancy will be irrelevant for LHC phenomenology. Similar threshold effects have been computed for the top-induced Higgs-gluon coupling and appear to be similarly irrelevant in practice [183].

The situation in Higgs pair production resembles the observations in the singlet model [152, 184, 185]. The agreement can be worse already at threshold if Higgs-top coupling shifts are not correctly captured by the effective model.

Summary

Eventually, the 2HDM discussion leads us to a similar conclusion as the singlet model: as long as the mixing is small and Higgs-gauge coupling shifts are neglible, all the LHC probes in single Higgs production is a set of three coupling modifications Δ_t, Δ_b, Δ_τ, and the charged Higgs loop contribution to the Higgs-photon coupling. These aspects of Higgs phenomenology are generally well captured by an appropriately defined EFT. Problems arise in scenarios with very light new Higgs bosons; when the Higgs-W and Higgs-Z couplings are modified, which requires dimension-eight operators; or in the special case of Higgs pair production.

A naive construction of the EFT by matching the effective dimension-six Lagrangian to the 2HDM in the gauge symmetric phase fails to correctly describe the modified Higgs boson dynamics in typical 2HDM scenarios, since terms formally suppressed by powers of v^2/Λ^2 can be crucial for phenomenologically relevant scenarios.

3.3.4 Scalar top partners

Model setup

New coloured scalar particles are, strictly speaking, not an extension of the SM Higgs sector, but they can lead to interesting modifications of the LHC observables. We consider a scalar top-partner sector mimicking the stop and sbottom sector of the MSSM. Its Lagrangian has the form

$$\begin{aligned}\mathcal{L}_{\text{top partners}} \supset\ & (D_\mu \tilde{Q})^\dagger D^\mu \tilde{Q} + (D_\mu \tilde{t}_R)^* D^\mu \tilde{t}_R - M^2\, \tilde{Q}^\dagger \tilde{Q} - M^2\, \tilde{t}_R^* \tilde{t}_R \\ & - \kappa_{LL}\, (\phi \cdot \tilde{Q})^\dagger\, (\phi \cdot \tilde{Q}) - \kappa_{RR}\, (\tilde{t}_R^* \tilde{t}_R)\, (\phi^\dagger\, \phi) - \left[\kappa_{LR}\, M\, \tilde{t}_R^*\, (\phi \cdot \tilde{Q}) + \text{h. c.}\right] . \end{aligned} \tag{3.50}$$

Here, $\tilde{Q}$ and $\tilde{t}_R$ are the additional isospin doublet and singlet in the fundamental representation of $SU(3)_C$. Their mass terms can be different, but for the sake of simplicity we unify them to a single heavy mass scale M. The singlet state $\tilde{b}_R$ is assumed to be heavier and integrated out.

This leaves us with three physical degrees of freedom, the scalars $\tilde{t}_1$, $\tilde{t}_2$ and $\tilde{b}_2 = \tilde{b}_L$. The eigenvalues of the stop mass matrix

$$\mathcal{M}_{\tilde{t}} = \begin{pmatrix} M^2 + \kappa_{LL}\, \dfrac{v^2}{2} & \kappa_{LR}\, \dfrac{Mv}{\sqrt{2}} \\ \kappa_{LR}\, \dfrac{Mv}{\sqrt{2}} & M^2 + \kappa_{RR}\, \dfrac{v^2}{2} \end{pmatrix} \tag{3.51}$$

define two masses $m_{\tilde{t}_1} < m_{\tilde{t}_2}$ and a mixing angle $\theta_{\tilde{t}}$. Again, we provide a detailed description of the model setup in Appendix 2.3.

Signatures and decoupling patterns

The main new physics effects in the Higgs sector are loop-induced modifications of the Higgs interactions, most notably to Δ_g, Δ_γ, Δ_W, and Δ_Z, possibly including new Lorentz structures. The Yukawa couplings do not change at one loop because we do not include gauge boson partners. As a side remark, the 2HDM described in Section 3.3.3 combined with the scalar top partners given here corresponds to an effective description of the Minimal Supersymmetric Standard Model in the limit of infinitely heavy gauginos, sleptons, and light-flavour squarks.

In the limit of small $\theta_{\tilde{t}}$, the leading correction to the hVV coupling scales like

$$\Delta_V \approx \frac{\kappa_{LL}^2}{16\pi^2} \left(\frac{v}{m_{\tilde{t}_1}} \right)^2 . \tag{3.52}$$

This shift can be sizeable for relatively low stop and sbottom masses combined with large couplings κ_{ij} to the Higgs sector.

As already noted for the 2HDM, the decoupling of the heavy scalars becomes non-trivial in the presence of a Higgs VEV. Following Equation (3.51), the masses of the heavy scalars $m_{\tilde{t}_1}$, $m_{\tilde{t}_2}$ are not only controlled by the mass scale in the symmetric phase of the electroweak symmetry M, but they receive additional contributions of the type $\kappa_{LR}\, vM$, $\kappa_{LL} v^2$, or $\kappa_{RR} v^2$ after electroweak symmetry breaking. This leads to a mass splitting of order v between masses of order M, which is increased by large values of the couplings κ_i.

Dimension-six description

This motivates us to again define two different matching schemes. First, we stick to our default prescription and carry out the matching of the linear EFT Lagrangian to the full model in the unbroken phase. The matching scale it then dictated by the intrinsic mass scale of the heavy fields,

$$\Lambda_{\text{default}} = M\,, \tag{3.53}$$

completely oblivious to contributions to the masses from the electroweak VEV.The suppression scale of loop effects in the complete model and this matching scale in the EFT only agree in the limit $M - m_{\tilde{t}_1} \sim v \ll M$.

In this dimension-six approach the stop loops generate a number of operators [60, 64, 119],

$$f_{\phi,1} = -\frac{1}{2(4\pi)^2} \left[\kappa_{LL}^2 - \frac{\kappa_{LL}\,\kappa_{LR}^2}{2} + \frac{\kappa_{LR}^4}{10} \right],$$
$$f_{\phi,2} = \frac{1}{4(4\pi)^2} \left[2\kappa_{RR}^2 - \kappa_{RR}\kappa_{LR}^2 + \frac{\kappa_{LR}^4}{5} \right],$$

	Scalar top-partner model						
	M	κ_{LL}	κ_{RR}	κ_{LR}	$m_{\tilde{t}_1}$	$m_{\tilde{t}_2}$	$\theta_{\tilde{t}}$
P1	500	−1.16	2.85	0.147	500	580	−0.15
P2	350	−3.16	−2.82	0.017	173	200	−0.10
P3	500	−7.51	−7.17	0.012	173	200	−0.10

Table 3.9: Benchmarks for the scalar top-partner scenario. We show Lagrangian parameters (left) and physical parameters (right). All masses are given in GeV.

$$
\begin{aligned}
f_{GG} &= \frac{g_s^2}{24\,(4\pi)^2}\left[\kappa_{LL}+\kappa_{RR}-\kappa_{LR}^2\right], \\
f_{BB} &= -\frac{1}{36\,(4\pi)^2}\left[\kappa_{LL}+16\kappa_{RR}-\frac{67}{10}\kappa_{LR}^2\right], \\
f_{WW} &= -\frac{1}{4\,(4\pi)^2}\left[\kappa_{LL}-\frac{3}{10}\kappa_{LR}^2\right], \\
f_{BW} &= \frac{1}{12\,(4\pi)^2}\left[2\kappa_{LL}-\frac{11}{5}\kappa_{LR}^2\right], \\
f_B &= \frac{1}{20\,(4\pi)^2}\,\kappa_{LR}^2, \\
f_W &= \frac{1}{20\,(4\pi)^2}\,\kappa_{LR}^2 .
\end{aligned}
\tag{3.54}
$$

Unlike the tree-level effects in the previous two models, the top partner loops do not only induce modifications to the SM Higgs couplings, but induce new Lorentz structures. Note that some of these operators are tightly constrained from electroweak precision data, see Section 2.3.2. We will ignore these constraints for our discussion of Higgs physics.

In addition, we define a v-improved matching. Like in the 2HDM we pick the matching scale as a physical mass in the broken phase,

$$\Lambda = m_{\tilde{t}_1} . \tag{3.55}$$

The Wilson are the same as in Equation (3.54).

Benchmark points

As Equation (3.52) suggests, sizeable loop corrections to the hVV coupling require light top partners with unrealistically strong couplings to the Higgs sector [186]. In Table 3.9 we define a set of benchmark points with this aim in mind. The corresponding Wilson coefficients in our two matching schemes are given in Table 3.10.

	EFT				EFT (v-improved)			
	Λ	$f_{\phi,2}$	f_{WW}	f_W	Λ	$f_{\phi,2}$	f_{WW}	f_W
P1	500	0.026	0.000	0.000	500	0.026	0.000	0.000
P2	350	0.023	0.005	0.000	173	0.023	0.005	0.000
P3	500	0.152	0.115	−0.207	173	0.152	0.115	−0.207

Table 3.10: Matching scales (in GeV) and selected Wilson coefficient for the top-partner benchmarks, both for default and v-improved matching.

Benchmark	$\sigma_{\text{EFT}}/\sigma_{\text{triplet}}$		$\sigma_{v\text{-improved EFT}}/\sigma_{\text{triplet}}$	
	WBF	Vh	WBF	Vh
P1	1.000	0.999	1.000	0.999
P2	1.095	1.100	1.074	1.049
P3	2.081	1.904	1.749	1.363

Table 3.11: Cross section ratios of the matched dimension-six EFT approximation to the full scalar top-partner model at the LHC. We give the results both for the default matching scheme with matching scale $\Lambda = M$ as well as for the v-improved matching at $\Lambda = m_{\tilde{t}_1}$. The statistical uncertainties on these ratios are below 0.4%.

Higgs production rates and distributions

The contributions from scalar top partners to Higgs production in gluon fusion are well known [187–191] and the validity of the EFT approach for this process has been thoroughly scrutinised [115, 119]. We therefore focus on corrections to the hVV coupling in WBF and Higgs-strahlung.

The total Higgs production rates in these channels are given in Table 3.11. In benchmark P1 the WBF cross section is reduced by about 0.6% compared to the Standard Model, with good agreement between effective and full description. Clearly, such a scenario is not relevant for LHC measurements in the foreseeable future. In more extreme corners of the parameter space the loop effects in the full model grow, higher-dimensional terms in the EFT become larger, the validity of the latter worsens, and discrepancies between both increase. In benchmarks P2 and P3 the WBF rate is reduced by 9.1% and 43.5% with respect to the Standard Model. By construction, the EFT based on the default matching captures only the formally leading term at $\mathcal{O}\left(v^2/\Lambda^2\right)$, only giving a reduction of 0.5% and 2.0%. The corresponding difference is again independent for example of the tagging jet's transverse momentum. With the v-improved matching, the cross section is reduced by 2.4% and 17.7%, still far from the result of the full model.

The results for Higgs-strahlung look similar: in the moderate benchmark P1 the predictions

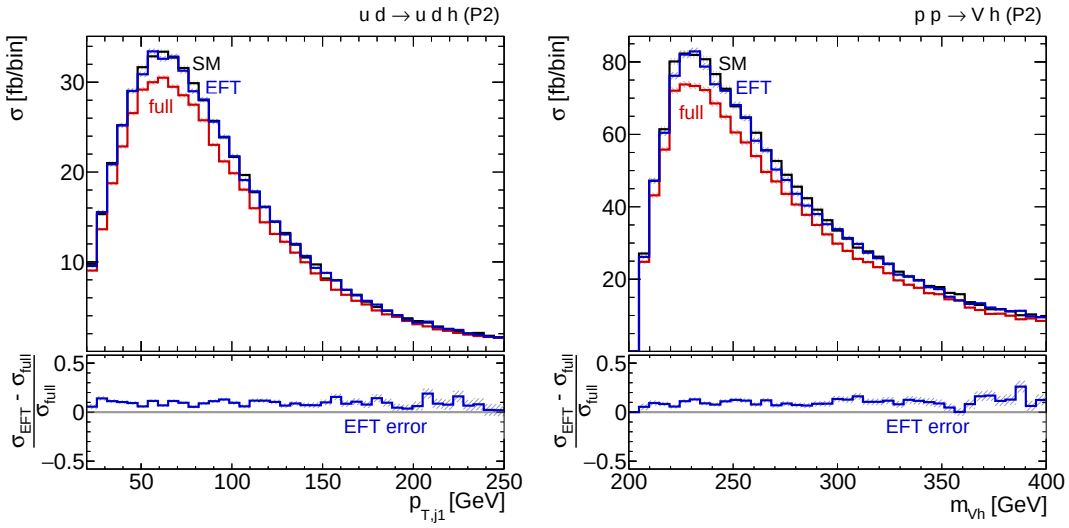

Figure 3.3: Kinematic distributions for the top partner model in benchmark P2. Left: tagging jet properties in WBF Higgs production. Right: m_{Vh} distribution in Higgs-strahlung.

of the full model and the dimension-six Lagrangian agree within 0.1%, but in this scenario the overall deviation from the Standard Model is negligible. In scenarios with larger loop effects, the dimension-six predictions fails to capture most of the full top partner loops, with numerical results similar to those given for WBF Higgs production. Again switching to the v-improved matching does not improve the EFT approximation significantly.

In Figure 3.3 we finally show that these changes in the total rates do not have a dramatic effect on the kinematic distributions. This is not surprising, since the largest Wilson coefficient generated in our benchmark points is consistently that of $\mathcal{O}_{\phi,2}$, see Table 3.10, which corresponds to a universal rescaling of the SM Higgs couplings.

Summary

Scalar top partners generate a large set of dimension-six operators through electroweak loops. However, in realistic scenarios with a large scale separation the loop corrections for example to the hVV vertex are tiny. Pushing for loop effects that are large enough to leave a visible imprint in WBF and Higgs-strahlung requires breaking the scale separation between the observed Higgs scalar and the top partners dramatically. In that case the EFT fails already for the total rates, kinematic distributions hardly add to this discrepancy.

3.3.5 Vector triplet

Model setup

Heavy vector bosons appear in many new physics scenarios, for instance when a larger gauge group is spontaneously broken down to the SM gauge group at higher energies. Often such particles are connected to the gauge-Higgs sector of the SM, predicting signatures in Higgs measurements [110, 192, 193]. As an example, we study a massive vector field[3] V_μ^a which is a triplet under $SU(2)_L$ and uncharged under $SU(3)_c$ and $U(1)_Y$. These charges allow it to mix with the W bosons of the Standard Model and to couple to Higgs and fermion currents [110, 193]. For simplicity, we assume CP invariance and a flavour-universal coupling to the fermion current. Following the conventions of Reference [193], the Lagrangian then reads

$$\begin{aligned}\mathcal{L}_{\text{vector triplet}} \supset & -\frac{1}{4} V_{\mu\nu}^a V^{\mu\nu\, a} + \frac{M_V^2}{2} V_\mu^a V^{\mu\, a} \\ & + \mathrm{i}\frac{g_V}{2} c_H V_\mu^a \left[\phi^\dagger \sigma^a \overleftrightarrow{D}^\mu \phi\right] + \frac{g_W^2}{2 g_V} V_\mu^a \sum_f c_F \bar{f}_L \gamma^\mu \sigma^a f_L \\ & + g_V^2 c_{VVHH} V_\mu^a V^{\mu a} \phi^\dagger \phi \\ & + \frac{g_V}{2} c_{VVV} \varepsilon_{abc} V_\mu^a V_\nu^b D^{[\mu} V^{\nu]c} - \frac{g_W}{2} c_{VVW} \varepsilon_{abc} W^{\mu\nu} V_\mu^b V_\nu^c \end{aligned} \tag{3.56}$$

with the field strength $V_{\mu\nu}^a = D_\mu V_\nu^a - D_\nu V_\mu^a$ and where $D_\mu V_\nu^a = \partial_\mu V_\nu^a + g_V \varepsilon^{abc} V_\mu^b V_\nu^c$.

The coupling g_V characterises the interactions of the heavy vector, while g_W is the $SU(2)_L$ coupling constant. After mixing, the original fields V^a and W^a combine to the mass eigenstates $W^\pm$, $\xi^\pm$, and ξ^0, while a combination of the couplings g_w and g_V becomes the observed weak gauge coupling g. c_{VVW} and c_{VVV} are irrelevant for Higgs phenomenology at the LHC. For more details, see Appendix 2.4.

Signatures and decoupling patterns

In addition to the new heavy resonances ξ^0 and $\xi^\pm$, the signature feature of the vector triplet is that the mixing of the new states with the W and Z bosons affects the properties of the electroweak gauge bosons at tree level. In particular, the shift from the Lagrangian parameter g_w to the observable weak coupling g combined with the direct heavy vector coupling to the Higgs doublet

[3] Note that such a model is not UV-complete: as fundamental particles, massive vector bosons are not renormalisable. However, such a mass can easily be generated from a consistent gauge theory with a Higgs mechanism at a higher scale [193]. The details of such an embedding do not matter for the discussion here.

modify the Higgs couplings as

$$\begin{aligned}\Delta_V &\approx \frac{g^2 c_F c_H}{4}\left(\frac{v}{M_V}\right)^2 - \frac{3 g_V^2 c_H^2}{8}\left(\frac{v}{M_V}\right)^2 \\ \Delta_f &\approx \frac{g^2 c_F c_H}{4}\left(\frac{v}{M_V}\right)^2 - \frac{g_V^2 c_H^2}{8}\left(\frac{v}{M_V}\right)^2 .\end{aligned} \tag{3.57}$$

In addition, contributions from virtual heavy states ξ modify the phase-space behaviour of Higgs signals in many ways.

Just as for the 2HDM and the top partners, the mass matrix for the massive vectors contains both the intrinsic mass scale M_V and terms proportional to some power of v multiplied by a combination of couplings. The new vector states have roughly degenerate masses

$$m_\xi^2 \approx M_V^2\left(1 + g_V^2 c_{VVHH}\frac{v^2}{M_V^2} + \frac{g_V^2 c_H^2}{4}\frac{v^2}{M_V^2} + \mathcal{O}\left(\frac{v^4}{M_V^4}\right)\right) . \tag{3.58}$$

Even if there appears to be a clear scale separation $M_V \gg v$, large values of g_V, c_{VVHH}, or c_H can change m_ξ significantly and effectively induce a second mass scale.

Dimension-six description

The obvious choice of the matching scale in the unbroken electroweak phase is the heavy mass scale in the Lagrangian

$$\Lambda_{\text{default}} = M_V , \tag{3.59}$$

which we use for our default matching scheme.

Integrating out the heavy vector triplet at tree level generates a number of operators with Wilson coefficients

$$\begin{aligned} f_{WW} &= c_F\, c_H , & f_{\phi 2} &= \frac{3}{4}\, c_H \left(c_H\, g_V^2 - 2\, c_F\, g^2\right) , \\ f_{BB} &= c_F\, c_H , & f_{\phi 3} &= -3\,\lambda\, c_H \left(c_H\, g_V^2 - 2\, c_F\, g^2\right) , \\ f_{BW} &= c_F\, c_H , & f_f &= -\frac{1}{4}\, y_f\, c_H \left(c_H\, g_V^2 - 2\, c_F\, g^2\right) , \\ f_W &= -2\, c_F\, c_H . \end{aligned} \tag{3.60}$$

Additional four-fermion contributions are irrelevant for Higgs physics. Loop-induced contributions will be further suppressed and do not add qualitatively new features, so we neglect them here.

Once again, we compare this default matching to an alternative v-improved matching, where as a cutoff we now use the physical mass

$$\Lambda_{v\text{-improved}} = m_{\xi^0} . \tag{3.61}$$

	Triplet model					
	M_V	g_V	c_H	c_F	c_{VVHH}	m_ξ
T1	591	3.0	−0.47	−5.0	2.0	1200
T2	946	3.0	−0.47	−5.0	1.0	1200
T3	941	3.0	−0.28	3.0	1.0	1200
T4	1246	3.0	−0.50	3.0	−0.2	1200
T5	846	1.0	−0.56	−1.32	0.08	849

Table 3.12: Benchmark points for the vector triplet model. The masses are given in GeV.

The coefficients in Equation (3.60) remain unchanged.[4]

Unlike the previous models, the vector triplet generates $\mathcal{O}_W$, $\mathcal{O}_{WW}$, and $\mathcal{O}_{BB}$ at tree level. As discussed in Section 2.3.3, these induce new kinematic structures in the hWW and hZZ couplings.

Benchmark points

As for the other models we study a set of benchmark points, defined in Table 3.12 and Table 3.13. Unlike additional scalars, light new vector triplets with masses just above the electroweak scale are unrealistic given the constraints from electroweak precision measurements and direct searches. We therefore focus on new vector bosons around the TeV scale. The different setups are motivated phenomenologically, from experimental constraints, or based on specific UV completions:

T1-2 **Higgs-gauge dynamics**: designed for large momentum-dependent effects in the hVV couplings. $\mathcal{O}_W$ and $\mathcal{O}_{WW}$ receive large Wilson coefficients, while $\mathcal{O}_{\phi,2}$, $\mathcal{O}_{\phi,3}$, and $\mathcal{O}_f$ vanish along the line

$$\frac{c_H}{c_F} = 2\frac{g^2}{g_V^2}\,. \tag{3.62}$$

The large couplings also imply a large difference between M_V and m_ξ.

T3 **Interference patterns**: changes the sign of c_W or the Wilson coefficients compared to T1 and T2. This allows us to compare constructive and destructive interference patterns between SM amplitudes and new physics contributions.

T4 **Realistic:** the vector triplet couplings and masses satisfy the leading constraints from direct collider searches at the time of publication of Reference [2]. The most stringent bounds come from di-lepton and di-boson channels [193, 194].

[4] In the spirit of v-improvement we could alternatively parametrise the Wilson coefficients with the physical mixing angles between the W, Z and V bosons, but this does not significantly change the results.

	Default EFT					v-improved EFT				
	Λ	$f_{\phi 2}$	f_{WW}	f_W	f_t	Λ	$f_{\phi 2}$	f_{WW}	f_W	f_t
T1	591	0.00	2.45	−4.90	0.00	1200	0.00	2.45	−4.90	0.00
T2	946	0.00	2.35	−4.71	0.00	1200	0.00	2.35	−4.71	0.00
T3	941	1.09	−0.82	1.64	−0.36	1200	1.09	−0.82	1.64	−0.36
T4	1246	2.64	−1.56	3.12	−0.87	1200	2.64	−1.56	3.12	−0.87
T5	846	−0.24	0.78	−1.55	0.08	849	−0.24	0.78	−1.55	0.08

Table 3.13: Matching scales (in GeV) and selected Wilson coefficients for the effective theory matched to the vector triplet model. We give these results both for the EFT matching in the unbroken phase as well as for the v-improved matching with $\Lambda = m_{\xi^0}$.

T5 **UV completion:** typical coupling patterns from a weakly coupled UV completion based on the extended gauge group $SU(3) \times SU(2) \times SU(2) \times U(1)$ [195]. Such a scenario could for instance arise from deconstructed extra dimensions [196]. The vector triplet phenomenology is effectively described by the parameter $\alpha = g_V/\sqrt{g_V^2 - g_w^2}$ together with the symmetry breaking scale f [193], with the couplings

$$M_V^2 = \alpha^2 g_V^2 f^2\,, \qquad c_H = -\alpha \frac{g_W^2}{g_V^2}\,, \qquad c_{VVHH} = \alpha^2 \left[\frac{g_W^4}{4 g_V^4}\right],$$
$$c_F = -\alpha\,, \qquad c_{VVW} = 1\,, \qquad c_{VVV} = -\frac{\alpha^3}{g_V}\left[1 - \frac{3g_W^2}{g_V^2} + \frac{2g_W^2}{g_V^4}\right]. \tag{3.63}$$

Benchmarks T1 to T3 are meant to emphasise the phenomenological possibilities of the vector triplet model, ignoring experimental constraints or parameter correlations from an underlying UV completion.

Higgs production rates and distributions

As shown in Figure 3.4, virtual heavy vector bosons contribute to as intermediate t-channel mediators to WBF Higgs production and in the s-channel to Higgs-strahlung, promising non-trivial kinematic features in these channels. In the EFT these effects are mapped onto large Wilson coefficients like $\mathcal{O}_W$ and $\mathcal{O}_{WW}$, adding a momentum dependence to the hVV couplings. Therefore our analysis focuses on these electroweak Higgs production modes.

Table 3.14 shows the agreement between EFT and full model for the total Higgs production rates in WBF Higgs production and Higgs-strahlung. The default dimension-six model matched in the unbroken phase, oblivious to the difference between the Lagrangian mass term M_V and the actual physical mass m_ξ, struggles with the first three benchmark points, in which this splitting is large. The discrepancies to the full model are particularly evident in Vh production.

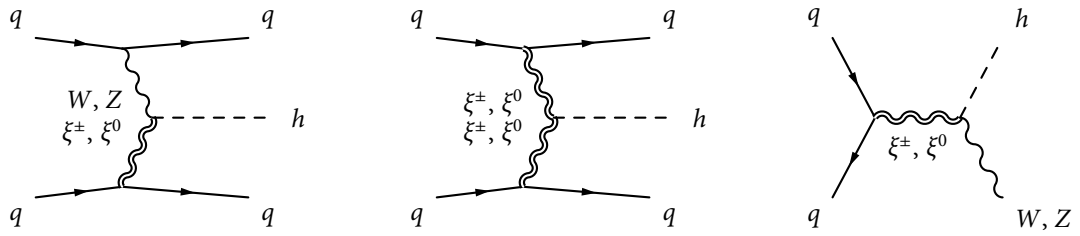

Figure 3.4: Example Feynman diagrams with contributions from virtual heavy vector bosons ξ to Higgs production in weak boson fusion (left, middle) or Higgs-strahlung (right).

	$\sigma_{\text{default EFT}}/\sigma_{\text{triplet}}$		$\sigma_{v\text{-improved EFT}}/\sigma_{\text{triplet}}$	
	WBF	Vh	WBF	Vh
T1	1.299	0.299	0.977	0.794
T2	1.045	0.737	0.992	0.907
T3	0.921	1.066	0.966	1.024
T4	1.026	0.970	1.012	0.978
T5	1.001	1.043	1.002	1.043

Table 3.14: Cross section ratios of the matched dimension-six EFT approximation to the full vector triplet at the LHC. To avoid large contributions from the ξ resonance in the Vh channel, we only take into account the region $m_{Vh} < 600$ GeV. The statistical uncertainties on these ratios are below 0.4%.

The v-improved EFT, on the other hand, performs better and describes the rate accurately in most of the scenarios. Only in Higgs-strahlung and only in the extreme scenarios T1 and T2 we find significant deviations.

To better understand these differences, we have to look at kinematic distributions. Figure 3.5 shows different properties of the tagging jets in WBF Higgs production. In addition to the predictions of the full vector triplet model and the default and v-improved EFT, we show distributions of the vector triplet model where we have artificially removed all contributions from virtual ξ propagators.

We find that the vector triplet significantly modifies the WBF rate with respect to the Standard Model. Its effect increases with momentum transfer, measured as transverse jet momentum. This modification can be traced to contributions from ξ fusion and mixed W-ξ fusion diagrams as given in Figure 3.4. These contributions from ξ propagators can become relevant already at energy scales well below m_ξ and further increase with the energy flow. In addition to the high-energy tails of the transverse momenta, large effects are visible in the azimuthal angle between the tagging jets, as shown in the bottom left panel of Figure 3.5. This angular correlation is well known to be sensitive to the modified Lorentz structure of the hWW vertex [77, 124–126, 197–199].

The EFT approach qualitatively captures these features of the full model, now parametrised by momentum-dependent operators such as $\mathcal{O}_W$ and $\mathcal{O}_{WW}$. The signs of the Wilson coefficients in benchmarks T1 and T2 yields a non-linear increase of the cross section with energy. Conversely, the switched signs in T3 reduces the rate with energy, eventually driving the combined amplitude through zero.

Comparing full and effective model for the more realistic benchmark points T4 and T5, we find good agreement in the bulk of the distribution. The deviations from the Standard Model are entirely captured by the dimension-six operators, including the momentum dependence coming from the ξ diagrams. Only at very large momentum transfer, likely beyond the sensitivity of the LHC, the validity of the EFT breaks down.

In the more strongly coupled benchmark points T1 to T3, the full model predicts shifts in the jet distributions that are large enough to be relevant for the upcoming LHC run. We find good agreement between the full model and the default EFT only at low momentum transfer, where the effects of new physics are small. This naive dimension-six model fails to reproduce the full model results already at energy scales $p_{T,j} \gtrsim 80$ GeV, a phase space region highly relevant for constraints on new physics [23]. Perhaps counter-intuitively, this discrepancy does not signal a breakdown of the E/Λ expansion, but is linked to the difference between the physical mass m_ξ, which suppresses the ξ fusion diagrams, and the matching scale $\Lambda_{\text{default}} = M_V$, which suppresses the dimension-six operators. This can be seen by comparing the results to those based on v-improved matching, where the EFT cutoff scale matches the physical mass. Here the agreement is significantly better, and the dimension-six description succesfully describes the momentum dependence up to large momentum transfer. Only at very high energies, $p_{T,j1} \gtrsim 300$ GeV, even the v-improved EFT

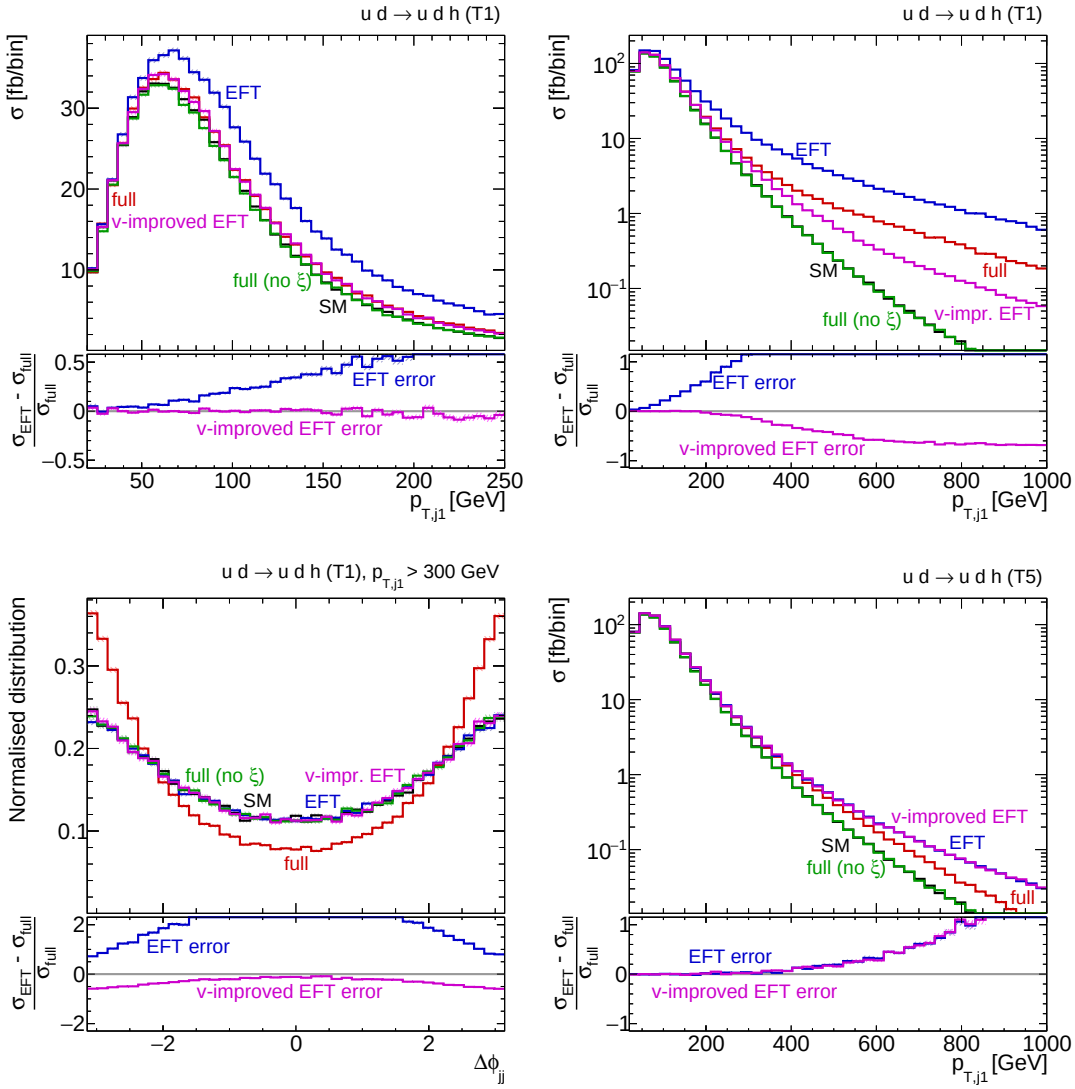

Figure 3.5: Tagging jet distributions in WBF Higgs production in the vector triplet model. Top: $p_{T,j1}$ distribution in benchmark T1, focusing on the low (left) and high (right) transverse momentum regions. Bottom left: $\Delta\phi_{jj}$ distribution above a certain $p_{T,j1}$ threshold for T1. Bottom right: $p_{T,j1}$ distribution for scenario T5.

breaks down.

The situation is similar in Higgs-strahlung, shown in Figure 3.6. Again, the dominant new physics effect is the interference with ξ-mediated diagrams rather than the modified hWW interaction. Not only does this lead to a significant change of the rate, it also introduces a strong dependence on the momentum transfer, probed by either the invariant mass of the gauge-Higgs system or the transverse momentum of the final vector boson. The relative sign of the interference between ξ amplitudes and SM-like diagrams is opposite to that in WBF: in T3 and T4 we find a non-linear increase of the cross section with the energy scale. The other benchmarks predict a decrease of the amplitude with energy, eventually including a sign flip when the amplitude is driven through zero.

In the more weakly coupled benchmarks T4 and T5, the full and effective models agree well over most of the phase space, and the dimension-six operators succesfully capture how the ξ contributions affect the Higgs-strahlung kinematics. At larger momentum transfer, higher-order terms in the EFT expansion become important, and dimension-six operators alone cannot describe the kinematics accurately any more. Ultimately, the ξ resonance in the full model marks the obvious failure of the effective theory.

For benchmarks T1 to T3, the default EFT has a more limited validity range. The large couplings lead to a failure of this dimension-six model already at low energies $m_{Vh} \gtrsim 220$ GeV, even though the actual ξ resonances only appear at $m_\xi = 1.2$ TeV. The EFT approximation can again be significantly improved by switching to the v-improved matching. But even then, there is a pronounced mismatch between full and effective model. This EFT error is larger in Higgs-strahlung than in WBF, showing how ξ contributions play a larger role in this s-channel process than in the t-channel WBF diagrams.

Summary

Heavy vector bosons can induce large kinematic effects in Higgs-gauge interactions, providing a perfect test case for the EFT approach. For realistic scenarios, the EFT works up to large momentum transfer. Operators such as $\mathcal{O}_W$ and $\mathcal{O}_{WW}$ successfully capture the effects from virtual ξ contributions to WBF Higgs production, including non-trivial momentum dependencies. In Higgs-strahlung, s-channel ξ contributions are more difficult to map onto effective operators, but the agreement is still good realistic parameter choices.

Again, this good performance of the dimension-six model requires particular care in the matching to the full theory. When the mixing with the SM gauge bosons is large, a naive matching procedure, defined in the unbroken electroweak phase, can lead to substantial errors already in the bulk of the WBF distributions. A v-improved dimension-six description, however, improves the EFT accuracy such that large deviations only occur in the high-energy tails of distributions.

To here

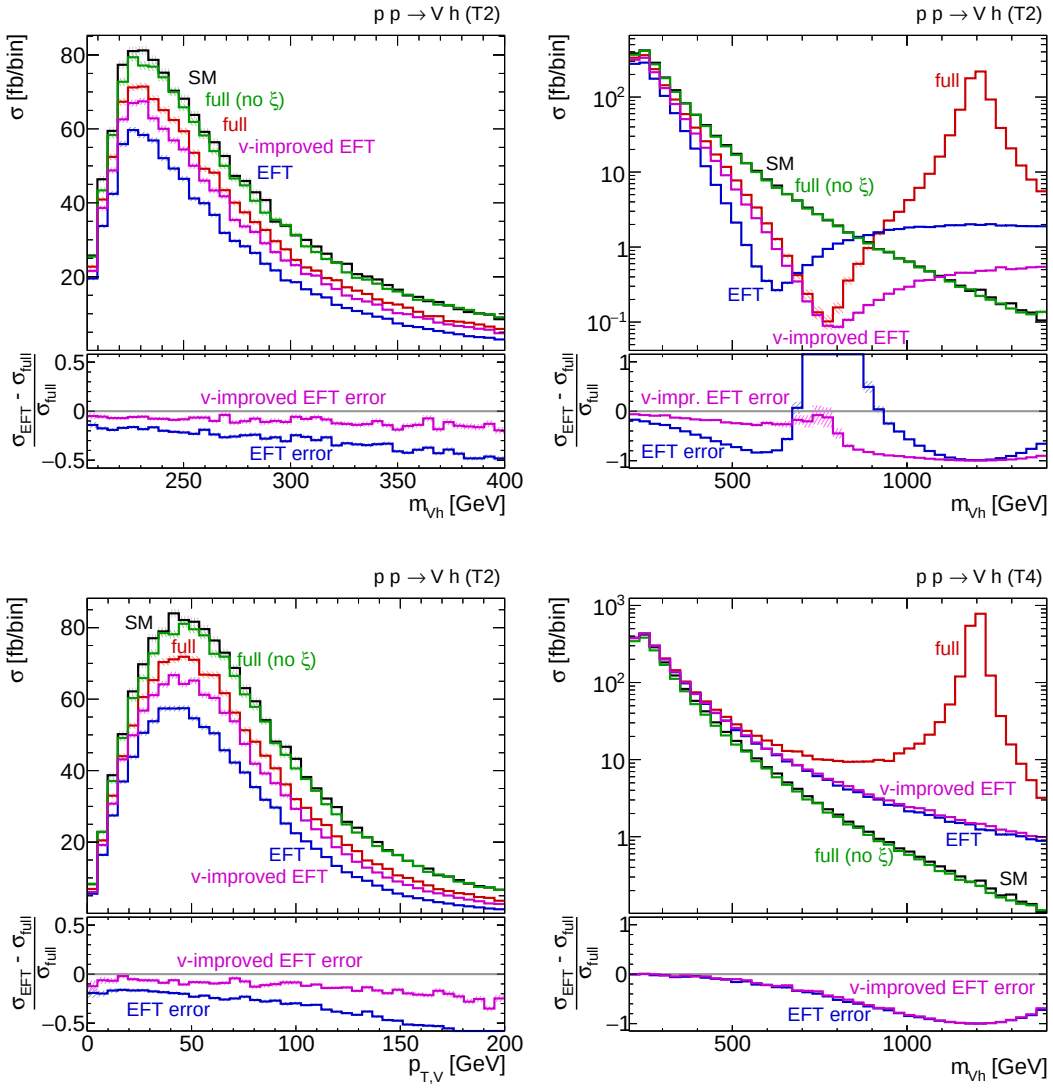

Figure 3.6: Higgs-strahlung distributions in the vector triplet model. Top: m_{Vh} distribution for benchmark T2, focusing on the low (left) and high (right) invariant mass regions. Bottom left: $p_{T,V}$ distribution for the same benchmark. Bottom right: m_{Vh} distribution for T4.

3.4 Practical questions

3.4.1 To square or not to square

If we accept that a dimension-six Lagrangian describing Higgs signatures at the LHC is not necessarily part of a consistent effective field theory, but rather a successful and reproducible parametrisation of weakly interacting new physics, there exists no fundamental motivation [**? ? ? ? ?**] to include or to not include the dimension-six squared term in

$$|\mathcal{M}_{4+6}|^2 = |\mathcal{M}_4|^2 + 2\,\text{Re}\mathcal{M}_4^*\mathcal{M}_6 \overset{?}{+} |\mathcal{M}_6|^2 \,. \tag{3.64}$$

A dimension-six squared term of comparable or larger size than the interference term can appear in phase-space regions with a suppressed dimension-4 prediction, even when the EFT expansion in E/Λ holds and dimension-eight effects are negligible. In the absence of any first-principle reason how to treat this term, we need to test the different possibilities from a practical perspective.

Higgs-strahlung

We first analyse associated Vh production with $V = W^\pm, Z$ at 13 TeV LHC energy. To retain as much phase space as possible we only consider the parton-level process

$$pp \to Vh \tag{3.65}$$

simulated in `MadGraph` [**?**] without cuts or decays. It is easy to see where in phase space the effective theory breaks down: for on-shell outgoing Higgs and gauge bosons a large momentum flow through the Higgs operator can only be generated through the virtual s-channel propagator. We can directly test this in the observable m_{Vh} distribution, comparing the full model with the dimension-six approach at large momentum flow.

We show the m_{Vh} distributions in the left panels of Figure 3.7. While theoretically the m_{Vh} distribution is cleaner, for example when we include initial state radiation, we can see the same effects in the highly correlated $p_{T,V}$ distribution (right panels), due to the simple $2 \to 2$ signal kinematics [**? ?**]. The T1 benchmark point is constructed with a low new physics scale and a destructive interference between Standard Model and dimension-six term. We see that the squared dimension-six terms are clearly needed to avoid negative cross sections in the high-energy tails of the distributions. Driven by the light new particles, inconsistencies otherwise occur around

$$m_{Vh} > 600\,\text{GeV} \approx \frac{m_\xi^{(\text{T1})}}{2} \qquad \text{or} \qquad p_{T,V} > 300\,\text{GeV} \approx \frac{m_\xi^{(\text{T1})}}{4} \,, \tag{3.66}$$

clearly within reach of Run II. The reason why differences appear much below $m_{Vh} = m_\xi$ is that the new states are wide and their pole contribution extends through a large interference effect.

Because for this benchmark point the discrepancies signal the onset of a new s-channel propagator pole, the agreement between full model and dimension-six operators is limited and will hardly improve once we include for example dimension-eight terms [**?**].[5]

For the constructively interfering benchmark point T4 we observe no dramatic effects in the tails, but the agreement between the full model and the dimension-six approximation is improved when we include these terms. Both benchmark points therefore suggest to include the dimension-six squared terms in the LHC analysis, to improve the agreement between the model and the dimension-six Lagrangian.

WBF Higgs production

Weak-boson-fusion Higgs production is a $2 \to 3$ process with two t-channel gauge bosons carrying the momentum to the Higgs vertex. The relevant kinematic variables are the two virtualities of the weak bosons. Following many studies in the framework of the effective W approximation [**? ?**] it is straightforward to link them to the p_T of the tagging jets, which even for multiple jet radiation can be linked to the transverse momentum of the Higgs [183] (even though it is not clear if this distribution is theoretically or experimentally favoured). Again, we start with the parton-level signal process

$$ud \to u'd'h \tag{3.67}$$

with only one minimal cut $p_{T,j} > 20$ GeV for the two tagging jets. We show the results for the now constructively interfering benchmark point T1 and the now destructively interfering benchmark point T4 in Figure 3.8. Negative event rates for T4 appear around

$$p_{T,j_1} > 600 \text{ GeV} \approx \frac{m_\xi^{(\text{T4})}}{2} , \tag{3.68}$$

forcing us to either disregard the corresponding model hypothesis or to add the dimension-six squared term. For the less critical point T1 the agreement between the vector triplet model and its dimension-six approximation including the squared terms extends well into the range where deviations from the Standard Model become visible.

In the middle panels of Figure 3.8 we see that indeed the $p_{T,h}$ distribution looks almost identical to p_{T,j_1}. Both of them can be traced back to the unobservable virtualities of the weak bosons. Due to the preferred collinear direction of the quark-vector splittings, the W-mediated and Z-mediated diagrams populate very different parton-level phase-space regions, with basically no interference

[5] We should note that if the LHC experiments should observe such a new resonance, the justification of a dimension-six description will most likely not be of experimental or theoretical concern.

between them. We can thus define the virtuality variable [**? ?**]

$$q = \begin{cases} \max\left(\sqrt{|(p_{u'} - p_d)^2|}, \sqrt{|(p_{d'} - p_u)^2|}\right) & \text{for } W\text{-like phase-space points,} \\ \max\left(\sqrt{|(p_{u'} - p_u)^2|}, \sqrt{|(p_{d'} - p_d)^2|}\right) & \text{for } Z\text{-like phase-space points,} \end{cases} \tag{3.69}$$

with the distribution shown in the bottom panels of Figure 3.8. Comparing it to $p_{T,h}$ and p_{T,j_1} we see essentially the same behaviour. The strong correlation of q with the observable transverse momenta of the leading tagging jet and the Higgs is explicitly shown in Figure 3.9.

Finally, we compare expected exclusion limits on the vector triplet in the absence of a signal, based on the full model vs the dimension-six approach. For the process shown in Equation (3.67) we multiply the cross sections with a branching ratio $\text{BR}(h \to 2\ell 2\nu) \approx 0.01$. We disregard non-Higgs backgrounds as well as parton-shower or detector effects. We then count events in two high-energy bins of the p_{T,j_1} distributions, defining a parameter point to be excluded if $S/\sqrt{S+B} > 2$. While this statistical analysis is not designed to be realistic, it illustrates how the validity of our dimension-six approach affects possible limits. For our limit setting procedure we choose a two-dimensional plane defined by m_ξ versus a universal coupling rescaling c,

$$g_V = 1\,, \qquad c_H = c\,, \qquad c_F = \frac{g_V^2}{2g^2}\,c\,, \qquad c_{HHVV} = c^2\,. \tag{3.70}$$

This reduces the list of generated dimension-six operators to

$$f_{WW} = f_{BW} = \frac{c^2}{2g^2} \qquad \text{and} \qquad f_W = -\frac{c^2}{g^2}\,, \tag{3.71}$$

and all dimension-six deviations scale like c^2/m_ξ^2. To avoid effects from strongly interacting theories we limit our analysis to $\Gamma_\xi/m_\xi < 1/4$.

In the left panel of Figure 3.10 we see that based on event numbers in the range 150 GeV $< p_{T,j_1} <$ 300 GeV, the dimension-six approximation with the squared terms gives the same limits as the full model, as long as we ensure that the new resonance remains narrow. In the high-energy tail $p_{T,j_1} > 300$ GeV including the squared terms also improves the validity of the dimension-six approach, but it only leads to identical limits for large m_ξ, combined with strong couplings. Indeed, limiting the momentum transfer of events for example through an upper limit on $p_{T,j}$ is well known to reduce the dependence on model assumptions [**? ?**].

Just as for the Vh production process, at least as long as the event numbers remain small the square of the dimension-six operators always improves the agreement with the full theory in weak boson fusion. With improved statistics the differences become smaller and ultimately negligible, and the question of whether the squared dimension-six amplitudes should be taken into account is rendered irrelevant.

3.4.2 Realistic tagging jets

Before we attempt to further improve the description of the full vector triplet model for example in the benchmark point T1, we briefly test if the parton-level effects described above survive a realistic environment. We add a parton shower and jet reconstruction now for the full process

$$pp \to h\ jj\,(+j)\,, \tag{3.72}$$

simulated in `MadGraph` [**?**]. Parton showering is performed by `PYTHIA6` [**?**] using the k_T-jet MLM matching scheme [**?**] with a minimum k_T jet measure between partons of `xqcut=20` GeV. `Fastjet` [**?**] is used to construct jets based on the k_T algorithm with $R = 0.4$. We do not include a Higgs decay because we are only interested in production-side kinematics. The standard WBF cuts then are

$$p_{T,j} > 20\ \text{GeV}\,, \qquad m_{jj} > 500\ \text{GeV}\,, \qquad \Delta\eta_{jj}\ >\ 3.6 \tag{3.73}$$

on the two hardest jets. We veto additional jets with $p_{T,j} > 20$ GeV between these two tagging jets. To analyse the effects of the $\Delta\eta_{jj}$ cut [**?**], we generate additional samples explicitly excluding Higgs-strahlung diagrams, in spite of the fact that it might break gauge invariance.

In Figure 3.11 we show that the distributions are generally robust under parton shower and jet reconstruction, but two complications arise. First, on-shell ξ production contributes to this process and is not entirely removed by the WBF cuts in Equation (3.73), leading to visible differences between the full and effective model already at low momenta. Such a resonance peak would be easy to identify experimentally and does not present a major problem for the dimension-six approximation.

Second, the tension between the full model and the dimension-six approximation at large momenta now remains below 10 %. This means that the $\Delta\eta_{jj}$ cut not only removes large contributions from Higgs-strahlung–like diagrams, it also gets rid of phase-space regions where the full model and the dimension-six description differ the most. At the same time, the $\Delta\eta_{jj}$ removes some of its well-known discrimination power for new physics effects versus the Standard Model [**?**].

3.4.3 Towards a simplified model

In the first part of the paper we have shown where in phase space a dimension-six description of LHC observables breaks down, both for Vh production and for weak boson fusion. For Vh production with its simple $2 \to 2$ kinematics problems are clearly linked to a possible s-channel resonance, as seen in Equation (3.66). For weak boson fusion there appears no resonance, but the result of Equation (3.68) suggests that the new states in the t-channel have a similar effect. In Figure 3.12 we show different tagging jet distributions, separating the Feynman diagrams including the heavy ξ states. In particular for the critical p_{T,j_1} distribution, the $\Delta\eta_{jj}$ distribution,

and the $\Delta\phi_{jj}$ distribution these diagrams are only very poorly described by the dimension-six approach. In practice this is not a problem because these contributions are strongly suppressed by the heavy mass m_ξ, but it poses the question how we can improve the agreement. The obvious solution to these problems in the s-channel of Vh production and in the t-channel of weak boson fusion is a simplified model [**?** **?**]. A new vector field mixing with the weak bosons as described by the Lagrangian shown in Equation (**??**) is such a simplified model, but its structure is still relatively complex. Obviously, an additional heavy scalar with mass around m_ξ and the appropriate couplings will improve the $2 \to 2$ kinematics for Vh production. The question we want to study in this section is if such a scalar can also improve the weak boson fusion kinematics.

A pseudo-scalar as a simplified vector

The simplest simplified model we can write down includes one new massive scalar S with a Higgs portal and a Yukawa coupling. However, a scalar state will not interfere with the Standard Model diagrams. In analogy to the CP properties of the Goldstone mode contributing to the massive Z boson we define our simplified model with a pseudo-scalar state as

$$\mathcal{L} \supset \frac{1}{2}(\partial_\mu S)^2 - \frac{m_S}{2} S^2 + \sum_{\text{fermions}} g_F \, S \overline{F} \gamma_5 F + g_S \, S^2 \phi^\dagger \phi \,. \tag{3.74}$$

In Figure 3.13 we show the same WBF distributions as in Figure 3.12, but including the simplified scalar model. For the $p_{T,j}$ distribution the squared new-physics amplitudes in the full vector model and the simplified scalar model indeed agree well, improving upon the dimension-six description which breaks down in this distribution. However, the interference term with the Standard Model, which is numerically dominant for most of the distribution and well described in the dimension-six model, poses a problem. The $\Delta\eta_{jj}$ distributions show even poorer agreement: the spin-1 amplitudes of the Standard Model and the vector triplet have similar phase-space distributions and give two forward tagging jets, while the scalar mediator favours central jets [**?**]. The $\Delta\phi_{jj}$ distribution, known to be sensitive to the tensor structure of the hard VVh interaction [**?**], exposes similar differences between the full and simplified model. Altogether, our simplified scalar model with its very different VVh interaction structure does improve the description in the region where the dimension-six approach breaks down, but it fails to describe interference patterns and angular correlations of the tagging jets.

Splitting functions and equivalence theorem

We can understand this very different behaviour of the scalar t-channel mediator as compared to the vector from the splitting kernels in the collinear limit. The matrix element squared for the

weak boson fusion process mediated by pseudo-scalars S has the form

$$|\mathcal{M}(qq \to q'q'h)|^2 \propto \frac{g_F^4\, t_1 t_2}{(t_1 - m_S^2)^2\,(t_2 - m_S^2)^2} \xrightarrow{m_S \to 0} \frac{\text{const}}{t_1 t_2}\,, \tag{3.75}$$

where t_1 and t_2 denote the respective momentum flow through each scalar propagator. For $m_S \to 0$ the Jacobians from the phase-space integration cancel a possible collinear divergence, while for a light vector boson a soft and a collinear divergence remains. Unlike in the usual WBF process, the tagging jets in our simplified scalar model will not be forward. The reason for this difference in the infrared is the (pseudo-)scalar coupling to quarks: since the scalar carries no Lorentz index, a $q \to qS$ splitting will be expressed in terms of the momentum combinations $(p_q p_q')$, $p_q^2 = m_q^2$, and $p_q'^2 = m_q^2$. In the limit of massless quarks only the first term remains as $t = 2(p_q p_q')$. This factor in the numerator cancels the apparent divergence of the t-channel propagator.

Adding higher-dimensional couplings of the (pseudo-)scalar to fermions, such as

$$\mathcal{L} \supset \sum_{\text{fermions}} \left[g_{F,2} S\overline{F}F + g_{F,3}(\partial_\mu S)\overline{F}\gamma^\mu F + g_{F,4} S(\partial_\mu S)\overline{F}\gamma^\mu\gamma_5 F + g_{F,5} S(\partial_\mu\partial_\nu S)\overline{F}[\gamma^\mu,\gamma^\nu]F \right], \tag{3.76}$$

does not change this result qualitatively. After partial integration and using the Dirac equation for the on-shell quarks the coupling $g_{F,3}$ is equivalent to the simple scalar coupling, $g_{F,2} = m_q^2 g_{F,3}$. In the limit of massless quarks, only two of the new structures listed in Equation (3.76) contribute at all: $g_{F,2}$ gives exactly the same result as g_F, while $g_{F,5}$ leads to even higher powers of t in the numerator,

$$|\mathcal{M}(qq \to q'q'h)|^2 \propto \frac{g_{F,5}^4\, t_1^3 t_2^3}{(t_1 - m_s^2)^2\,(t_2 - m_s^2)^2}\,. \tag{3.77}$$

No matter how we couple the (pseudo-)scalar of the simplified model to the external quarks, it never reproduces the collinear splitting kernel of a vector boson.

To be a little more precise, we can write out the spin-averaged matrix element squared for the $q \to q'S$ splitting in terms of the energy of the initial quark E, the longitudinal momentum fraction x, and the transverse momentum p_T, both carried by S,

$$\begin{aligned} |\mathcal{M}(q \to q'S)|^2 &= -2g_F^2 x m_q^2 + 2g_F^2 E^2(1-x)\left[\sqrt{1 + \frac{p_T^2}{E^2(1-x)^2} + \frac{m_q^2(1-(1-x)^2)}{E^2(1-x)^2}} - 1\right] \\ &= g_F^2\,\frac{x^2\, m_q^2}{1-x} + g_F^2\,\frac{p_T^2}{1-x} + \mathcal{O}\left(\frac{m_q^2 p_T^2}{E^2}, \frac{m_q^4}{E^2}, \frac{p_T^4}{E^2}\right)\,. \end{aligned} \tag{3.78}$$

From Equation (3.78) one can derive an effective Higgs approximation or **effective scalar approximation** [**?**]: in the collinear and high-energy limit, a process $qX \to q'Y$ mediated by a (pseudo-)scalar S is described by

$$\sigma(qX \to q'Y) = \int \mathrm{d}x\, \mathrm{d}p_T\, F_S(x, p_T)\, \sigma(SX \to Y) \tag{3.79}$$

with the splitting function

$$F_S(x, p_T) = \frac{g_F^2}{16\pi^2} \frac{x\, p_T^3}{\left(m_S^2(1-x) + p_T^2\right)^2} \,. \tag{3.80}$$

Unlike for vector emission, there is no soft divergence for $x \to 0$. The p_T dependence is the same as for transverse vector bosons [**? ?**], as we discuss in some detail in the appendix.

It might seem surprising that our pseudo-scalar is emitted with a fundamentally different phase-space dependence than longitudinal W and Z bosons, in apparent contradiction of the Goldstone boson equivalence theorem. However, the latter only makes a statement about the leading term in an expansion in m_W/E, where $\varepsilon_L^\mu \sim p^\mu/m_W$. At this order the squared matrix element for the splitting $q \to q' W_L$ agrees with the pseudo-scalar result, but is suppressed by a factor of m_q^2/E^2. Higher orders in the m_W/E expansion, outside the validity range of the equivalence theorem, are not suppressed by quark masses. The equivalence theorem is therefore of very limited use in describing the W or Z couplings to quarks except the top.

In Sec. 3.4.3 we have introduced a pseudo-scalar in the t-channel of weak boson fusion to describe some of the features which we find in the full vector triplet model and which our dimension-six description does not describe well. In this appendix we collect some of the main formulas and compare the kinematics of fermions radiating scalars, transverse, or longitudinal gauge bosons. Our formalism follows the effective W approximation [**?**] as well as the effective Higgs approximation [**?**] and allows us to analytically describe the soft and collinear behaviour. If we do not need to describe interference terms with SM gauge bosons we can start with a CP-even scalar splitting $q \to qS$, in terms of the energy of the initial quark E, the longitudinal momentum fraction x, carried by S, and the scalar's transverse momentum p_T:

$$\begin{aligned} |\mathcal{M}(q \to q'S)|^2 &= 2g_F^2(2-x)m_q^2 + 2g_F^2E^2(1-x)\left[\sqrt{1 + \frac{p_T^2}{E^2(1-x)^2} + \frac{m_q^2(1-(1-x)^2)}{E^2(1-x)^2}} - 1\right] \\ &= g_F^2\left(4 + \frac{x^2}{1-x}\right)m_q^2 + g_F^2\,\frac{p_T^2}{1-x} + \mathcal{O}\left(\frac{m_q^2p_T^2}{E^2}, \frac{m_q^4}{E^2}, \frac{p_T^4}{E^2}\right) . \end{aligned} \tag{3.81}$$

The main feature of this splitting is that the infrared behaviour is different for the term proportional to the quark mass and for the surviving term in the realistic limit $m_q \to 0$: in the absence of a fermion mass the collinear divergence from a t-channel propagator is cancelled by the coupling

structure. If the term proportional to m_q dominates there will be the usual collinear divergence once we include a scalar propagator. For a pseudo-scalar the structure shown in Equation (3.78) is very similar,

$$\begin{aligned} |\mathcal{M}(q \to q'S)|^2 &= -2g_F^2 x m_q^2 + 2g_F^2 E^2 (1-x) \left[\sqrt{1 + \frac{p_T^2}{E^2(1-x)^2} + \frac{m_q^2(1-(1-x)^2)}{E^2(1-x)^2}} - 1 \right] \\ &= g_F^2 \frac{x^2\, m_q^2}{1-x} + g_F^2 \frac{p_T^2}{1-x} + \mathcal{O}\left(\frac{m_q^2 p_T^2}{E^2}, \frac{m_q^4}{E^2}, \frac{p_T^4}{E^2} \right) . \end{aligned} \tag{3.82}$$

In the limit $m_q \to 0$ we can compute universal splitting kernels including only the leading term in p_T, as defined in Equation (3.79). Obviously, the scalar and pseudoscalar case given in Equation (3.80) are identical, and we can compare them with the splitting kernels for longitudinal or transverse W bosons [**?**],

$$\begin{aligned} F_S(x, p_T) &= \frac{g_F^2}{16\pi^2}\, x\, \frac{p_T^3}{\left(m_S^2(1-x) + p_T^2\right)^2} , \\ F_T(x, p_T) &= \frac{g^2}{16\pi^2}\, \frac{1+(1-x)^2}{x}\, \frac{p_T^3}{\left(m_W^2(1-x) + p_T^2\right)^2} , \\ F_L(x, p_T) &= \frac{g^2}{16\pi^2}\, \frac{(1-x)^2}{x}\, \frac{2m_W^2\, p_T}{\left(m_W^2(1-x) + p_T^2\right)^2} . \end{aligned} \tag{3.83}$$

In Figure 3.14 we show how these different splittings translate into WBF distributions and compare full simulations in `MadGraph` to the predictions of Equation (3.83). A heavy Higgs, $m_h = 1$ TeV, is needed to guarantee a large energy scale $E \sim m_h \gg p_T \sim m_W, m_S$. In this case we find that the effective scalar approximation quite accurately describes the transverse momentum distribution of the tagging jets. For $m_h = 125$ GeV the assumption of on-shell W bosons or scalars breaks down and the effective descriptions lose their validity.

3.4.4 Which observables to study

Now that it is clear that we cannot further improve the agreement between the vector triplet and its dimension-six approximation by adding a heavy scalar as a simplified model, we go back to the original problem: how can we best use the dimension-six approximation for limit setting, and do the shortcomings shown in Figure 3.12 harm this approach?

We know that in our LHC analysis we should avoid angular correlations of the tagging jets, like $\Delta\eta_{jj}$ or $\Delta\phi_{jj}$. Instead, we can use momentum-related kinematic variables like

$$x \in \left\{ q,\, p_{T,j_1},\, p_{T,j_2},\, p_{T,h} \right\} . \tag{3.84}$$

An acceptance cut $x > x_{\text{min}}$ on any of those variables projects out the interesting phase-space regions, while the cut $x < x_{\text{max}}$ ensures the validity of an effective theory description. If $x_{\text{min}} > x_{\text{max}}$ the dimension-six description is not useful. For each window $x_{\text{min,max}}$ we can compute the contribution to the theoretical uncertainty

$$\Delta_{\text{theo}}(x_{\text{min,max}}) = \left| \frac{\sigma_{\text{D6}} - \sigma_{\text{full}}}{\sigma_{\text{full}}} \right| , \tag{3.85}$$

as well as the statistics-driven and systematics-driven significances

$$\frac{S}{B}(x_{\text{min,max}}) = \left| \frac{\sigma_{\text{full}} - \sigma_{\text{SM}}}{\sigma_{\text{SM}}} \right| \qquad \text{and} \qquad \frac{S}{\sqrt{B}}(x_{\text{min,max}}) = \sqrt{L} \left| \frac{\sigma_{\text{full}} - \sigma_{\text{SM}}}{\sqrt{\sigma_{\text{SM}}}} \right| , \tag{3.86}$$

where $L = 30\ \text{fb}^{-1}$ is used as a toy number.

The question is for which observable x we find the largest S/B and $S/\sqrt{B}$ values while keeping Δ_{theo} small. In Figure 3.15 we show the correlations between theoretical uncertainty and experimental reach for the variables defined in Equation (3.84) for a parton-level analysis as defined in Equation (3.67). We see that the momentum transfer q or the leading tagging jet's p_{T,j_1} lead to the envelopes with the highest significance for a given theoretical uncertainty Δ_{theo}. This indicates that the leading tagging jet's transverse momentum is the best way of experimentally accessing the momentum flow through the hard process, at least for the hard parton-level process with only two tagging jets.

3.5 Conclusions

An effective field theory for the Higgs sector offers a theoretically well-defined, efficient, and largely model-independent language to analyse extensions of the Standard Model in both rate measurements and kinematic distributions. A fit of dimension-six operators to LHC Higgs measurements works fine [23] and constitutes the natural extension of the Higgs couplings analyses of Run I. Most of the relevant higher-dimensional operators correspond to simple coupling modifications, supplemented by four operators describing new Lorentz structures in the Higgs coupling to weak bosons [23].

In this paper we have studied the validity of this approach from the theoretical side. We know that at the LHC a clear hierarchy of electroweak and new physics scales cannot be guaranteed, the question is whether dimension-six operators nevertheless capture the phenomenology of specific UV-complete theories with sufficient accuracy. We have systematically compared a singlet Higgs portal model, a two-Higgs doublet model, scalar top partners, and a heavy vector triplet to their dimension-six EFT descriptions, based on the linear realisation of electroweak symmetry breaking with a Higgs doublet. We have analysed the main Higgs production and decay signatures, covering rates as well as kinematic distributions.

Model	Process	EFT failure		
		resonance	kinematics	matching
singlet	on-shell $h \to 4\ell$, WBF, Vh, …			×
	off-shell WBF, …		(×)	×
	hh	×	×	×
2HDM	on-shell $h \to 4\ell$, WBF, Vh, …			×
	off-shell $h \to \gamma\gamma$, …		(×)	×
	hh	×	×	×
top partner	WBF, Vh			×
vector triplet	WBF		(×)	×
	Vh	×	(×)	×

Table 3.15: Possible sources of failure of dimension-six Lagrangian at the LHC. We use parentheses where deviations in kinematic distributions appear, but are unlikely to be observed in realistic scenarios.

We have found that the dimension-six operators provide an adequate description in almost all realistic weakly coupled scenarios. Shifts in the total rates are well described by effective operators. Kinematic distributions typically do not probe weakly interacting new physics with sufficient precision in the high-energy tails to challenge the effective operator ansatz. This is obvious for the extended scalar models, where new Lorentz structures and momentum-dependent couplings with dramatic effects in LHC distributions only appear at the loop level. A loop-suppressed effective scale suppression $E^2/(4\pi\Lambda)^2$ has to be compared with on-shell couplings modifications proportional to v^2/Λ^2. Only phase space regions probing energies around $4\pi v \approx 3$ TeV significantly constrain loop contributions in the Higgs sector and eventually lead to breakdown of the effective field theory. In turn, a simple dimension-six descriptions will capture all effects that are expected to be measurable with sufficient statistics at the LHC Run II. On the other hand, the vector triplet model shows that modifications of the gauge sector can generate effects in LHC kinematics at tree level. However, we again find that for weakly interacting models and phenomenologically viable benchmark points they are described well by an appropriate set of dimension-six operators.

Three sources for a possible breakdown of the dimension-six description are illustrated in Table 3.15[6]: First, the EFT cannot describe light new resonances. Such a signature at the LHC would be an obvious signal to stop using the EFT and switch to appropriate simplified models.

[6] Forcing the EFT approach into a spectacular breakdown was the original aim of this paper, but to our surprise this did not happen.

Second, selected kinematic distributions fail to be described by the dimension-six Lagrangian, in particular for Higgs pair production. Deviations in the high-energy tails of WBF and Higgs-strahlung distributions on the other hand are too small to be relevant in realistic weakly coupled scenarios. These two cases do not threaten LHC analyses in practice.

The third issue with the dimension-six EFT description is linked to matching in the absence of a well-defined scale hierarchy. Even with only one heavy mass scale in the Lagrangian, the electroweak VEV together with large couplings can generate several new physics scales, defined by the masses of the new particles. A linear EFT description, which is justified by the SM-like properties of the newly discovered Higgs boson, should in principle be matched in the phase where the electroweak symmetry is unbroken. Such a procedure is blind to additional scales induced by the electroweak VEV, potentially leading to large errors in the dimension-six approximation. Including v-dependent terms in the Wilson coefficients, which corresponds to matching in the broken phase, can significantly improve the EFT performance. We have explicitly demonstrated this for all the models considered in this paper.

None of these complications with the dimension-six description presents a problem in using effective operators to fit LHC Higgs data. They are purely theoretical issues that need to be considered for the interpretation of the results.

While a dimension-six Higgs analysis at the LHC cannot be considered the leading part of a consistent effective theory, it describes the effects of weakly interacting extensions of the Higgs-gauge sector very well [**?**]. In this brief study we have answered two practical question concerning such a dimension-six analysis for Run II.

First, a priori it is not clear if squared dimension-six terms should be included in calculations. We have studied two particularly challenging parameter points of a vector triplet model for Vh production and for weak-boson-fusion Higgs production. For both processes we find that the dimension-six squared term avoids negative rate predictions in the m_{Vh} or $p_{T,V}$ distributions of Vh production and in the p_{T,j_1} distribution of weak boson fusion. Even for cases with a constructive interference between the dimension-six and the Standard Model contributions, it turns out that including the dimension-six squared term improves the agreement of kinematic distributions between the full model and the dimension-six approximation. Ultimately, this translates into a better agreement in the expected exclusion limits[7].

Second, we have attempted to improve the agreement between the full model and our approximation by using a simplified model. The only significantly simpler model than a mixing gauge extension is an extended scalar sector. While the corresponding deviations between the full model and the dimension-six approximation are phenomenologically hardly relevant, we find that such an additional scalar improves the modelling of kinematic distributions of the kind m_{Vh} and p_{T,j_1} where the dimension-six description breaks down. However, this comes at the cost of significant deviations in the dominant interference terms. Moreover, once we include angular correlations

[7] Similar conclusions in a different framework have recently been published in Reference [**?**].

like $\Delta\eta_{jj}$ or $\Delta\phi_{jj}$ in weak boson fusion, the simplified model fails badly. The difference can be traced to the divergence structure of the corresponding splittings.

Seeing that the dimension-six approach is still the better simple model to describe new physics in WBF distributions, we have finally analysed which phase-space regions provide an interesting window to new physics while being well described by the dimension-six approximation. We have demonstrated that the leading tagging jet's p_T distribution is particularly suited for such a search for new physics.

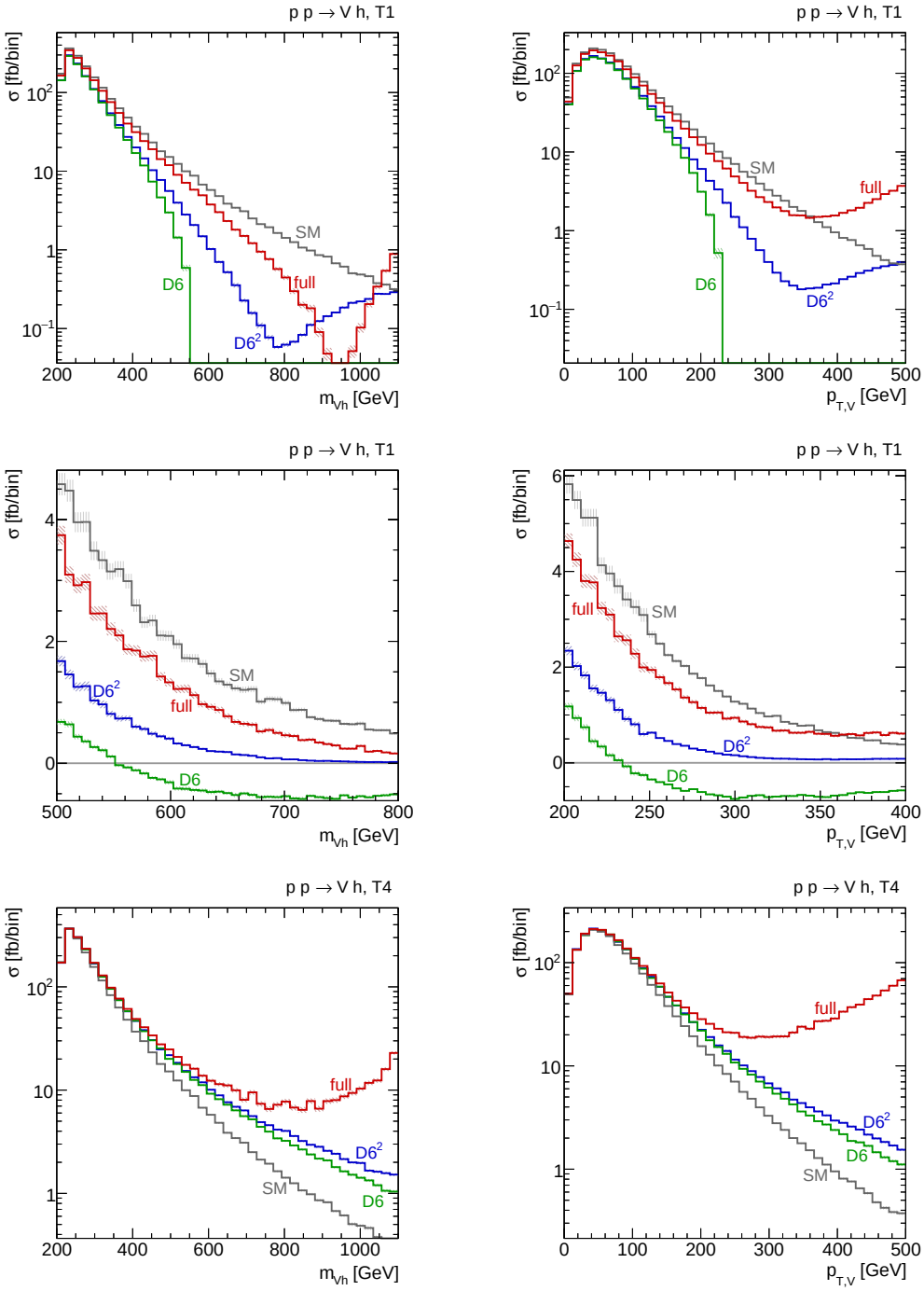

Figure 3.7: Vh distributions with ("D6^2") and without ("D6") the dimension-six squared term. The left panels show m_{VH}, the right panels $p_{T,V}$. The central panels show the region where leaving out the squared dimension-six terms leads to a negative cross section.

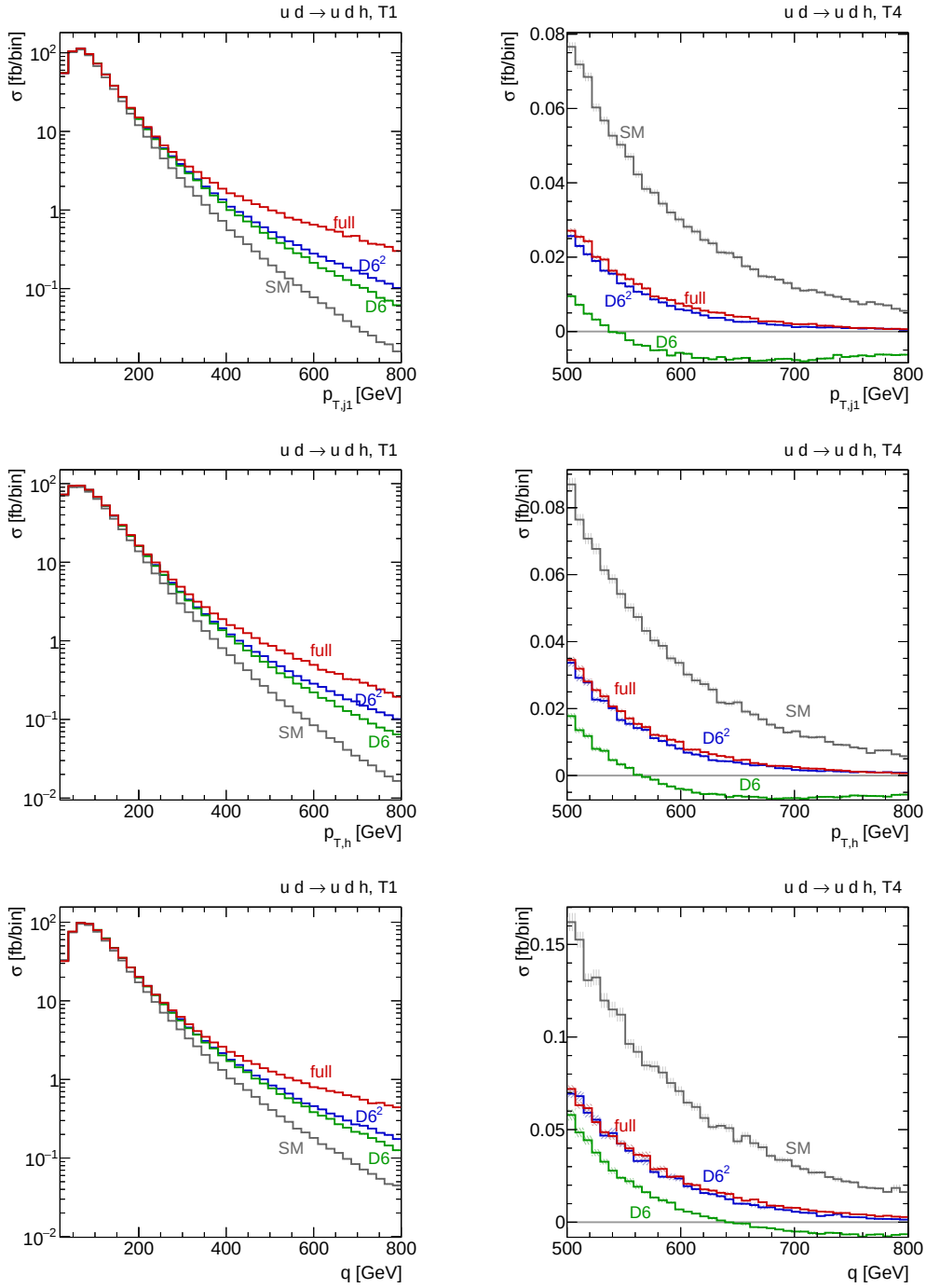

Figure 3.8: WBF distributions with ("D6^2") and without ("D6") the dimension-six squared term. From top to bottom: $p_{T,j1}$, $p_{T,h}$, and virtuality q defined in Equation (3.69). The right panels show the region where leaving out the squared dimension-six terms leads to a negative cross section.

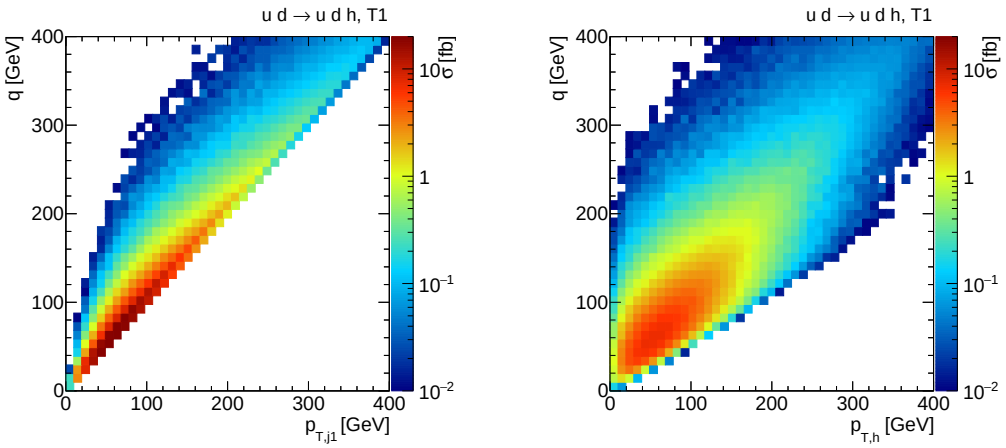

Figure 3.9: WBF correlations between the virtuality q and p_{T,j_1} (left) or $p_{T,h}$ (right).

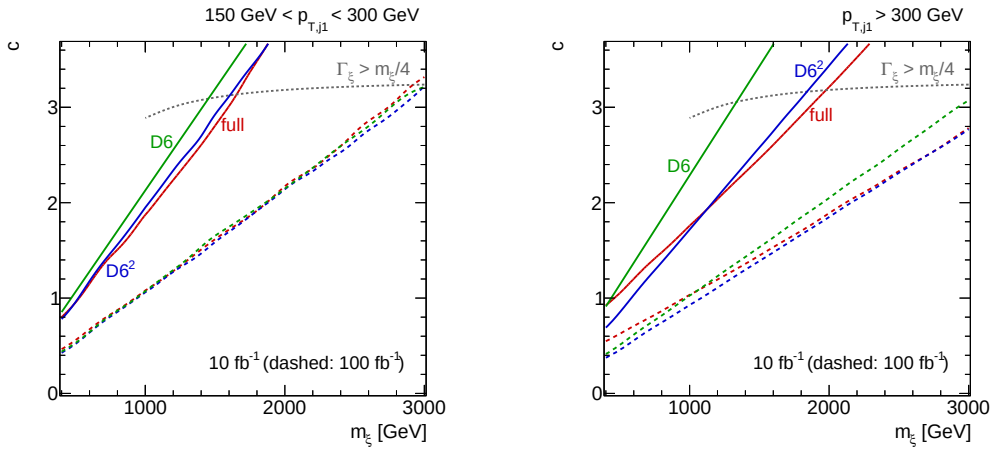

Figure 3.10: Expected limits on a two-dimensional slice of the vector triplet parameter space. We show the analysis based on the event numbers in 150 GeV < p_{T,j_1} < 300 GeV (left) and based on the tail p_{T,j_1} > 300 GeV.

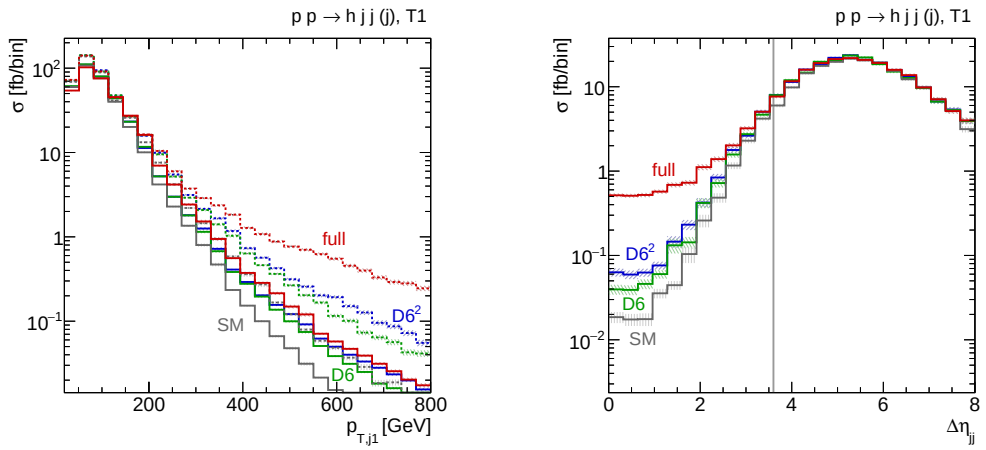

Figure 3.11: WBF distribution at hadron level. Left: p_{T,j_1} distribution based on the full process, the dashed lines show the distributions based on WBF diagrams only and without a $\Delta\eta_{jj}$ cut. Right: $\Delta\eta_{jj}$ based on WBF diagrams only, the vertical line marks the standard WBF cut following Equation (3.73).

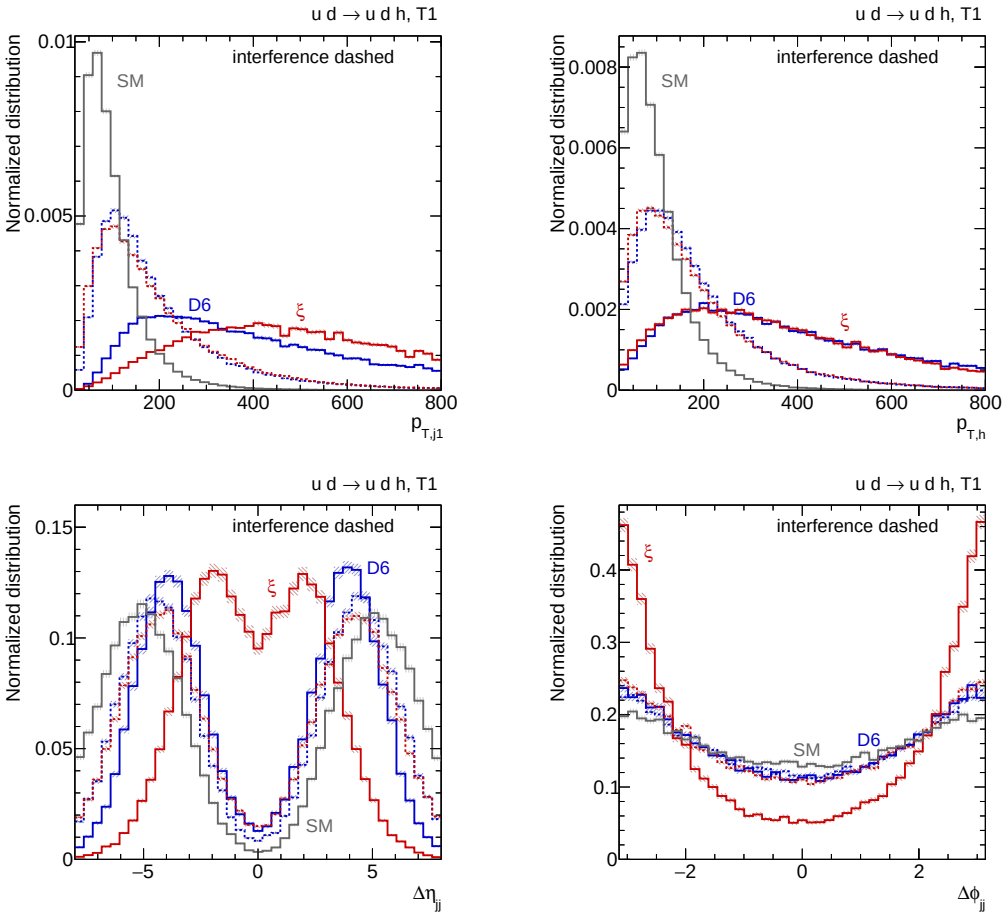

Figure 3.12: Normalised WBF distributions of the tagging jets. We separate the squared new-physics amplitudes, shown as solid lines, from the interference with the SM-like diagrams (dashed).

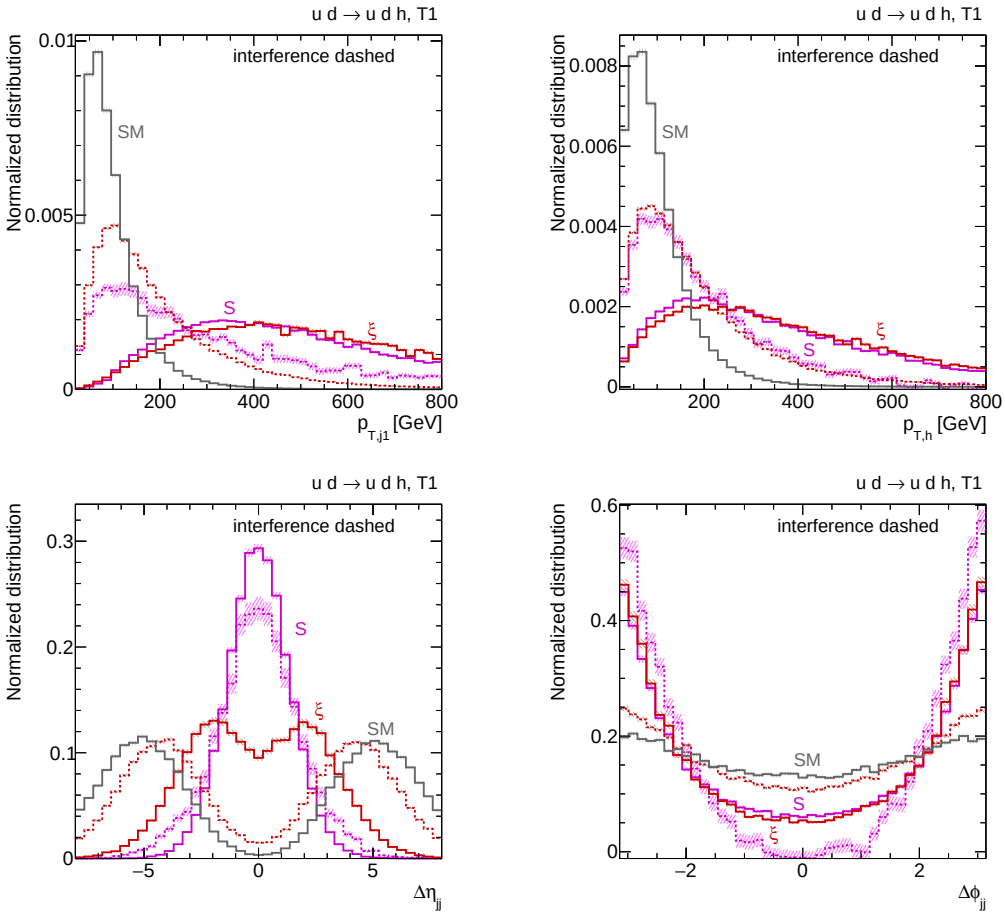

Figure 3.13: Normalised WBF distributions for a scalar simplified model defined in Equation (3.74) vs the vector triplet benchmark.

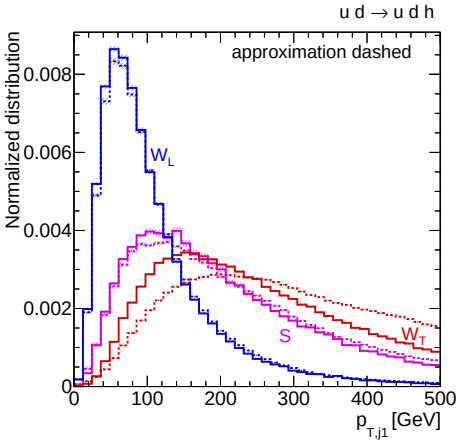

Figure 3.14: Normalised WBF distributions of the tagging jets in the SM with a heavy Higgs, $m_h = 1$ TeV. Scalar mediators are compared to longitudinal and transverse W bosons following Reference [**?**]. The dotted lines give the corresponding predictions of the effective W and scalar approximations, Equation (3.83).

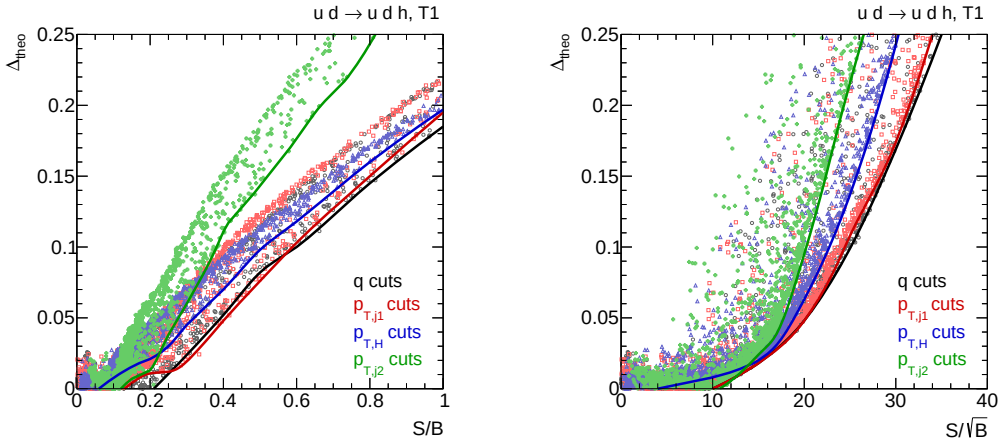

Figure 3.15: Experimental reach in systematics-driven and statistics-driven channels vs theoretical uncertainties of the dimension-six description. Each point corresponds to a window $x_{\text{min,max}}$ in one of the four momentum observables that leaves a signal cross section of at least 20 fb.

Chapter 4

Better Higgs measurements through information geometry

Some funny quote.

— Someone

4.1 Introduction

4.2 Information geometry

4.2.1 Fisher information and Cramér-Rao bound

4.2.2 Simple example

4.3 Information in LHC processes

4.3.1 Information in event counts

4.3.2 Information in histograms

4.3.3 Information in full process and differential information

4.3.4 Nuisance parameters and profiling

4.3.5 The MadFisher algorithm

4.3.6 Geometry of effective field theories

4.4 Higgs signatures from CP-even operators

4.4.1 Weak-boson-fusion Higgs to taus

4.4.2 Weak-boson-fusion Higgs to four leptons

4.4.3 Higgs plus single top

4.5 CP violation in the Higgs sector

4.6 Technical questions

4.6.1 Systematic uncertainties

4.6.2 Comparison with other tools

4.7 Conclusions

Chapter 5

Conclusions

Can we actually know the universe? My God, it's hard enough finding your way around in Chinatown.

— W. Allen [200]

Acknowledgements

Did you know that in my PhD defence, I didn't answer a single question correctly?
— T. Plehn [201]

Without doubt, the three years of my PhD were an amazing time.

For that, I first and foremost want to thank my advisor Tilman Plehn: for taking me on as a student, for working with me on interesting questions, and for disagreeing with me on many points over coffee. In particular I want to thank him for always having my back, including coming into the office on a Sunday morning to get me a backup laptop when mine broke down days before a deadline. And last but certainly not least, I am very grateful to him for clearing the way to an academic career for me, even though I finally decided against this path.

I would like to express my gratitude to Björn Malte Schäfer for reading and refereeing this thesis, and to Monica Dunford and Susanne Westhoff for completing my examination committee. Further praise is reserved until after the defence.

The Research Training Group "Particle physics at the LHC" (DFG GRK 1940) paid my salary and, together with the Heidelberg Graduate School of Fundamental Physics, my travels. I am grateful for their support.

During the different PhD projects, I had the great pleasure to collaborate with a number of amazing scientists. Together with Tilman Plehn, Ayres Freitas and David López-Val saw me off to a great start. Anke Biekötter joined us a little later. Chasing the diboson ambulance with JoAnne Hewett, Joachim Kopp, Tom Rizzo, and Jamie Tattersall was a wild and fun ride. One of the best ideas during my PhD was to invite Kyle Cranmer to a beer in Café Botanik. Working with him was truly inspiring, and was even more fun when Felix Kling joined our team. Heartfelt thanks to all of my collaborators.

Much of the work presented in this thesis would not have been possible without the help

from others. In particular I would like to express my gratitude to Juan Gonzalez-Fraile for many discussions about effective field theories; Peter Schichtel for helping me set up and use `MadMax`; and Torben Schell, who was an unwavering source of physics knowledge as well as a saviour in the hour of incomprehensible linker errors.

From Marstall lunches to "class trips" to Pheno, with nut cakes, PhD hats and the eternal coffee list, the Heidelberg pheno group was akin to a second home in the last three years. I would like to thank Martin Bauer, Anke Biekötter, Katja Böhnke, Anja Butter, Nishita Desai, Karin Firnkes, Josua Göcking, Juan Gonzalez-Fraile, Jamil Hetzel, Sebastian Hoof, Jan Horak, Thomas Hugle, Jörg Jäckel, Florian Jetter, Martin Klassen, Lara Kuhn, Rabea Link, Viraf Mehta, Luminita Mihaila, Rhea Moutafis, Tilman Plehn, Peter Reimitz, Michael Russel, Torben Schell, Sebastian Schenk, Peter Schichtel, Linda Shen, Beatriz Tapia Oregui, Jamie Tattersall, Valentin Tenorth, Jennifer Thompson, Susanne Westhoff, and Nikolai Zerf. I am grateful to Anke, Patrick, and Sebastian for the awesome wine & cheese seminar. But most of all, I would like to thank Anja and Torben, who shared nearly the entire PhD journey with me. Without the two, these three years would not have been half as much fun.

…

Appendix

Here we collect various technical details and intermediate results that are not too interesting on their own, but should be included for completeness and reproducibility. We begin with a definition of different EFT bases and provide a dictionary to translate between them. Appendix 2 then contains some additional details on the models considered in Chapter 3. Finally, in Appendix 3 we derive some of the key results of Chapter 4.

1 Effective field theory conventions

1.1 Standard Model conventions

Bla

HISZ basis		
$\mathcal{O}_{\phi 1} = (D_\mu \phi)^\dagger \, (\phi \, \phi^\dagger) \, (D^\mu \phi)$	$\mathcal{O}_{\phi 2} = \frac{1}{2} \partial^\mu (\phi^\dagger \phi) \, \partial_\mu (\phi^\dagger \phi)$	$\mathcal{O}_{\phi 3} = \frac{1}{3} (\phi^\dagger \phi)^3$
$\mathcal{O}_{GG} = (\phi^\dagger \phi) \, G^A_{\mu\nu} \, G^{\mu\nu \, A}$		
$\mathcal{O}_{BB} = -\frac{g'^2}{4} (\phi^\dagger \phi) \, B_{\mu\nu} \, B^{\mu\nu}$	$\mathcal{O}_{WW} = -\frac{g^2}{4} (\phi^\dagger \phi) \, W^k_{\mu\nu} \, W^{\mu\nu \, k}$	$\mathcal{O}_{BW} = -\frac{g \, g'}{4} (\phi^\dagger \sigma^k \phi) \, B_{\mu\nu} \, W^{\mu\nu \, k}$
$\mathcal{O}_B = \frac{ig}{2} (D^\mu \phi^\dagger)(D^\nu \phi) \, B_{\mu\nu}$	$\mathcal{O}_W = \frac{ig}{2} (D^\mu \phi^\dagger) \sigma^k (D^\nu \phi) \, W^k_{\mu\nu}$	

Table 1: Bosonic CP-conserving Higgs operators in the HISZ basis.

1.2 HISZ basis

1.3 SILH basis

The SILH Lagrangian reads

$$\begin{aligned}\mathcal{L}_{\rm EFT} =& \mathcal{L}_{\rm SM} + \frac{\bar{c}_H}{2v^2}\,\partial^\mu(\phi^\dagger\phi)\,\partial_\mu(\phi^\dagger\phi) + \frac{\bar{c}_T}{2v^2}\,(\phi^\dagger \overleftrightarrow{D}^\mu \phi)\,(\phi^\dagger \overleftrightarrow{D}_\mu \phi) - \frac{\bar{c}_6\lambda}{v^2}(\phi^\dagger\phi)^3 \\ &+ \frac{ig\bar{c}_W}{2m_W^2}\,(\phi^\dagger\,\sigma^k \overleftrightarrow{D}^\mu \phi)\,D^\nu\,W^k{}_{\mu\nu} + \frac{ig'\bar{c}_B}{2m_W^2}\,(\phi^\dagger \overleftrightarrow{D}^\mu \phi)\,\partial^\nu B_{\mu\nu} \\ &+ \frac{ig\,\bar{c}_{HW}}{m_W^2}\,(D^\mu\,\phi^\dagger)\,\sigma^k\,(D^\nu\,\phi)\,W^k_{\mu\nu} + \frac{ig'\bar{c}_{HB}}{m_W^2}(D^\mu\phi^\dagger)\,(D^\nu\,\phi)\,B_{\mu\nu} \\ &+ \frac{g'^2\bar{c}_\gamma}{m_W^2}\,(\phi^\dagger\phi)\,B_{\mu\nu}\,B^{\mu\nu} + \frac{g_s^2\bar{c}_g}{m_W^2}\,(\phi^\dagger\phi)\,G^A_{\mu\nu}\,G^{\mu\nu\,A} \\ &- \left[\frac{\bar{c}_u}{v^2}\,y_u\,(\phi^\dagger\phi)(\phi^\dagger\cdot\overline{Q}_L)\,u_R + \frac{\bar{c}_d}{v^2}\,y_d\,(\phi^\dagger\phi)(\phi\,\overline{Q}_L)\,d_R + \frac{\bar{c}_\ell}{v^2}\,y_\ell\,(\phi^\dagger\phi)(\phi\,\overline{L}_L)\,\ell_R + \text{h.c.}\right].\end{aligned} \tag{1}$$

Here, $g = e/s_w, g' = e/c_w$, and g_s stand for the SM gauge couplings and λ denotes the usual Higgs quartic coupling. The normalization of the dimension-6 Wilson coefficients $\bar{c}_i$ includes conventional prefactors which reflect a bias concerning their origin. We present further details on the EFT setup, the translation between the different bases, and the connection to Higgs observables in Appendix **??**.

As mentioned in Sec. **??**, we here adopt the notation and conventions of Reference [149], which is based on the SILH framework with the decomposition and normalization of the Wilson coefficients defined in Reference [**?**]. For our purposes, it is enough to single out the subset that encodes all possible new physics contributions to the Higgs sector compatible with CP conservation and the flavor structure of the SM. These are given in Tab. **??** and correspond to the Lagrangian in Equation (1).

The conventions for how covariant derivatives act on the Higgs, fermion and gauge vector fields are fixed as follows:

$$\begin{aligned} D_\mu\phi &= \partial_\mu\phi - \frac{ig'}{2}B_\mu\phi - ig\frac{\sigma^a}{2}\,W^a_\mu\,\phi\,, \\ D_\mu F_L &= \partial_\mu F_L - ig'\frac{Y_{F_L}}{2}B_\mu F_L - ig\frac{\sigma^a}{2}\,W^a_\mu\,F_L\,, \\ D_\mu V^a_\nu &= \partial_\mu V^a_\nu + g\,\varepsilon^{abc}\,W^b_\mu\,V^c_\nu\,, \\ D_\mu W^a_{\nu\rho} &= \partial_\mu W^a_{\nu\rho} + g\,\varepsilon^{abc}\,W^b_\mu\,W^c_{\nu\rho}\,. \end{aligned} \tag{2}$$

While the effective Lagrangian in Equation (1) is written in terms of the fundamental SM gauge fields, the connection to physics observables is more easily seen in the mass-eigenstate basis,

which we can write as

$$\begin{aligned}\mathcal{L} \supset & -\frac{m_H^2}{2v}\, g^{(1)}_{HHH}\, HHH + \frac{1}{2}\, g^{(2)}_{HHH}\, H(\partial_\mu H)\,(\partial^\mu H) \\ & - \frac{1}{4}\, g_{ggH}\, G^{\mu\nu\,A}\, G^A_{\mu\nu}\, H - \frac{1}{4}\, g_{\gamma\gamma H}\, F^{\mu\nu}\, F_{\mu\nu}\, H \\ & - \frac{1}{4}\, g^{(1)}_Z\, Z_{\mu\nu}\, Z^{\mu\nu}\, H - g^{(2)}_Z\, Z_\nu\, \partial_\mu\, Z^{\mu\nu}\, H + \frac{1}{2}\, g^{(3)}_Z\, Z_\mu Z^\mu\, H \\ & - \frac{1}{2}\, g^{(1)}_W\, W^{\mu\nu}\, W^\dagger_{\mu\nu}\, H - \left[g^{(2)}_W\, W^\nu\, \partial^\mu\, W^\dagger_{\mu\nu} H + \text{h.c.} \right] + g^{(3)}_W\, m_W\, W^\dagger_\mu W^\mu\, H \\ & - \left[g_u \frac{1}{\sqrt{2}}\, (\bar{u} P_R u)\, H + g_d \frac{1}{\sqrt{2}} \left(\bar{d} P_R d\right) H + g_\ell \frac{1}{\sqrt{2}} \left(\bar{\ell} P_R \ell\right) H + \text{h.c.} \right], \end{aligned} \tag{3}$$

with the different effective couplings g_i quoted in Tab. 2. More details on the notation and conventions can be found in Reference [149].

Note that the Higgs-fermion coupling shift is given by $g_f \propto y_f(1 - \bar{c}_H/2 + 3\bar{c}_f/2)$, but $\mathcal{O}_f$ also shifts the fermion masses to $m_f = y_f v(1 + \bar{c}_f/2)/\sqrt{2}$, yielding the result given above. Similarly, $\mathcal{O}_H$ and $\mathcal{O}_\gamma$ generate additional contributions to the Higgs-boson and gauge-boson kinetic terms, which are restored to their canonical form by the field re-definitions

$$\begin{aligned} H \to H \left(1 - \frac{1}{2} c_H\right), \qquad & Z_\mu \to Z_\mu \left(1 + \frac{4 s_w^4}{c_w^2} c_\gamma\right), \\ & A_\mu \to A_\mu \left(1 + 4 s_w^2\, c_\gamma\right) - Z_\mu \left(\frac{8 s_w^3}{c_w} c_\gamma\right). \end{aligned} \tag{4}$$

None of the operators considered in this basis affects the relations between g, m_W, v and G_F, so the SM relations

$$m_W = \frac{g\, v}{2}, \qquad G_F = \frac{\sqrt{2}\, g^2}{8\, m_W^2} = \frac{1}{\sqrt{2} v^2}, \tag{5}$$

can always be used to translate these coupling shifts from one scheme of input parameters to another.

Dimension-6 operators result in a modified pattern of Higgs interactions, leading to coupling shifts $g_{xxH} \equiv g^{\text{SM}}_{xxH}(1 + \Delta_x)$ and also genuinely novel Lorentz structures. Interestingly, in general more than one of the effective operators in Tab. **??** contributes to a given Higgs interaction in the mass basis, implying that it is in general not possible to establish a one-to-one mapping between Wilson coefficients and distorted Higgs couplings.

Note that the Wilson coefficients of the operators $\mathcal{O}_T$ and $\mathcal{O}_B + \mathcal{O}_W$ are strongly constrained by electroweak precision data [**?**]. In this work, we allow ourselves, on occasion, to ignore these bounds to more distinctly illustrate the effects in the Higgs sector.

Coupling	Operators	Expression
$g_Z^{(1)}$	$\mathcal{O}_{HB}, \mathcal{O}_{HW}, \mathcal{O}_H gam$	$\frac{2g}{m_W c_w^2}\left[\bar{c}_{HB} s_w^2 - 4\bar{c}_\gamma s_w^4 + c_w^2\,\bar{c}_{HW}\right]$
$g_Z^{(2)}$	$\mathcal{O}_{HW}, \mathcal{O}_{HB}, \mathcal{O}_W, \mathcal{O}_B$	$\frac{g}{m_W c_w^2}\left[(\bar{c}_{HW} + \bar{c}_W)c_w^2 + (\bar{c}_B + \bar{c}_{HB})s_w^2\right]$
$g_Z^{(3)}$	$\mathcal{O}_H, \mathcal{O}_T, \mathcal{O}_\gamma$	$\frac{g m_W}{c_w^2}\left[1 - \frac{1}{2}\bar{c}_H - 2\bar{c}_T + 8\bar{c}_\gamma \frac{s_w^4}{c_w^2}\right]$
$g_W^{(1)}$	$\mathcal{O}_{HW}$	$\frac{2g}{m_W}\,\bar{c}_{HW}$
$g_W^{(2)}$	$\mathcal{O}_{HW}, \mathcal{O}_W$	$\frac{g}{m_W}\left[\bar{c}_W + \bar{c}_{HW}\right]$
$g_W^{(3)}$	$\mathcal{O}_H$	$g\left(1 - \frac{1}{2}\bar{c}_H\right)$
g_f	$\mathcal{O}_H, \mathcal{O}_f \quad (f = u, d, \ell)$	$\frac{\sqrt{2} m_f}{v}\left[1 - \frac{1}{2}\bar{c}_H + \bar{c}_f\right]$
g_g	$\mathcal{O}_H, \mathcal{O}_g$	$g_H - \frac{4\bar{c}_g g_s^2 v}{m_W^2}$
g_γ	$\mathcal{O}_H, \mathcal{O}_\gamma$	$a_H - \frac{8 g \bar{c}_\gamma s_w^2}{m_W}$
$g_{HHH}^{(1)}$	$\mathcal{O}_H, \mathcal{O}_6$	$1 + \frac{5}{2}\bar{c}_6 - \frac{1}{2}\bar{c}_H$
$g_{HHH}^{(2)}$	$\mathcal{O}_H$	$\frac{g}{m_W}\,\bar{c}_H$

Table 2: Subset of the dimension-6 operators which enter the different leading-order Higgs couplings which are relevant for LHC phenomenology, in the notation and conventions of Reference [149] (see text). The different superscripts denote the various terms in the Lagrangian in Equation (3) and correspond to either a SM-like interaction with a rescaled coupling strength or to genuinely new Lorentz structures. The weak coupling constant is written as $g \equiv e/s_w$. The SM contribution to the loop-induced Higgs coupling to the gluons (photons) is denoted by g_H (a_H).

Translations between effective operator bases can be performed with the help of equations of motion, field redefinitions, integration by parts and Fierz identities. Here we quote a number of such relations which turn out to be particularly useful for the practitioner. For example, in addition to the effective operators in the SILH basis, we often find the operators

$$\begin{aligned} \mathcal{O}_r &= \phi^\dagger\phi\,(D_\mu\phi)^2\,, & \mathcal{O}'_{HF} &= \left(\bar{f}_L\,\gamma^\mu\,\sigma^a\,f_L\right)\left(\phi^\dagger\,\sigma^a\overleftrightarrow{D}_\mu\,\phi\right), \\ \mathcal{O}_D &= \left(D^2\,\phi\right)^2\,, & \hat{\mathcal{O}}'_{HH} &= \left(\phi^\dagger\,\sigma^a\overleftrightarrow{D}_\mu\,\phi\right)\left(\phi^\dagger\,\sigma^a\overleftrightarrow{D}_\mu\,\phi\right). \end{aligned} \tag{6}$$

$\hat{\mathcal{O}}'_{HH}$ can be replaced by using the completeness relation of the Pauli matrices, which for arbitrary SU(2) doublets ξ, χ, η, ψ leads to

$$\begin{aligned} (\xi^\dagger\sigma^a\chi)(\eta^\dagger\sigma^a\psi) &= \sum_{ijkl}\xi_i^*\,\sigma^a_{ij}\chi_j\,\eta_k^*\sigma^a_{kl}\psi_l \\ &= \sum_{ijkl}(2\delta_{il}\delta_{jk}-\delta_{ij}\delta_{kl})\,\xi_i^*\,\chi_j\,\eta_k^*\psi_l = 2(\xi^\dagger\psi)(\eta^\dagger\chi)-(\xi^\dagger\chi)(\eta^\dagger\psi)\,. \end{aligned} \tag{7}$$

Thus we find

$$\begin{aligned} \hat{\mathcal{O}}'_{HH} &= (\phi^\dagger\,\sigma^a\,D^\mu\phi)^2+((D^\mu\phi^\dagger)\,\sigma^a\,\phi)^2-2((D^\mu\phi^\dagger)\,\sigma^a\,\phi)(\phi^\dagger\,\sigma^a\,D_\mu\phi) \\ &= (\phi^\dagger\,D^\mu\phi)^2+((D^\mu\phi^\dagger)\,\phi)^2-2\left[2((D^\mu\phi^\dagger)\,D^\mu\phi)(\phi^\dagger\phi)-((D^\mu\phi^\dagger)\,\phi)(\phi^\dagger\,D^\mu\phi)\right] \\ &= \mathcal{O}_H-4\mathcal{O}_r\,. \end{aligned} \tag{8}$$

The equation of motion for the W fields,

$$D^\nu W^a_{\mu\nu} = -ig\,\phi^\dagger\frac{\sigma^a}{2}\overleftrightarrow{D}_\mu\phi - g\sum_f\bar{f}_L\frac{\sigma^a}{2}\gamma_\mu f_L\,, \tag{9}$$

gives rise to the identity

$$\sum_f\mathcal{O}'_{HF}=\frac{2}{g}\,\mathcal{O}_W-i\,\mathcal{O}_H+4i\,\mathcal{O}_r\,. \tag{10}$$

A global redefinition $\phi\to\phi+\alpha\,(\phi^\dagger\phi)\phi/v^2$ generates a shift in the Wilson coefficients

$$c_H\to c_H+2\alpha\,,\quad c_r\to c_r+2\alpha\,,\quad c_6\to c_6+4\alpha\,,\quad c_f\to c_f+\alpha\,, \tag{11}$$

so that with the choice $\alpha=-c_r/2$ one can eliminate the operator $\mathcal{O}_r$ in favor of other operators:

$$\mathcal{O}_r\leftrightarrow\left\{-\frac{1}{2}\,\mathcal{O}_H+2\,\lambda\,\mathcal{O}_6+\sum_f\left[\frac{1}{2}\,y_f\,\mathcal{O}_f+\text{h.c.}\right]\right\}. \tag{12}$$

Finally, $\mathcal{O}_D$ can be exchanged for others using the equation of motion for ϕ,

$$D^2\phi = -\mu^2\,\phi - 2\,\lambda\,\phi^\dagger\phi\,\phi - \sum_{\text{gen.}}\left[y_u\,\bar{Q}_L^T\,u_R + y_d\,\bar{d}_R\,Q_L + y_\ell\,\bar{\ell}_R\,L_L\right]. \tag{13}$$

This leads to

$$\mathcal{O}_D = \mu^4\,\phi^\dagger\phi + 4\,\lambda\,\mu^2\,(\phi^\dagger\phi)^2 + \mu^2\sum_f y_f\,\bar{f}_L\phi f_R\; + 4\,\lambda^2\,(\phi^\dagger\phi)^3 + 2\,\lambda\sum_f y_f\,\phi^\dagger\phi\,\left(\bar{f}_L\phi f_R\right). \tag{14}$$

The first three terms lead to a renormalization of the SM parameters μ, λ, y_f, without any impact on physical observables. The last two terms, however, means that $\mathcal{O}_D$ is equivalent to the combination

$$\mathcal{O}_D \leftrightarrow 4\,\lambda^2\,\mathcal{O}_6 + 2\,\lambda\sum_f\left(y_f\,\mathcal{O}_f + \text{h.c.}\right). \tag{15}$$

1.4 HLM basis

Aside from the relatively simple case of the multi-Higgs sector extensions, we make use of the covariant derivative expansion [62, 63] to analytically carry out the matching between the different UV completions to their corresponding EFT description. The method has been recently reappraised in Reference [60] and employed in a number of studies [**? ? ? ?**]. By applying this method, the Wilson coefficients are readily obtained in a different operator basis (henceforth dubbed HLM),

$$\mathcal{L}_{\text{HLM}} = \sum_i \frac{k_i}{\Lambda^2}\mathcal{O}_i''. \tag{16}$$

The HLM operators involving Higgs fields and their interaction with gauge bosons are listed in Tab. 3. In addition, the HLM basis contains a subset of operators with no direct correspondence to the bosonic SILH operators, which must be rewritten with the help of equations of motion and field redefinitions, as we discuss below.

The operators in Tab. 3 translate to the SILH basis via

$$\begin{aligned}
&\mathcal{O}_H'' = \frac{1}{2}\mathcal{O}_H\,, \qquad \mathcal{O}_6'' = \mathcal{O}_6\,, \qquad \mathcal{O}_T'' = \frac{1}{2}\mathcal{O}_T\,, \qquad \mathcal{O}_B'' = \frac{ig'}{2}\mathcal{O}_B\,, \qquad \mathcal{O}_W'' = \frac{ig}{2}\mathcal{O}_W\,,\\
&\mathcal{O}_{GG}'' = g_s^2\mathcal{O}_g\,, \qquad \mathcal{O}_{BB}'' = g'^2\mathcal{O}_\gamma\,, \qquad \mathcal{O}_{WB}'' = 2ig'\mathcal{O}_B - 4ig'\mathcal{O}_{HB} - g'^2\mathcal{O}_\gamma\,,\\
&\mathcal{O}_{WW}'' = -2ig'\mathcal{O}_B + 2ig\mathcal{O}_W + 4ig'\mathcal{O}_{HB} - 4ig\mathcal{O}_{HW} + g'^2\mathcal{O}_\gamma\,.
\end{aligned} \tag{17}$$

In addition, the HLM basis contains extra operators with no SILH counterpart,

$$\mathcal{O}_R'' = \phi^\dagger\phi\left(D_\mu\,\phi\right)^\dagger\left(D^\mu\,\phi\right), \qquad \mathcal{O}_D'' = \left(D^2\phi\right)^2, \tag{18}$$

HLM basis
$\mathcal{O}''_H = \frac{1}{2}\,\partial^\mu(\phi^\dagger\phi)\,\partial_\mu(\phi^\dagger\phi)$
$\mathcal{O}''_6 = (\phi^\dagger\phi)^3$
$\mathcal{O}''_T = \frac{1}{2}\left(\phi^\dagger \overleftrightarrow{D}^\mu \phi\right)\left(\phi^\dagger \overleftrightarrow{D}_\mu \phi\right)$
$\mathcal{O}''_B = \frac{ig'}{2}\left(\phi^\dagger \overleftrightarrow{D}^\mu \phi\right)\partial^\nu B_{\mu\nu}$
$\mathcal{O}''_W = \frac{ig}{2}\left(\phi^\dagger \sigma^k \overleftrightarrow{D}^\mu \phi\right)(D^\nu W^k_{\mu\nu})$
$\mathcal{O}''_{GG} = g_s^2(\phi^\dagger\phi)\,G^A_{\mu\nu}\,G^{\mu\nu A}$
$\mathcal{O}''_{BB} = g'^2(\phi^\dagger\phi)\,B_{\mu\nu}\,B^{\mu\nu}$
$\mathcal{O}''_{WW} = g^2(\phi^\dagger\phi)\,W^k_{\mu\nu}\,W^{\mu\nu k}$
$\mathcal{O}''_{WB} = gg'\left(\phi^\dagger\sigma^k\phi\right)B_{\mu\nu}\,W^{\mu\nu k}$

HISZ basis
$\mathcal{O}'_{\phi 1} = (D_\mu\phi)^\dagger\phi\,\phi^\dagger(D^\mu\phi)$
$\mathcal{O}'_{\phi 2} = \frac{1}{2}\partial^\mu(\phi^\dagger\phi)\,\partial_\mu(\phi^\dagger\phi)$
$\mathcal{O}'_{\phi 3} = \frac{1}{3}(\phi^\dagger\phi)^3$
$\mathcal{O}'_{GG} = (\phi^\dagger\phi)\,G^A_{\mu\nu}\,G^{\mu\nu A}$
$\mathcal{O}'_{BB} = \phi^\dagger\,\hat{B}_{\mu\nu}\,\hat{B}^{\mu\nu}\,\phi = -\frac{g'^2}{4}\phi^\dagger\phi\,B_{\mu\nu}\,B^{\mu\nu}$
$\mathcal{O}'_{WW} = \phi^\dagger\,\hat{W}_{\mu\nu}\,\hat{W}^{\mu\nu}\,\phi = -\frac{g^2}{4}\phi^\dagger\phi\,W^k_{\mu\nu}\,W^{\mu\nu k}$
$\mathcal{O}'_{BW} = \phi^\dagger\,\hat{B}_{\mu\nu}\,\hat{W}^{\mu\nu}\,\phi = -\frac{g\,g'}{4}(\phi^\dagger\sigma^k\phi)\,B_{\mu\nu}\,W^{\mu\nu k}$
$\mathcal{O}'_B = (D^\mu\phi)^\dagger\hat{B}_{\mu\nu}(D^\nu\phi) = i\frac{g}{2}(D^\mu\phi^\dagger)(D^\nu\phi)\,B_{\mu\nu}$
$\mathcal{O}'_W = (D^\mu\phi)^\dagger\hat{W}_{\mu\nu}(D^\nu\phi) = i\frac{g}{2}(D^\mu\phi^\dagger)\sigma^k(D^\nu\phi)\,W^k_{\mu\nu}$

Table 3: Bosonic CP-conserving Higgs operators in the HLM basis (left) and the HISZ basis (right). Here $\hat{B}_{\mu\nu} = ig'/2B_{\mu\nu}$ and $\hat{W}_{\mu\nu} = ig\sigma^k/2W^k_{\mu\nu}$.

which can be eliminated using Equation (12) and Equation (15), respectively. The Wilson coefficients k_i of the HLM basis translate to the SILH coefficients $\bar{c}_i$ as follows:

$$\begin{aligned}
\bar{c}_H &= \frac{v^2}{\Lambda^2}\,(k_H - k_R)\,, & \bar{c}_B &= \frac{v^2}{\Lambda^2}\frac{g^2}{4}\,(k_B + 4\,k_{WB} - 4\,k_{WW})\,,\\
\bar{c}_T &= \frac{v^2}{\Lambda^2}\,k_T\,, & \bar{c}_W &= \frac{v^2}{\Lambda^2}\frac{g^2}{4}\,(k_W + 4\,k_{WW})\,,\\
\bar{c}_6 &= -\frac{v^2}{\Lambda^2}\left(\frac{k_6}{\lambda} + 2\,k_R + 4\,\lambda\,k_D\right), & \bar{c}_{HB} &= \frac{v^2}{\Lambda^2}\,g^2\,(k_{WW} - k_{WB})\,,\\
\bar{c}_g &= \frac{v^2}{\Lambda^2}\frac{g^2}{4}\,k_{GG}\,, & \bar{c}_{HW} &= -\frac{v^2}{\Lambda^2}\,g^2\,k_{WW}\,,\\
\bar{c}_\gamma &= \frac{v^2}{\Lambda^2}\frac{g^2}{4}\,(k_{BB} - k_{WB} + k_{WW})\,, & \bar{c}_f &= -\frac{v^2}{\Lambda^2}\left(\frac{1}{2}\,k_R + 2\,\lambda\,k_D\right),
\end{aligned} \tag{19}$$

where for the sake of completeness we have included the coefficients of the redundant operators given in Equation (18).

1.5 SILH to HISZ

We also give the conversion to the popular HISZ basis [73] (see also References [22**?**] for recent studies in this framework)

$$\mathcal{L}_{\text{HISZ}} = \sum_i \frac{f_i}{\Lambda^2}\mathcal{O}'_i\,, \tag{20}$$

with Higgs-gauge operators given in Tab. 3. We use the same conventions for the covariant derivative as above (note that this is not the case in some of the cited literature). The operators can then be translated via the relations

$$\begin{aligned}
\mathcal{O}_H &= 2\mathcal{O}'_{\phi 2}\,, & \mathcal{O}_W &= \frac{2i}{g}\left(\mathcal{O}'_{WW} + \mathcal{O}'_{BW} - 2\mathcal{O}'_W\right), & \mathcal{O}_{HW} &= -\frac{2i}{g}\mathcal{O}'_W\,,\\
\mathcal{O}_T &= 2\mathcal{O}'_{\phi 2} - 4\mathcal{O}'_{\phi 1}\,, & \mathcal{O}_B &= \frac{2i}{g'}\left(\mathcal{O}'_{BB} + \mathcal{O}'_{BW} - 2\mathcal{O}'_B\right), & \mathcal{O}_g &= \mathcal{O}'_{GG}\,,\\
\mathcal{O}_6 &= 3\mathcal{O}'_{\phi 3}\,, & \mathcal{O}_{HB} &= -\frac{2i}{g'}\mathcal{O}'_B\,, & \mathcal{O}_\gamma &= -\frac{4}{g'^2}\mathcal{O}'_{BB}\,.
\end{aligned} \tag{21}$$

The HISZ basis also includes the redundant operator $\mathcal{O}'_{\phi 4} = (D_\mu \phi)^\dagger (D^\mu \phi)\, \phi^\dagger \phi$, which can be removed using Equation (12). For the coefficients, we find

$$\begin{aligned}
\bar{c}_H &= \frac{v^2}{\Lambda^2}\left(\frac{1}{2} f_{\phi 1} + f_{\phi 2}\right), & \bar{c}_W &= -\frac{v^2}{\Lambda^2}\frac{g^2}{4} f_{WW}, \\
\bar{c}_T &= -\frac{v^2}{\Lambda^2}\frac{1}{2} f_{\phi 1}, & \bar{c}_B &= \frac{v^2}{\Lambda^2}\frac{g^2}{4}(f_{WW} - f_{BW}), \\
\bar{c}_6 &= -\frac{v^2}{\Lambda^2}\frac{1}{3\lambda} f_{\phi 3}, & \bar{c}_{HW} &= \frac{v^2}{\Lambda^2}\frac{g^2}{8}(f_W + 2 f_{WW}), \\
\bar{c}_g &= \frac{v^2}{\Lambda^2}\frac{g^2}{4 g_s^2} f_{GG}, & \bar{c}_{HB} &= \frac{v^2}{\Lambda^2}\frac{g^2}{8}(f_B + 2 f_{BW} - 2 f_{WW}), \\
\bar{c}_\gamma &= \frac{v^2}{\Lambda^2}\frac{g^2}{16}(f_{BW} - f_{BB} - f_{WW}).
\end{aligned} \tag{22}$$

2 Model fineprint

2.1 Singlet extension

The singlet model is defined in Equations (3.22) and (3.23) in Section 3.3.2. Ignoring the Goldstones, the scalar doublet and singlets fields can be expanded into components as

$$\begin{aligned}
\phi &= \frac{1}{\sqrt{2}}\begin{pmatrix} 1 \\ v + \phi^0 \end{pmatrix}, \\
S &= \frac{1}{\sqrt{2}}(v_s + s^0),
\end{aligned} \tag{23}$$

where $v \equiv \sqrt{2}\langle\phi\rangle = 246$ GeV and $v_s \equiv \sqrt{2}\langle S\rangle$ denote their respective VEVs. The minimisation condition for this potential can be used to eliminate the parameters $\mu_{1,2}$ in favor of v and v_s. ϕ^0 and s^0 mix to form a light (h) and a heavy (H) mass eigenstate,

$$\begin{aligned}
h &= \phi^0 \cos\alpha - s^0 \sin\alpha, \\
H &= \phi^0 \sin\alpha + s^0 \cos\alpha,
\end{aligned} \tag{24}$$

where

$$\tan(2\alpha) = \frac{\lambda_3 v v_s}{\lambda_2 v_s^2 - \lambda_1 v^2}. \tag{25}$$

Their masses are

$$m^2_{h,H} = \lambda_1 v^2 + \lambda_2 v_s^2 \mp |\lambda_1 v^2 - \lambda_2 v_s^2| \sqrt{1 + \tan^2(2\alpha)} \tag{26}$$

with $m_H^2 \approx 2\lambda_2 v_s^2 \gg m_h^2$ in the limit $v^2 \ll v_s^2$.

2.2 Two-Higgs-doublet model

Model setup

We analyse the most general gauge invariant, CP-even theory for two scalar fields with an additional $\mathbb{Z}_2$ symmetry, as defined in Equation (3.38) in Section 3.3.3. The Higgs mass-eigenstates follow from the set of rotations

$$\begin{pmatrix} H^0 \\ h^0 \end{pmatrix} = R(\alpha) \begin{pmatrix} h_1^0 \\ h_2^0 \end{pmatrix}, \qquad \begin{pmatrix} w^0 \\ A^0 \end{pmatrix} = R(\beta) \begin{pmatrix} a_1^0 \\ a_2^0 \end{pmatrix}, \qquad \begin{pmatrix} w^\pm \\ H^\pm \end{pmatrix} = R(\beta) \begin{pmatrix} h_1^\pm \\ h_2^\pm \end{pmatrix}, \quad (27)$$

with

$$\phi_k = \begin{pmatrix} h_k^+ \\ \frac{1}{\sqrt{2}}(v_k + h_k^0 + \mathrm{i}a_k) \end{pmatrix} \quad (28)$$

and

$$R(\theta) = \begin{pmatrix} \cos\theta & \sin\theta \\ -\sin\theta & \cos\theta \end{pmatrix}. \quad (29)$$

Since the two doublets contribute to giving masses to the weak gauge bosons, custodial symmetry will impose tight constraints on the viable mass spectrum of the model [202–210]. Analytic relations linking the different Higgs masses and mixing angles with the Lagrangian parameters in Equation (3.38) can be found e. g. in Appendix A of [101]. The conventions

$$0 < \beta < \pi/2 \quad \text{and} \quad 0 \leq \beta - \alpha < \pi \quad (30)$$

guarantee that the Higgs coupling to vector bosons has the same sign in the 2HDM and in the SM. As we will next show, the decoupling limit implies that the light Higgs interactions approach the alignment limit, where $\cos\beta \sim |\sin\alpha|$ and the couplings become SM-like [167].

Couplings

The tree-level coupling shifts of the light Higgs follow from these rotations and are given in Eqs. (3.39) to (3.43). The light Higgs coupling to a charged Higgs pair reads

$$\frac{g_{h^0H^+H^-}}{g_{hhh}^{\mathrm{SM}}} = \frac{1}{3m_{h^0}^2}\left[\sin(\beta-\alpha)\left(2m_{H^\pm}^2 - m_{h^0}^2\right) + \frac{\cos(\alpha+\beta)}{\sin(2\beta)}\left(2m_{h^0}^2 - \frac{2m_{12}^2}{\sin\beta\cos\beta}\right)\right], \quad (31)$$

with $g_{hhh}^{\mathrm{SM}} = -3m_h^2/v$.

The loop-induced couplings are more involved, giving

$$1 + \Delta_g = \frac{1}{A_{gg}^{\mathrm{SM}}} \left[\sum_{f=t,b} (1 + \Delta_f)\, A_f(\tau_f) \right], \tag{32}$$

$$1 + \Delta_\gamma = \frac{1}{A_{\gamma\gamma}^{\mathrm{SM}}} \left[\sum_{f=t,b} N_C\, Q_f^2\, (1 + \Delta_f)\, A_f(\tau_f) + Q_\tau^2\, (1 + \Delta_\tau)\, A_f(\tau_\tau) + (1 + \Delta_W)\, A_v(\tau_W) \right.$$
$$\left. - g_{h^0 H^+ H^-}\, \frac{m_W s_w}{e m_{H^\pm}^2}\, A_s(\tau_{H^\pm}) \right], \tag{33}$$

where A_{xx}^{SM} are the corresponding contributions in the SM. The conventional loop form factors read

$$\begin{aligned} A_s(\tau) &= -\frac{\tau}{2}\,[1 - \tau f(\tau)] && = 1/6 + \mathcal{O}(\tau^{-1})\,, \\ A_f(\tau) &= \tau\,[1 + (1 - \tau)\, f(\tau)] && = 2/3 + \mathcal{O}(\tau^{-1})\,, \\ A_V(\tau) &= -\frac{1}{2}\,\left[2 + 3\tau + 3(2\tau - \tau^2)\, f(\tau)\right] && = -7/2 + \mathcal{O}(\tau^{-1})\,, \end{aligned} \tag{34}$$

where

$$f(\tau) = \begin{cases} -\frac{1}{4}\left[\log \frac{1+\sqrt{1-\tau}}{1-\sqrt{1-\tau}} - i\pi\right]^2 & \text{for } \tau < 1 \\ \left[\arcsin \frac{1}{\sqrt{\tau}}\right]^2 & \text{for } \tau \geq 1\,, \end{cases} \tag{35}$$

and $\tau_x = 4m_x^2/m_{h^0}^2$.

Matching

The effect of the second doublet on the phenomenology of the light Higgs consists purely of shifted couplings Δ_x. This allows us to match the dimension-six model by setting equal the coupling shifts from the full model, given by Eqs. (3.39) to (3.43) and (33), to the corresponding couplings in the dimension-six Lagrangian, Equation (2.73).

In a second step we then expand in $1/\Lambda$ and keep terms up to $\mathcal{O}\left(1/\Lambda^2\right)$, where Λ is defined in the unbroken phase for the default matching or as the physical mass m_{A^0} in the v-improved matching, as described in Section 3.3.3.

This defines the effective model in a straightforward way. For more details see Appendix A.3 of Reference [2].

2.3 Scalar top partners

Model setup

The potential for the simplified scalar top-partner model consists of three parts,

$$\mathcal{L}_{\text{top partners}} \supset (D_\mu \tilde{Q})^\dagger D^\mu \tilde{Q} + (D_\mu \tilde{t}_R)^* D^\mu \tilde{t}_R - \underbrace{M^2\, \tilde{Q}^\dagger \tilde{Q} - M^2\, \tilde{t}_R^* \tilde{t}_R}_{\mathcal{L}_{\text{mass}}}$$
$$- \underbrace{\kappa_{LL}\, (\phi \cdot \tilde{Q})^\dagger\, (\phi \cdot \tilde{Q}) - \kappa_{RR}\, (\tilde{t}_R^* \tilde{t}_R)\, (\phi^\dagger\, \phi)}_{\mathcal{L}_{\text{Higgs}}} - \underbrace{\left[\kappa_{LR}\, M\, \tilde{t}_R^*\, (\phi \cdot \tilde{Q}) + \text{h. c.}\right]}_{\mathcal{L}_{\text{mixing}}} . \quad (36)$$

We use the customary notation for the $SU(2)_L$ invariant product $\phi \cdot \tilde{Q} \equiv \epsilon_{ab}\, \phi^a\, \tilde{Q}^b$, with the help of the antisymmetric pseudo-tensor $\epsilon^{ab} \equiv (i\sigma^2)^{ab}$ such that $\epsilon^{12} = -\epsilon^{21} = 1$.

The term $\mathcal{L}_{\text{Higgs}}$ gives rise to scalar partner masses proportional to the Higgs vev, mirroring the supersymmetric F-term contribution to the squark masses. By a similar token, the explicit mass terms $\mathcal{L}_{\text{mass}}$ are analogous to the squark soft-SUSY breaking mass terms. $\mathcal{L}_{\text{mixing}}$ is responsible for the mixing between the gauge eigenstates, reminiscent of the MSSM A-terms. In the absence of an underlying supersymmetry, the Lagrangian features no equivalent of the D-term contributions.

Collecting all bilinear terms from Equation (36), we get

$$\mathcal{L}_{\text{top partners}} \supset (\tilde{t}_L^*\ \tilde{t}_R^*)\, \mathcal{M}_{\tilde{t}} \begin{pmatrix} \tilde{t}_L \\ \tilde{t}_R \end{pmatrix} , \quad (37)$$

with the mass matrix $\mathcal{M}_{\tilde{t}}$ given in Equation (3.51). Assuming all parameters in Equation (36) to be real, m_{ij} can be diagonalized through the usual orthogonal transformation $R(\theta_{\tilde{t}})$ given in Equation (29). This rotates the gauge eigenstates $(\tilde{t}_L, \tilde{t}_R)$ into the mass basis $(\tilde{t}_1, \tilde{t}_2)$,

$$\begin{pmatrix} \tilde{t}_1 \\ \tilde{t}_2 \end{pmatrix} = R(\theta_{\tilde{t}}) \begin{pmatrix} \tilde{t}_L \\ \tilde{t}_R \end{pmatrix} . \quad (38)$$

The physical scalar partner masses and the mixing angle are then given by

$$\begin{aligned} m_{\tilde{t}_1}^2 &= M_{LL}^2 \cos^2\theta_{\tilde{t}} + M_{RR}^2 \sin^2\theta_{\tilde{t}} + 2M_{LR}^2 \sin\theta_{\tilde{t}} \cos\theta_{\tilde{t}} , \\ m_{\tilde{t}_2}^2 &= M_{LL}^2 \sin^2\theta_{\tilde{t}} + M_{RR}^2 \cos^2\theta_{\tilde{t}} - 2M_{LR}^2 \sin\theta_{\tilde{t}} \cos\theta_{\tilde{t}} , \end{aligned} \quad (39)$$

$$\tan(2\theta_{\tilde{t}}) = \frac{2M_{LR}^2}{M_{LL}^2 - M_{RR}^2} . \quad (40)$$

As we assume the right-handed bottom partner $\tilde{b}_R$ to be heavy and thus decoupled, the sbottom-like scalar eigenstate $\tilde{b}_L$ undergoes no mixing and can be readily identified with the physical eigenstate.

Matching

We compute the effective action at one loop with the help of the covariant derivative expansion [60, 62], which is fully consistent with our mass degeneracy setup. Since the Lagrangian Equation (36) lacks any linear terms in the heavy scalar fields $\Psi \equiv (\tilde{Q}, \tilde{t}_R^*)$, the tree-level exchange of such heavy partners cannot generate any effective interaction at dimension six. Our results are in agreement with References [60, 64, 119] and given in Equation (3.54). To here

2.4 Vector triplet

Our final example is the heavy vector triplet defined in **??**. This Lagrangian includes conventional factors of coupling constants, introduced for a convenient power counting in certain UV embeddings [193]: insertions of V and ϕ are weighted by one factor of g_V, while SM gauge bosons come with a factor of g_w. In addition, the coupling to fermions is weighted with an additional factor of g_W^2/g_V^2. For simplicity, it is assumed that the fermion current in **??** is universal.

We can add an explicit kinetic V-W mixing term

$$\mathcal{L} \supset c_{WV}\, \frac{g_W}{2g_V}\, D_{[\mu}\, V_{\nu]}^a\, W^{\mu\nu\, a} \tag{41}$$

to the Lagrangian in Equation (3.56). As it turns out, this term is redundant and can be removed with field redefinitions, shifting its effects into the other model parameters [193, 211]. For more details, see Appendix A.5 of Reference [2].

In this model, seven gauge eigenstates W^a, B, V^a mix into mass eigenstates A, $W^\pm$, Z, $\xi^\pm$, and ξ^0. The photon is as usual defined as the component that remains massless during EWSB, $A_\mu = c_w\, B_\mu + s_w\, W_\mu^3$, where the Weinberg angle is linked to the gauge couplings $e = g_W\, s_w = g'\, c_w$. For the remaining fields we have to diagonalize the neutral and charged mass matrices, giving the mass eigenstates

$$\begin{aligned}
Z_\mu &= \cos\theta_N \left(-s_w B_\mu + c_w W_\mu^3\right) + \sin\theta_N\, V_\mu^3\,, \\
\xi_\mu^0 &= -\sin\theta_N \left(-s_w B_\mu + c_w W_\mu^3\right) + \cos\theta_N\, V_\mu^3\,, \\
W_\mu^\pm &= \cos\theta_C\, \frac{W_\mu^1 \mp W_\mu^2}{\sqrt{2}} + \sin\theta_C\, \frac{V_\mu^1 \mp V_\mu^2}{\sqrt{2}}\,, \\
\xi_\mu^\pm &= -\sin\theta_C\, \frac{W_\mu^1 \mp W_\mu^2}{\sqrt{2}} + \cos\theta_C\, \frac{V_\mu^1 \mp V_\mu^2}{\sqrt{2}}\,.
\end{aligned} \tag{42}$$

The corresponding mass eigenvalues read

$$\begin{aligned} m^2_{Z/\xi^0} &= \frac{1}{2}\left[\hat{m}^2_V + \hat{m}^2_Z \mp \sqrt{\left(\hat{m}^2_Z - \hat{m}^2_V\right)^2 + c^2_H\, g^2_V\, \hat{m}^2_Z\, \hat{v}^2}\right] \\ &= \begin{cases} \hat{m}^2_Z \left(1 - \dfrac{c^2_H g^2_V}{4}\, \dfrac{\hat{v}^2}{\hat{m}^2_V} + \mathcal{O}\left(\hat{v}^4/\hat{m}^4_V\right)\right) \\ \hat{m}^2_V \left(1 + \dfrac{c^2_H g^2_V}{4}\, \dfrac{\hat{v}^2}{\hat{m}^2_V} + \mathcal{O}\left(\hat{v}^4/\hat{m}^4_V\right)\right), \end{cases} \end{aligned} \tag{43}$$

and

$$\begin{aligned} m^2_{W^\pm/\xi^\pm} &= \frac{1}{2}\left[\hat{m}^2_V + \hat{m}^2_W \mp \sqrt{\left(\hat{m}^2_W - \hat{m}^2_V\right)^2 + c^2_H\, g^2_V\, \hat{m}^2_W\, \hat{v}^2}\right] \\ &= \begin{cases} \hat{m}^2_W \left(1 - \dfrac{c^2_H g^2_V}{4}\, \dfrac{\hat{v}^2}{\hat{m}^2_V} + \mathcal{O}\left(\hat{v}^4/\hat{m}^4_V\right)\right) \\ \hat{m}^2_V \left(1 + \dfrac{c^2_H g^2_V}{4}\, \dfrac{\hat{v}^2}{\hat{m}^2_V} + \mathcal{O}\left(\hat{v}^4/\hat{m}^4_V\right)\right). \end{cases} \end{aligned} \tag{44}$$

For the mixing angles, we find

$$\begin{aligned} \tan(2\theta_N) &= \frac{c_H\, g_V\, \hat{v}\, \hat{m}_Z}{\hat{m}^2_V - \hat{m}^2_Z} = \frac{c_H\, g\, g_V}{2\, c_w}\, \frac{\hat{v}^2}{\hat{m}^2_V} + \mathcal{O}\left(\hat{v}^4/\hat{m}^4_V\right), \\ \tan(2\theta_C) &= \frac{c_H\, g_V\, \hat{v}\, \hat{m}_W}{\hat{m}^2_V - \hat{m}^2_W} = \frac{c_H\, g\, g_V}{2}\, \frac{\hat{v}^2}{\hat{m}^2_V} + \mathcal{O}\left(\hat{v}^4/\hat{m}^4_V\right), \end{aligned} \tag{45}$$

or

$$\sin\theta_C = \frac{c_H\, g\, g_V}{4}\, \frac{v^2}{M^2_V} + \mathcal{O}\left(\hat{v}^4/\hat{m}^4_V\right). \tag{46}$$

Here we use the definitions

$$\hat{m}_Z = \frac{g_W\, \hat{v}}{2\, c_w}, \qquad \hat{m}_W = \frac{g_W\, \hat{v}}{2}, \qquad \hat{m}^2_V = M^2_V + g^2_V\, c_{VVHH}\, \hat{v}^2, \tag{47}$$

where $\hat{v}$ is the actual vev of ϕ, which does not necessarily have the SM value of $v = 2m_W/g \approx 246$ GeV.

This mixing affects the weak current interactions: instead of being simply governed by the $SU(2)_L$ coupling constant g_W, the physical Wff' couplings are now determined by

$$g = \cos\theta_C\, g_W - \sin\theta_C\, c_F\, \frac{g^2_W}{g_V} = g_W \left(1 - \frac{c_F\, c_H\, g^2_W}{4}\, \frac{v^2}{M^2_V}\right) + \mathcal{O}\left(v^4/M^4_V\right). \tag{48}$$

The relation between $\hat{v}$ and v can be read off from Equation (44):

$$\frac{\hat{v}}{v} = 1 + \frac{c_H^2\, g_V^2}{8}\,\frac{v^2}{M_V^2} - \frac{c_F\, c_H\, g_W^2}{4}\,\frac{v^2}{M_V^2} + \mathcal{O}\big(v^4/M_V^4\big)\,. \tag{49}$$

Finally, note that to ensure compatibility with electroweak precision measurements, the neutral and charged states ξ^0 and $\xi^\pm$ have to be nearly mass-degenerate,

$$m_{\xi^0} \approx m_{\xi^\pm} \equiv m_\xi\,. \tag{50}$$

In practice, we set up our model in the m_W-g scheme, i. e. based on the input parameters g, m_W, α, m_{h^0}, α_s, the vector triplet couplings g_V and c_i, as well as the physical mass $m_{\xi^\pm}$. The remaining Lagrangian parameters, mixing angles, and couplings are calculated by solving Equations (43) and (44) iteratively.

Couplings

The mismatch between g and g_w as well as between v and $\hat{v}$ leads to a shift of the Higgs couplings to fermions,

$$\begin{aligned}\Delta_f &= \frac{g_W}{g}\,\frac{v}{\hat{v}} - 1 = \frac{1}{\cos\theta_C - c_F\,\frac{g_W}{g_V}\,\sin\theta_C}\,\frac{v}{\hat{v}} - 1 \\ &= c_H^2\,\frac{g_V^2 v^2}{8M_V^2} + c_F c_H\,\frac{g^2 v^2}{4M_V^2} + \mathcal{O}\big(M_V^{-4}\big)\,,\end{aligned} \tag{51}$$

and to (on-shell) W bosons,

$$\begin{aligned}\Delta_W &= \frac{1}{g m_W}\left(\frac{\cos^2\theta_C\, g^2\,\hat{v}}{2(\cos\theta_C - c_F\frac{g_W}{g_V}\sin\theta_C)^2} - c_H\frac{\sin\theta_C\,\cos\theta_C\, g\, g_V\,\hat{v}}{\cos\theta_C - c_F\,\frac{g_W}{g_V}\,\sin\theta_C}\right. \\ &\qquad\qquad \left. + 2\,c_{VVHH}\,\sin^2\theta_C\, g_V^2\,\hat{v}\right) - 1 \\ &= c_H^2\,\frac{3 g_V^2 v^2}{8M_V^2} + c_F c_H\,\frac{g^2 v^2}{4M_V^2} + \mathcal{O}\big(M_V^{-4}\big)\,.\end{aligned} \tag{52}$$

Matching

Since we are only interested in tree-level effects, we can construct the effective theory in our default matching procedure with the classical equation of motion for V_μ^a, corresponding to the first term in Equation (2.28). To simplify the notation, we define currents

$$J_F^{\mu,a} \equiv \bar{f}_L \gamma^\mu \sigma^a f_L\,, \qquad J_H^{\mu,a} \equiv \phi^\dagger \sigma^a \overleftrightarrow{D}^\mu \phi\,. \tag{53}$$

This Euler-Lagrange equation then reads

$$[\partial^\mu \partial^\nu - g^{\mu\nu}\,\partial^2 - M_V^2]\,V_\nu^a = g_V\,c_H\,J_H^{\mu,a} + \frac{g_W^2}{2g_V}\,c_F \sum_F J_F^{\mu,a} + \mathcal{O}\big(V^2\big) \tag{54}$$

or

$$V^{\mu,a} = -\frac{1}{M_V^2}\left[g_V\,c_H\,J_H^{\mu,a} + \frac{g_W^2}{2g_V}\,c_F \sum_F J_F^{\mu,a}\right] + \mathcal{O}\big(p_V^2/\tilde{M}_V^4\big) + \mathcal{O}\big(V^2\big)\,, \tag{55}$$

where we neglect higher powers of V that are irrelevant for our analysis.

Inserting this into the Lagrangian in Equation (3.56), we find the effective theory

$$\mathcal{L}_{\text{EFT}} \supset -\frac{g_W^4\,c_F^2}{8g_V^2\,M_V^2}\,J_F^{\mu,a}\,J_\mu^{F\,a} - \frac{g_V^2\,c_H^2}{2\,M_V^2}\,J_H^{\mu,a}\,J_\mu^{H\,a} - \frac{g_W^2\,c_F\,c_H}{2\,M_V^2}\,J_H^{\mu,a}\,J_\mu^{F\,a}\,. \tag{56}$$

$J_F^{\mu,a}\,J_\mu^{F\,a}$ only contains four-fermion operators irrelevant for our analysis. The remaining current products can be expressed in terms of dimension-six operators as

$$\begin{aligned} J_H^{\mu,a}\,J_\mu^{H\,a} &= -\frac{1}{2}\,(\mathcal{O}_{\phi,2} - 2\,\phi^\dagger\phi\,(D_\mu\phi)^2) \\ &= -\frac{1}{2}\left[3\mathcal{O}_{\phi,2} - 12\lambda\mathcal{O}_{\phi,3} - \sum_f y_f\mathcal{O}_f\right], \end{aligned} \tag{57}$$

$$\begin{aligned} J_F^{\mu,a}\,J_\mu^{H\,a} &= \frac{\mathrm{i}}{2}\,\big(\bar{f}_L\,\gamma^\mu\,\sigma^a\,f_L\big)\Big(\phi^\dagger\,\sigma^a\,\overleftrightarrow{D}_\mu\,\phi\Big) \\ &= \frac{-2}{g_W^2}\,[\mathcal{O}_{WW} + \mathcal{O}_{BW} - 2\mathcal{O}_W] + 3\mathcal{O}_{\phi,2} - 12\lambda\mathcal{O}_{\phi,3} - \sum_f y_f\mathcal{O}_f\,. \end{aligned} \tag{58}$$

Here we have used the equations of motions in Equations (2.54) to (2.56) to bring the operators to our HISZ basis.

Combining the pieces, we finally arrive at

$$\mathcal{L}_{\text{EFT}} \supset \left(\frac{g_V^2\,c_H^2}{4\,M_V^2} - \frac{g_W^2\,c_F\,c_H}{2\,M_V^2}\right)\left[3\mathcal{O}_{\phi,2} - 12\lambda\mathcal{O}_{\phi,3} - \sum_f y_f\mathcal{O}_f\right] + \frac{c_F\,c_H}{M_V^2}\,[\mathcal{O}_{WW} + \mathcal{O}_{BW} - 2\mathcal{O}_W]\,, \tag{59}$$

To here

corresponding to the Wilson coefficients given in Equation (3.60).

3 Fisher information derivations

References

[1] J. Cullum: 'Twentysomething', 2003.

[2] J. Brehmer, A. Freitas, D. Lopez-Val, and T. Plehn: 'Pushing Higgs Effective Theory to its Limits'. Phys. Rev. D93 (7): p. 075 014, 2016. arXiv:1510.03443.

[3] A. Biekötter, J. Brehmer, and T. Plehn: 'Extending the limits of Higgs effective theory'. Phys. Rev. D94 (5): p. 055 032, 2016. arXiv:1602.05202.

[4] D. de Florian et al. (LHC Higgs Cross Section Working Group): 'Handbook of LHC Higgs Cross Sections: 4. Deciphering the Nature of the Higgs Sector' 2016. arXiv:1610.07922.

[5] J. Brehmer, K. Cranmer, F. Kling, and T. Plehn: 'Better Higgs Measurements Through Information Geometry' 2016. arXiv:1612.05261.

[6] J. Brehmer: 'Higgs Effective Field Theory'. Student lecture, research training group "Particle Physics Beyond the Standard Model" 2016. URL http://www.thphys.uni-heidelberg.de/~gk_ppbsm/lib/exe/fetch.php?media=students:lectures:student_lecture_eft.pdf.

[7] J. Brehmer, J. Hewett, J. Kopp, T. Rizzo, and J. Tattersall: 'Symmetry Restored in Dibosons at the LHC?' JHEP 10: p. 182, 2015. arXiv:1507.00013.

[8] J. Brehmer et al.: 'The Diboson Excess: Experimental Situation and Classification of Explanations; A Les Houches Pre-Proceeding' 2015. arXiv:1512.04357.

[9] G. Brooijmans et al.: 'Les Houches 2015: Physics at TeV colliders - new physics working group report' 2016. arXiv:1605.02684.

[10] L. Carroll: Alice's Adventures in Wonderland. Macmillan, 1865.

[11] P. W. Higgs: 'Broken symmetries, massless particles and gauge fields'. Phys. Lett. 12: pp. 132–133, 1964.

[12] P. W. Higgs: 'Broken Symmetries and the Masses of Gauge Bosons'. Phys. Rev. Lett. 13: pp. 508–509, 1964.

[13] F. Englert and R. Brout: 'Broken Symmetry and the Mass of Gauge Vector Mesons'. Phys. Rev. Lett. 13: pp. 321–323, 1964.

[14] G. Aad et al. (ATLAS): 'Observation of a new particle in the search for the Standard Model Higgs boson with the ATLAS detector at the LHC'. Phys. Lett. B716: pp. 1–29, 2012. arXiv:1207.7214.

[15] S. Chatrchyan et al. (CMS): 'Observation of a new boson at a mass of 125 GeV with the CMS experiment at the LHC'. Phys. Lett. B716: pp. 30–61, 2012. arXiv:1207.7235.

[16] S. R. Coleman, J. Wess, and B. Zumino: 'Structure of phenomenological Lagrangians. 1.' Phys. Rev. 177: pp. 2239–2247, 1969.

[17] C. G. Callan, Jr., S. R. Coleman, J. Wess, and B. Zumino: 'Structure of phenomenological Lagrangians. 2.' Phys. Rev. 177: pp. 2247–2250, 1969.

[18] S. Weinberg: 'Effective Gauge Theories'. Phys. Lett. B91: pp. 51–55, 1980.

[19] C. J. C. Burges and H. J. Schnitzer: 'Virtual Effects of Excited Quarks as Probes of a Possible New Hadronic Mass Scale'. Nucl. Phys. B228: pp. 464–500, 1983.

[20] C. N. Leung, S. T. Love, and S. Rao: 'Low-Energy Manifestations of a New Interaction Scale: Operator Analysis'. Z. Phys. C31: p. 433, 1986.

[21] W. Buchmuller and D. Wyler: 'Effective Lagrangian Analysis of New Interactions and Flavor Conservation'. Nucl. Phys. B268: pp. 621–653, 1986.

[22] T. Corbett, O. J. P. Eboli, J. Gonzalez-Fraile, and M. C. Gonzalez-Garcia: 'Robust Determination of the Higgs Couplings: Power to the Data'. Phys. Rev. D87: p. 015 022, 2013. arXiv:1211.4580.

[23] T. Corbett, O. J. P. Eboli, D. Goncalves, J. Gonzalez-Fraile, T. Plehn, and M. Rauch: 'The Higgs Legacy of the LHC Run I'. JHEP 08: p. 156, 2015. arXiv:1505.05516.

[24] A. Butter, O. J. P. Éboli, J. Gonzalez-Fraile, M. C. Gonzalez-Garcia, T. Plehn, and M. Rauch: 'The Gauge-Higgs Legacy of the LHC Run I'. JHEP 07: p. 152, 2016. arXiv:1604.03105.

[25] K. Kondo: 'Dynamical Likelihood Method for Reconstruction of Events With Missing Momentum. 1: Method and Toy Models'. J. Phys. Soc. Jap. 57: pp. 4126–4140, 1988.

[26] D. Atwood and A. Soni: 'Analysis for magnetic moment and electric dipole moment form-factors of the top quark via e+ e- —¿ t anti-t'. Phys. Rev. D45: pp. 2405–2413, 1992.

[27] Y. Gao, A. V. Gritsan, Z. Guo, K. Melnikov, M. Schulze, and N. V. Tran: 'Spin determination of single-produced resonances at hadron colliders'. Phys. Rev. D81: p. 075 022, 2010. arXiv:1001.3396.

[28] S. Bolognesi, Y. Gao, A. V. Gritsan, K. Melnikov, M. Schulze, N. V. Tran, and A. Whitbeck: 'On the spin and parity of a single-produced resonance at the LHC'. Phys. Rev. D86: p. 095 031, 2012. arXiv:1208.4018.

[29] K. Cranmer: 'Practical Statistics for the LHC'. In 'Proceedings, 2011 European School of High-Energy Physics (ESHEP 2011): Cheile Gradistei, Romania, September 7-20, 2011', pp. 267–308. 2015. [,247(2015)], arXiv:1503.07622, URL http://inspirehep.net/record/1356277/files/arXiv:1503.07622.pdf.

[30] K. Cranmer, J. Pavez, and G. Louppe: 'Approximating Likelihood Ratios with Calibrated Discriminative Classifiers' 2015. arXiv:1506.02169.

[31] G. Martin: A Game of Thrones. A Bantam spectra book: Fantasy. Bantam Books, 1997. ISBN 9780553573404.

[32] T. Plehn: 'Lectures on LHC Physics'. Lect. Notes Phys. 844: pp. 1–193, 2012. arXiv:0910.4182.

[33] H. Georgi: 'Effective field theory'. Ann. Rev. Nucl. Part. Sci. 43: pp. 209–252, 1993.

[34] D. B. Kaplan: 'Five lectures on effective field theory' 2005. arXiv:nucl-th/0510023.

[35] G. Aad et al. (ATLAS, CMS): 'Measurements of the Higgs boson production and decay rates and constraints on its couplings from a combined ATLAS and CMS analysis of the LHC pp collision data at $\sqrt{s}$ = 7 and 8 TeV'. JHEP 08: p. 045, 2016. arXiv:1606.02266.

[36] D. L. Rainwater, D. Zeppenfeld, and K. Hagiwara: 'Searching for $H \to \tau^+\tau^-$ in weak boson fusion at the CERN LHC'. Phys. Rev. D59: p. 014 037, 1998. arXiv:hep-ph/9808468.

[37] T. Plehn, M. Spira, and P. M. Zerwas: 'Pair production of neutral Higgs particles in gluon-gluon collisions'. Nucl. Phys. B479: pp. 46–64, 1996. [Erratum: Nucl. Phys.B531,655(1998)], arXiv:hep-ph/9603205.

[38] U. Baur, T. Plehn, and D. L. Rainwater: 'Measuring the Higgs boson self coupling at the LHC and finite top mass matrix elements'. Phys. Rev. Lett. 89: p. 151 801, 2002. arXiv:hep-ph/0206024.

[39] X. Li and M. B. Voloshin: 'Remarks on double Higgs boson production by gluon fusion at threshold'. Phys. Rev. D89 (1): p. 013 012, 2014. arXiv:1311.5156.

[40] S. Weinberg: 'Anthropic Bound on the Cosmological Constant'. Phys. Rev. Lett. 59: p. 2607, 1987.

[41] J. D. Barrow and F. J. Tipler: The Anthropic Cosmological Principle. Oxford U. Pr., Oxford, 1988. ISBN 0192821474, 9780192821478.

[42] V. Agrawal, S. M. Barr, J. F. Donoghue, and D. Seckel: 'The Anthropic principle and the mass scale of the standard model'. Phys. Rev. D57: pp. 5480–5492, 1998. arXiv:hep-ph/9707380.

[43] R. Harnik, G. D. Kribs, and G. Perez: 'A Universe without weak interactions'. Phys. Rev. D74: p. 035 006, 2006. arXiv:hep-ph/0604027.

[44] L. Clavelli and R. E. White, III: 'Problems in a weakless universe' 2006. arXiv:hep-ph/0609050.

[45] G. F. Giudice: 'Naturally Speaking: The Naturalness Criterion and Physics at the LHC' 2008. arXiv:0801.2562.

[46] J. F. Donoghue, K. Dutta, A. Ross, and M. Tegmark: 'Likely values of the Higgs vev'. Phys. Rev. D81: p. 073 003, 2010. arXiv:0903.1024.

[47] O. Gedalia, A. Jenkins, and G. Perez: 'Why do we observe a weak force? The Hierarchy problem in the multiverse'. Phys. Rev. D83: p. 115 020, 2011. arXiv:1010.2626.

[48] F. C. Adams: 'Constraints on Alternate Universes: Stars and habitable planets with different fundamental constants'. JCAP 1602 (02): p. 042, 2016. arXiv:1511.06958.

[49] P. W. Graham, D. E. Kaplan, and S. Rajendran: 'Cosmological Relaxation of the Electroweak Scale'. Phys. Rev. Lett. 115 (22): p. 221 801, 2015. arXiv:1504.07551.

[50] N. Arkani-Hamed, T. Cohen, R. T. D'Agnolo, A. Hook, H. D. Kim, and D. Pinner: 'Solving the Hierarchy Problem at Reheating with a Large Number of Degrees of Freedom'. Phys. Rev. Lett. 117 (25): p. 251 801, 2016. arXiv:1607.06821.

[51] W. A. Bardeen: 'On naturalness in the standard model'. In 'Ontake Summer Institute on Particle Physics Ontake Mountain, Japan, August 27-September 2, 1995', 1995. URL http://lss.fnal.gov/cgi-bin/find_paper.pl?conf-95-391.

[52] G. Degrassi, S. Di Vita, J. Elias-Miro, J. R. Espinosa, G. F. Giudice, G. Isidori, and A. Strumia: 'Higgs mass and vacuum stability in the Standard Model at NNLO'. JHEP 08: p. 098, 2012. arXiv:1205.6497.

[53] A. Eichhorn, H. Gies, J. Jaeckel, T. Plehn, M. M. Scherer, and R. Sondenheimer: 'The Higgs Mass and the Scale of New Physics'. JHEP 04: p. 022, 2015. arXiv:1501.02812.

[54] T. Plehn: 'Dark Matter from a Particle Theorist's Perspective' 2017. URL http://www.thphys.uni-heidelberg.de/~plehn/pics/dark_matter.pdf.

[55] H. D. Politzer: 'Power Corrections at Short Distances'. Nucl. Phys. B172: pp. 349–382, 1980.

[56] H. Georgi: 'On-shell effective field theory'. Nucl. Phys. B361: pp. 339–350, 1991.

[57] C. Arzt: 'Reduced effective Lagrangians'. Phys. Lett. B342: pp. 189–195, 1995. arXiv:hep-ph/9304230.

[58] H. Simma: 'Equations of motion for effective Lagrangians and penguins in rare B decays'. Z. Phys. C61: pp. 67–82, 1994. arXiv:hep-ph/9307274.

[59] M. K. Gaillard: 'Effective One Loop Scalar Actions in (Mostly) Four-Dimensions'. In '3rd Jerusalem Winter School for Theoretical Physics: Strings and Superstrings Jerusalem, Israel, 30 December 1985 - 9 January 1986', 1986.

[60] B. Henning, X. Lu, and H. Murayama: 'How to use the Standard Model effective field theory'. JHEP 01: p. 023, 2016. arXiv:1412.1837.

[61] B. Henning, X. Lu, and H. Murayama: 'One-loop Matching and Running with Covariant Derivative Expansion' 2016. arXiv:1604.01019.

[62] M. K. Gaillard: 'The Effective One Loop Lagrangian With Derivative Couplings'. Nucl. Phys. B268: pp. 669–692, 1986.

[63] O. Cheyette: 'Effective Action for the Standard Model With Large Higgs Mass'. Nucl. Phys. B297: pp. 183–204, 1988.

[64] A. Drozd, J. Ellis, J. Quevillon, and T. You: 'The Universal One-Loop Effective Action' 2015. arXiv:1512.03003.

[65] G. 't Hooft and M. J. G. Veltman: 'Scalar One Loop Integrals'. Nucl. Phys. B153: pp. 365–401, 1979.

[66] A. Denner: 'Techniques for calculation of electroweak radiative corrections at the one loop level and results for W physics at LEP-200'. Fortsch. Phys. 41: pp. 307–420, 1993. arXiv:0709.1075.

[67] C. Arzt, M. B. Einhorn, and J. Wudka: 'Patterns of deviation from the standard model'. Nucl. Phys. B433: pp. 41–66, 1995. arXiv:hep-ph/9405214.

[68] C. G. Krause: Higgs Effective Field Theories - Systematics and Applications. Ph.D. thesis, Munich U., 2016. arXiv:1610.08537.

[69] B. Grzadkowski, M. Iskrzynski, M. Misiak, and J. Rosiek: 'Dimension-Six Terms in the Standard Model Lagrangian'. JHEP 10: p. 085, 2010. arXiv:1008.4884.

[70] B. Henning, X. Lu, T. Melia, and H. Murayama: '2, 84, 30, 993, 560, 15456, 11962, 261485, ...: Higher dimension operators in the SM EFT' 2015. arXiv:1512.03433.

[71] G. F. Giudice, C. Grojean, A. Pomarol, and R. Rattazzi: 'The Strongly-Interacting Light Higgs'. JHEP 06: p. 045, 2007. arXiv:hep-ph/0703164.

[72] R. Contino, M. Ghezzi, C. Grojean, M. Muhlleitner, and M. Spira: 'Effective Lagrangian for a light Higgs-like scalar'. JHEP 07: p. 035, 2013. arXiv:1303.3876.

[73] K. Hagiwara, S. Ishihara, R. Szalapski, and D. Zeppenfeld: 'Low-energy effects of new interactions in the electroweak boson sector'. Phys. Rev. D48: pp. 2182–2203, 1993.

[74] A. Falkowski, B. Fuks, K. Mawatari, K. Mimasu, F. Riva, and V. sanz: 'Rosetta: an operator basis translator for Standard Model effective field theory'. Eur. Phys. J. C75 (12): p. 583, 2015. arXiv:1508.05895.

[75] J. Gonzalez-Fraile: On the origin of masses at the LHC. Ph.D. thesis, Universitat de Barcelona, 2014.

[76] M. B. Gavela, J. Gonzalez-Fraile, M. C. Gonzalez-Garcia, L. Merlo, S. Rigolin, and J. Yepes: 'CP violation with a dynamical Higgs'. JHEP 10: p. 044, 2014. arXiv:1406.6367.

[77] V. Hankele, G. Klamke, D. Zeppenfeld, and T. Figy: 'Anomalous Higgs boson couplings in vector boson fusion at the CERN LHC'. Phys. Rev. D74: p. 095001, 2006. arXiv:hep-ph/0609075.

[78] E. E. Jenkins, A. V. Manohar, and M. Trott: 'Renormalization Group Evolution of the Standard Model Dimension Six Operators I: Formalism and lambda Dependence'. JHEP 10: p. 087, 2013. arXiv:1308.2627.

[79] E. E. Jenkins, A. V. Manohar, and M. Trott: 'Renormalization Group Evolution of the Standard Model Dimension Six Operators II: Yukawa Dependence'. JHEP 01: p. 035, 2014. arXiv:1310.4838.

[80] R. Alonso, E. E. Jenkins, A. V. Manohar, and M. Trott: 'Renormalization Group Evolution of the Standard Model Dimension Six Operators III: Gauge Coupling Dependence and Phenomenology'. JHEP 04: p. 159, 2014. arXiv:1312.2014.

[81] D. B. Kaplan and H. Georgi: 'SU(2) x U(1) Breaking by Vacuum Misalignment'. Phys. Lett. B136: pp. 183–186, 1984.

[82] D. B. Kaplan, H. Georgi, and S. Dimopoulos: 'Composite Higgs Scalars'. Phys. Lett. B136: pp. 187–190, 1984.

[83] T. Banks: 'CONSTRAINTS ON SU(2) x U(1) BREAKING BY VACUUM MISALIGNMENT'. Nucl. Phys. B243: pp. 125–130, 1984.

[84] K. Agashe, R. Contino, and A. Pomarol: 'The Minimal composite Higgs model'. Nucl. Phys. B719: pp. 165–187, 2005. arXiv:hep-ph/0412089.

[85] B. Gripaios, A. Pomarol, F. Riva, and J. Serra: 'Beyond the Minimal Composite Higgs Model'. JHEP 04: p. 070, 2009. arXiv:0902.1483.

[86] T. Appelquist and C. W. Bernard: 'Strongly Interacting Higgs Bosons'. Phys. Rev. D22: p. 200, 1980.

[87] A. C. Longhitano: 'Heavy Higgs Bosons in the Weinberg-Salam Model'. Phys. Rev. D22: p. 1166, 1980.

[88] T. Appelquist, M. J. Bowick, E. Cohler, and A. I. Hauser: 'The Breaking of Isospin Symmetry in Theories With a Dynamical Higgs Mechanism'. Phys. Rev. D31: p. 1676, 1985.

[89] B. Grinstein and M. Trott: 'A Higgs-Higgs bound state due to new physics at a TeV'. Phys. Rev. D76: p. 073 002, 2007. arXiv:0704.1505.

[90] R. Alonso, M. B. Gavela, L. Merlo, S. Rigolin, and J. Yepes: 'The Effective Chiral Lagrangian for a Light Dynamical "Higgs Particle"'. Phys. Lett. B722: pp. 330–335, 2013. [Erratum: Phys. Lett.B726,926(2013)], arXiv:1212.3305.

[91] G. Buchalla, O. Catà, and C. Krause: 'Complete Electroweak Chiral Lagrangian with a Light Higgs at NLO'. Nucl. Phys. B880: pp. 552–573, 2014. [Erratum: Nucl. Phys.B913,475(2016)], arXiv:1307.5017.

[92] G. Buchalla, O. Catà, and C. Krause: 'On the Power Counting in Effective Field Theories'. Phys. Lett. B731: pp. 80–86, 2014. arXiv:1312.5624.

[93] I. Brivio, T. Corbett, O. J. P. Éboli, M. B. Gavela, J. Gonzalez-Fraile, M. C. Gonzalez-Garcia, L. Merlo, and S. Rigolin: 'Disentangling a dynamical Higgs'. JHEP 03: p. 024, 2014. arXiv:1311.1823.

[94] G. Buchalla, O. Catà, A. Celis, and C. Krause: 'Note on Anomalous Higgs-Boson Couplings in Effective Field Theory'. Phys. Lett. B750: pp. 298–301, 2015. arXiv:1504.01707.

[95] I. Brivio, J. Gonzalez-Fraile, M. C. Gonzalez-Garcia, and L. Merlo: 'The complete HEFT Lagrangian after the LHC Run I'. Eur. Phys. J. C76 (7): p. 416, 2016. arXiv:1604.06801.

[96] S. Scherer: 'Introduction to chiral perturbation theory'. Adv. Nucl. Phys. 27: p. 277, 2003. arXiv:hep-ph/0210398.

[97] A. N. Hiller Blin: Electromagnetic interactions of light hadrons in covariant chiral perturbation theory. Ph.D. thesis, Valencia U., IFIC, 2016-11-13. URL http://roderic.uv.es/bitstream/handle/10550/56957/Tesis.pdf?sequence=1&isAllowed=y.

[98] B. M. Gavela, E. E. Jenkins, A. V. Manohar, and L. Merlo: 'Analysis of General Power Counting Rules in Effective Field Theory'. Eur. Phys. J. C76 (9): p. 485, 2016. arXiv:1601.07551.

[99] A. David, A. Denner, M. Duehrssen, et al. (LHC Higgs Cross Section Working Group): 'LHC HXSWG interim recommendations to explore the coupling structure of a Higgs-like particle' 2012. arXiv:1209.0040.

[100] R. Lafaye, T. Plehn, M. Rauch, D. Zerwas, and M. Duhrssen: 'Measuring the Higgs Sector'. JHEP 08: p. 009, 2009. arXiv:0904.3866.

[101] D. López-Val, T. Plehn, and M. Rauch: 'Measuring extended Higgs sectors as a consistent free couplings model'. JHEP 10: p. 134, 2013. arXiv:1308.1979.

[102] G. Isidori and M. Trott: 'Higgs form factors in Associated Production'. JHEP 02: p. 082, 2014. arXiv:1307.4051.

[103] M. Bordone, A. Greljo, G. Isidori, D. Marzocca, and A. Pattori: 'Higgs Pseudo Observables and Radiative Corrections'. Eur. Phys. J. C75 (8): p. 385, 2015. arXiv:1507.02555.

[104] A. Greljo, G. Isidori, J. M. Lindert, and D. Marzocca: 'Pseudo-observables in electroweak Higgs production'. Eur. Phys. J. C76 (3): p. 158, 2016. arXiv:1512.06135.

[105] M. J. Dolan, J. L. Hewett, M. Krämer, and T. G. Rizzo: 'Simplified Models for Higgs Physics: Singlet Scalar and Vector-like Quark Phenomenology'. JHEP 07: p. 039, 2016. arXiv:1601.07208.

[106] B. Gripaios and D. Sutherland: 'An operator basis for the Standard Model with an added scalar singlet'. JHEP 08: p. 103, 2016. arXiv:1604.07365.

[107] M. Bauer, A. Butter, J. Gonzalez-Fraile, T. Plehn, and M. Rauch: 'Learning from the New Higgs-like Scalar before It Vanishes' 2016. arXiv:1607.04562.

[108] G. Box and N. Draper: Empirical model-building and response surfaces. Wiley series in probability and mathematical statistics: Applied probability and statistics. Wiley, 1987. ISBN 9780471810339.

[109] L. Berthier and M. Trott: 'Consistent constraints on the Standard Model Effective Field Theory'. JHEP 02: p. 069, 2016. arXiv:1508.05060.

[110] A. Biekötter, A. Knochel, M. Krämer, D. Liu, and F. Riva: 'Vices and virtues of Higgs effective field theories at large energy'. Phys. Rev. D91: p. 055 029, 2015. arXiv:1406.7320.

[111] C. Arnesen, I. Z. Rothstein, and J. Zupan: 'Smoking Guns for On-Shell New Physics at the LHC'. Phys. Rev. Lett. 103: p. 151 801, 2009. arXiv:0809.1429.

[112] C. Englert and M. Spannowsky: 'Effective Theories and Measurements at Colliders'. Phys. Lett. B740: pp. 8–15, 2015. arXiv:1408.5147.

[113] M. de Vries: 'Four-quark effective operators at hadron colliders'. JHEP 03: p. 095, 2015. arXiv:1409.4657.

[114] N. Craig, M. Farina, M. McCullough, and M. Perelstein: 'Precision Higgsstrahlung as a Probe of New Physics'. JHEP 03: p. 146, 2015. arXiv:1411.0676.

[115] S. Dawson, I. M. Lewis, and M. Zeng: 'Usefulness of effective field theory for boosted Higgs production'. Phys. Rev. D91: p. 074 012, 2015. arXiv:1501.04103.

[116] R. Edezhath: 'Dimension-6 Operator Constraints from Boosted VBF Higgs' 2015. arXiv:1501.00992.

[117] M. Gorbahn, J. M. No, and V. Sanz: 'Benchmarks for Higgs Effective Theory: Extended Higgs Sectors'. JHEP 10: p. 036, 2015. arXiv:1502.07352.

[118] L. Edelhäuser, A. Knochel, and T. Steeger: 'Applying EFT to Higgs Pair Production in Universal Extra Dimensions'. JHEP 11: p. 062, 2015. arXiv:1503.05078.

[119] A. Drozd, J. Ellis, J. Quevillon, and T. You: 'Comparing EFT and Exact One-Loop Analyses of Non-Degenerate Stops'. JHEP 06: p. 028, 2015. arXiv:1504.02409.

[120] C. Englert, R. Kogler, H. Schulz, and M. Spannowsky: 'Higgs coupling measurements at the LHC'. Eur. Phys. J. C76 (7): p. 393, 2016. arXiv:1511.05170.

[121] R. Contino, A. Falkowski, F. Goertz, C. Grojean, and F. Riva: 'On the Validity of the Effective Field Theory Approach to SM Precision Tests'. JHEP 07: p. 144, 2016. arXiv:1604.06444.

[122] A. Freitas, D. López-Val, and T. Plehn: 'When matching matters: Loop effects in Higgs effective theory'. Phys. Rev. D94 (9): p. 095 007, 2016. arXiv:1607.08251.

[123] J. Alwall, D. Rainwater, and T. Plehn: 'Same-Sign Charginos and Majorana Neutralinos at the CERN LHC'. Phys. Rev. D76: p. 055 006, 2007. arXiv:0706.0536.

[124] K. Hagiwara, Q. Li, and K. Mawatari: 'Jet angular correlation in vector-boson fusion processes at hadron colliders'. JHEP 07: p. 101, 2009. arXiv:0905.4314.

[125] C. Englert, D. Goncalves-Netto, K. Mawatari, and T. Plehn: 'Higgs Quantum Numbers in Weak Boson Fusion'. JHEP 01: p. 148, 2013. arXiv:1212.0843.

[126] J. Brehmer, J. Jaeckel, and T. Plehn: 'Polarized WW Scattering on the Higgs Pole'. Phys. Rev. D90 (5): p. 054 023, 2014. arXiv:1404.5951.

[127] A. Azatov, C. Grojean, A. Paul, and E. Salvioni: 'Taming the off-shell Higgs boson'. Zh. Eksp. Teor. Fiz. 147: pp. 410–425, 2015. [J. Exp. Theor. Phys.120,354(2015)], arXiv:1406.6338.

[128] M. Buschmann, D. Goncalves, S. Kuttimalai, M. Schonherr, F. Krauss, and T. Plehn: 'Mass Effects in the Higgs-Gluon Coupling: Boosted vs Off-Shell Production'. JHEP 02: p. 038, 2015. arXiv:1410.5806.

[129] A. Azatov, C. Grojean, A. Paul, and E. Salvioni: 'Resolving gluon fusion loops at current and future hadron colliders'. JHEP 09: p. 123, 2016. arXiv:1608.00977.

[130] I. M. Shoemaker and L. Vecchi: 'Unitarity and Monojet Bounds on Models for DAMA, CoGeNT, and CRESST-II'. Phys. Rev. D86: p. 015 023, 2012. arXiv:1112.5457.

[131] G. Busoni, A. De Simone, E. Morgante, and A. Riotto: 'On the Validity of the Effective Field Theory for Dark Matter Searches at the LHC'. Phys. Lett. B728: pp. 412–421, 2014. arXiv:1307.2253.

[132] O. Buchmueller, M. J. Dolan, and C. McCabe: 'Beyond Effective Field Theory for Dark Matter Searches at the LHC'. JHEP 01: p. 025, 2014. arXiv:1308.6799.

[133] G. Busoni, A. De Simone, J. Gramling, E. Morgante, and A. Riotto: 'On the Validity of the Effective Field Theory for Dark Matter Searches at the LHC, Part II: Complete Analysis for the *s*-channel'. JCAP 1406: p. 060, 2014. arXiv:1402.1275.

[134] D. Racco, A. Wulzer, and F. Zwirner: 'Robust collider limits on heavy-mediator Dark Matter'. JHEP 05: p. 009, 2015. arXiv:1502.04701.

[135] M. Bauer, A. Butter, N. Desai, J. Gonzalez-Fraile, and T. Plehn: 'On the Validity of Dark Matter Effective Theory' 2016. arXiv:1611.09908.

[136] J. M. Cornwall, D. N. Levin, and G. Tiktopoulos: 'Derivation of Gauge Invariance from High-Energy Unitarity Bounds on the s Matrix'. Phys. Rev. D10: p. 1145, 1974. [Erratum: Phys. Rev.D11,972(1975)].

[137] J. M. Cornwall, D. N. Levin, and G. Tiktopoulos: 'Uniqueness of spontaneously broken gauge theories'. Phys. Rev. Lett. 30: pp. 1268–1270, 1973. [Erratum: Phys. Rev. Lett.31,572(1973)].

[138] C. H. Llewellyn Smith: 'High-Energy Behavior and Gauge Symmetry'. Phys. Lett. B46: pp. 233–236, 1973.

[139] H. A. Weldon: 'CONSTRAINTS ON SCALAR MASSES IMPLIED BY SPONTANEOUS SYMMETRY BREAKING'. Phys. Lett. B146: pp. 59–62, 1984.

[140] H. A. Weldon: 'The Effects of Multiple Higgs Bosons on Tree Unitarity'. Phys. Rev. D30: p. 1547, 1984.

[141] J. F. Gunion, H. E. Haber, and J. Wudka: 'Sum rules for Higgs bosons'. Phys. Rev. D43: pp. 904–912, 1991.

[142] T. Corbett, O. J. P. Éboli, and M. C. Gonzalez-Garcia: 'Inverse amplitude method for the perturbative electroweak symmetry breaking sector: The singlet Higgs portal as a study case'. Phys. Rev. D93 (1): p. 015 005, 2016. arXiv:1509.01585.

[143] T. Han, D. Krohn, L.-T. Wang, and W. Zhu: 'New Physics Signals in Longitudinal Gauge Boson Scattering at the LHC'. JHEP 03: p. 082, 2010. arXiv:0911.3656.

[144] M. Gillioz, R. Grober, C. Grojean, M. Muhlleitner, and E. Salvioni: 'Higgs Low-Energy Theorem (and its corrections) in Composite Models'. JHEP 10: p. 004, 2012. arXiv:1206.7120.

[145] S. Dawson, E. Furlan, and I. Lewis: 'Unravelling an extended quark sector through multiple Higgs production?' Phys. Rev. D87 (1): p. 014 007, 2013. arXiv:1210.6663.

[146] J. Alwall, R. Frederix, S. Frixione, et al.: 'The automated computation of tree-level and next-to-leading order differential cross sections, and their matching to parton shower simulations'. JHEP 07: p. 079, 2014. arXiv:1405.0301.

[147] A. Alloul, N. D. Christensen, C. Degrande, C. Duhr, and B. Fuks: 'FeynRules 2.0 - A complete toolbox for tree-level phenomenology'. Comput. Phys. Commun. 185: pp. 2250–2300, 2014. arXiv:1310.1921, URL https://feynrules.irmp.ucl.ac.be/wiki/ModelDatabaseMainPage.

[148] C. Degrande, C. Duhr, B. Fuks, D. Grellscheid, O. Mattelaer, and T. Reiter: 'UFO - The Universal FeynRules Output'. Comput. Phys. Commun. 183: pp. 1201–1214, 2012. arXiv:1108.2040.

[149] A. Alloul, B. Fuks, and V. Sanz: 'Phenomenology of the Higgs Effective Lagrangian via FEYNRULES'. JHEP 04: p. 110, 2014. arXiv:1310.5150.

[150] A. Djouadi: 'The Anatomy of electro-weak symmetry breaking. I: The Higgs boson in the standard model'. Phys. Rept. 457: pp. 1–216, 2008. arXiv:hep-ph/0503172.

[151] B. Hespel and E. Vryonidou: 'Higgs pair production'. URL https://cp3.irmp.ucl.ac.be/projects/madgraph/wiki/HiggsPairProduction.

[152] B. Hespel, D. Lopez-Val, and E. Vryonidou: 'Higgs pair production via gluon fusion in the Two-Higgs-Doublet Model'. JHEP 09: p. 124, 2014. arXiv:1407.0281.

[153] T. Hahn: 'Generating Feynman diagrams and amplitudes with FeynArts 3'. Comput. Phys. Commun. 140: pp. 418–431, 2001. arXiv:hep-ph/0012260.

[154] T. Hahn and M. Perez-Victoria: 'Automatized one loop calculations in four-dimensions and D-dimensions'. Comput. Phys. Commun. 118: pp. 153–165, 1999. arXiv:hep-ph/9807565.

[155] J. Pumplin, D. R. Stump, J. Huston, H. L. Lai, P. M. Nadolsky, and W. K. Tung: 'New generation of parton distributions with uncertainties from global QCD analysis'. JHEP 07: p. 012, 2002. arXiv:hep-ph/0201195.

[156] G. Aad et al. (ATLAS, CMS): 'Combined Measurement of the Higgs Boson Mass in pp Collisions at $\sqrt{s}$ = 7 and 8 TeV with the ATLAS and CMS Experiments'. Phys. Rev. Lett. 114: p. 191 803, 2015. arXiv:1503.07589.

[157] T. E. W. Group (CDF, Do): 'Combination of CDF and Do results on the mass of the top quark using up to 9.7 fb^{-1} at the Tevatron' 2014. arXiv:1407.2682.

[158] 'First combination of Tevatron and LHC measurements of the top-quark mass' 2014. arXiv:1403.4427.

[159] A. Djouadi, J. Kalinowski, and M. Spira: 'HDECAY: A Program for Higgs boson decays in the standard model and its supersymmetric extension'. Comput. Phys. Commun. 108: pp. 56–74, 1998. arXiv:hep-ph/9704448.

[160] V. Silveira and A. Zee: 'SCALAR PHANTOMS'. Phys. Lett. B161: pp. 136–140, 1985.

[161] R. M. Schabinger and J. D. Wells: 'A Minimal spontaneously broken hidden sector and its impact on Higgs boson physics at the large hadron collider'. Phys. Rev. D72: p. 093 007, 2005. arXiv:hep-ph/0509209.

[162] B. Patt and F. Wilczek: 'Higgs-field portal into hidden sectors' 2006. arXiv:hep-ph/0605188.

[163] G. M. Pruna and T. Robens: 'Higgs singlet extension parameter space in the light of the LHC discovery'. Phys. Rev. D88 (11): p. 115 012, 2013. arXiv:1303.1150.

[164] D. Lóopez-Val and T. Robens: 'Δr and the W-boson mass in the singlet extension of the standard model'. Phys. Rev. D90: p. 114 018, 2014. arXiv:1406.1043.

[165] T. Robens and T. Stefaniak: 'Status of the Higgs Singlet Extension of the Standard Model after LHC Run 1'. Eur. Phys. J. C75: p. 104, 2015. arXiv:1501.02234.

[166] T. Robens and T. Stefaniak: 'LHC Benchmark Scenarios for the Real Higgs Singlet Extension of the Standard Model'. Eur. Phys. J. C76 (5): p. 268, 2016. arXiv:1601.07880.

[167] J. F. Gunion and H. E. Haber: 'The CP conserving two Higgs doublet model: The Approach to the decoupling limit'. Phys. Rev. D67: p. 075 019, 2003. arXiv:hep-ph/0207010.

[168] N. Craig, J. Galloway, and S. Thomas: 'Searching for Signs of the Second Higgs Doublet' 2013. arXiv:1305.2424.

[169] M. Carena, I. Low, N. R. Shah, and C. E. M. Wagner: 'Impersonating the Standard Model Higgs Boson: Alignment without Decoupling'. JHEP 04: p. 015, 2014. arXiv:1310.2248.

[170] A. Delgado, G. Nardini, and M. Quiros: 'A Light Supersymmetric Higgs Sector Hidden by a Standard Model-like Higgs'. JHEP 07: p. 054, 2013. arXiv:1303.0800.

[171] J. F. Gunion, H. E. Haber, G. L. Kane, and S. Dawson: 'The Higgs Hunter's Guide'. Front. Phys. 80: pp. 1–404, 2000.

[172] G. C. Branco, P. M. Ferreira, L. Lavoura, M. N. Rebelo, M. Sher, and J. P. Silva: 'Theory and phenomenology of two-Higgs-doublet models'. Phys. Rept. 516: pp. 1–102, 2012. arXiv:1106.0034.

[173] S. L. Glashow and S. Weinberg: 'Natural Conservation Laws for Neutral Currents'. Phys. Rev. D15: p. 1958, 1977.

[174] H. E. Haber, M. J. Herrero, H. E. Logan, S. Penaranda, S. Rigolin, and D. Temes: 'SUSY QCD corrections to the MSSM ho $b\bar{b}$ vertex in the decoupling limit'. Phys. Rev. D63: p. 055 004, 2001. arXiv:hep-ph/0007006.

[175] S. Davidson and H. E. Haber: 'Basis-independent methods for the two-Higgs-doublet model'. Phys. Rev. D72: p. 035 004, 2005. [Erratum: Phys. Rev.D72,099902(2005)], arXiv:hep-ph/0504050.

[176] D. Eriksson, J. Rathsman, and O. Stal: '2HDMC: Two-Higgs-Doublet Model Calculator Physics and Manual'. Comput. Phys. Commun. 181: pp. 189–205, 2010. arXiv:0902.0851.

[177] P. Bechtle, O. Brein, S. Heinemeyer, G. Weiglein, and K. E. Williams: 'HiggsBounds: Confronting Arbitrary Higgs Sectors with Exclusion Bounds from LEP and the Tevatron'. Comput. Phys. Commun. 181: pp. 138–167, 2010. arXiv:0811.4169.

[178] P. Bechtle, O. Brein, S. Heinemeyer, G. Weiglein, and K. E. Williams: 'HiggsBounds 2.0.0: Confronting Neutral and Charged Higgs Sector Predictions with Exclusion Bounds from LEP and the Tevatron'. Comput. Phys. Commun. 182: pp. 2605–2631, 2011. arXiv:1102.1898.

[179] F. Mahmoudi: 'SuperIso v2.3: A Program for calculating flavor physics observables in Supersymmetry'. Comput. Phys. Commun. 180: pp. 1579–1613, 2009. arXiv:0808.3144.

[180] P. Bechtle, S. Heinemeyer, O. Stål, T. Stefaniak, and G. Weiglein: '*HiggsSignals*: Confronting arbitrary Higgs sectors with measurements at the Tevatron and the LHC'. Eur. Phys. J. C74 (2): p. 2711, 2014. arXiv:1305.1933.

[181] M. Carena, S. Heinemeyer, O. Stål, C. E. M. Wagner, and G. Weiglein: 'MSSM Higgs Boson Searches at the LHC: Benchmark Scenarios after the Discovery of a Higgs-like Particle'. Eur. Phys. J. C73 (9): p. 2552, 2013. arXiv:1302.7033.

[182] P. M. Ferreira, J. F. Gunion, H. E. Haber, and R. Santos: 'Probing wrong-sign Yukawa couplings at the LHC and a future linear collider'. Phys. Rev. D89 (11): p. 115 003, 2014. arXiv:1403.4736.

[183] M. Buschmann, C. Englert, D. Goncalves, T. Plehn, and M. Spannowsky: 'Resolving the Higgs-Gluon Coupling with Jets'. Phys. Rev. D90 (1): p. 013 010, 2014. arXiv:1405.7651.

[184] U. Baur, T. Plehn, and D. L. Rainwater: 'Probing the Higgs selfcoupling at hadron colliders using rare decays'. Phys. Rev. D69: p. 053 004, 2004. arXiv:hep-ph/0310056.

[185] J. Baglio, O. Eberhardt, U. Nierste, and M. Wiebusch: 'Benchmarks for Higgs Pair Production and Heavy Higgs boson Searches in the Two-Higgs-Doublet Model of Type II'. Phys. Rev. D90 (1): p. 015 008, 2014. arXiv:1403.1264.

[186] W. Hollik, T. Plehn, M. Rauch, and H. Rzehak: 'Supersymmetric Higgs Bosons in Weak Boson Fusion'. Phys. Rev. Lett. 102: p. 091 802, 2009. arXiv:0804.2676.

[187] J. Berger, J. Hubisz, and M. Perelstein: 'A Fermionic Top Partner: Naturalness and the LHC'. JHEP 07: p. 016, 2012. arXiv:1205.0013.

[188] S. Dawson and E. Furlan: 'A Higgs Conundrum with Vector Fermions'. Phys. Rev. D86: p. 015 021, 2012. arXiv:1205.4733.

[189] S. Fajfer, A. Greljo, J. F. Kamenik, and I. Mustac: 'Light Higgs and Vector-like Quarks without Prejudice'. JHEP 07: p. 155, 2013. arXiv:1304.4219.

[190] S. A. R. Ellis, R. M. Godbole, S. Gopalakrishna, and J. D. Wells: 'Survey of vector-like fermion extensions of the Standard Model and their phenomenological implications'. JHEP 09: p. 130, 2014. arXiv:1404.4398.

[191] C.-Y. Chen, S. Dawson, and I. M. Lewis: 'Top Partners and Higgs Boson Production'. Phys. Rev. D90 (3): p. 035 016, 2014. arXiv:1406.3349.

[192] I. Low, R. Rattazzi, and A. Vichi: 'Theoretical Constraints on the Higgs Effective Couplings'. JHEP 04: p. 126, 2010. arXiv:0907.5413.

[193] D. Pappadopulo, A. Thamm, R. Torre, and A. Wulzer: 'Heavy Vector Triplets: Bridging Theory and Data'. JHEP 09: p. 060, 2014. arXiv:1402.4431.

[194] A. Kaminska: 'Improving LHC searches for strong EW symmetry breaking resonances'. In 'Proceedings, 50th Rencontres de Moriond Electroweak Interactions and Unified Theories: La Thuile, Italy, March 14-21, 2015', pp. 113–120. 2015. arXiv:1505.04645, URL http://inspirehep.net/record/1370708/files/arXiv:1505.04645.pdf.

[195] V. D. Barger, W.-Y. Keung, and E. Ma: 'Doubling of Weak Gauge Bosons in an Extension of the Standard Model'. Phys. Rev. Lett. 44: p. 1169, 1980.

[196] N. Arkani-Hamed, A. G. Cohen, and H. Georgi: 'Electroweak symmetry breaking from dimensional deconstruction'. Phys. Lett. B513: pp. 232–240, 2001. arXiv:hep-ph/0105239.

[197] O. J. P. Eboli and D. Zeppenfeld: 'Observing an invisible Higgs boson'. Phys. Lett. B495: pp. 147–154, 2000. arXiv:hep-ph/0009158.

[198] T. Plehn, D. L. Rainwater, and D. Zeppenfeld: 'Determining the structure of Higgs couplings at the LHC'. Phys. Rev. Lett. 88: p. 051 801, 2002. arXiv:hep-ph/0105325.

[199] M. R. Buckley, T. Plehn, and M. J. Ramsey-Musolf: 'Top squark with mass close to the top quark'. Phys. Rev. D90 (1): p. 014 046, 2014. arXiv:1403.2726.

[200] W. Allen: Getting even. Random House, 1971. ISBN 9780394473482.

[201] T. Plehn: private communication, 2017.

[202] M. J. G. Veltman: 'Second Threshold in Weak Interactions'. Acta Phys. Polon. B8: p. 475, 1977.

[203] D. Toussaint: 'Renormalization Effects From Superheavy Higgs Particles'. Phys. Rev. D18: p. 1626, 1978.

[204] J. M. Frere and J. A. M. Vermaseren: 'Radiative Corrections to Masses in the Standard Model With Two Scalar Doublets'. Z. Phys. C19: pp. 63–67, 1983.

[205] W. Grimus, L. Lavoura, O. M. Ogreid, and P. Osland: 'A Precision constraint on multi-Higgs-doublet models'. J. Phys. G35: p. 075 001, 2008. arXiv:0711.4022.

[206] W. Hollik: 'Nonstandard Higgs Bosons in SU(2) X U(1) Radiative Corrections'. Z. Phys. C32: p. 291, 1986.

[207] W. Beenakker and W. Hollik: 'The Width of the Z Boson'. Z. Phys. C40: p. 141, 1988.

[208] C. D. Froggatt, R. G. Moorhouse, and I. G. Knowles: 'Leading radiative corrections in two scalar doublet models'. Phys. Rev. D45: pp. 2471–2481, 1992.

[209] H.-J. He, N. Polonsky, and S.-f. Su: 'Extra families, Higgs spectrum and oblique corrections'. Phys. Rev. D64: p. 053 004, 2001. arXiv:hep-ph/0102144.

[210] W. Grimus, L. Lavoura, O. M. Ogreid, and P. Osland: 'The Oblique parameters in multi-Higgs-doublet models'. Nucl. Phys. B801: pp. 81–96, 2008. arXiv:0802.4353.

[211] F. del Aguila, J. de Blas, and M. Perez-Victoria: 'Electroweak Limits on General New Vector Bosons'. JHEP 09: p. 033, 2010. arXiv:1005.3998.

List of abbreviations

2HDM	two-Higgs doublet model
BSM	beyond the Standard Model
EFT	effective field theory
ggF	gluon fusion
IR	infrared
LHC	Large Hadron Collider
LLR	log likelihood ratio
PO	pseudo-observable
SM	Standard Model
UV	ultraviolet
VEV	vacuum expectation value
WBF	weak boson fusion